ADVANCED TECHNOLOGY LABORATORIES

183p.

DESIGN CRITERIA FOR ZERO-LEAKAGE CONNECTORS FOR LAUNCH VEHICLES. VOL. 4, DESIGN OF CONNECTORS

Edited by
S. LEVY

CONTRACT NAS 8-4012

MARCH 15, 1963

FINAL REPORT FOR FIRST CONTRACT PERIOD

(March 1962 through February 1963)

DESIGN CRITERIA
FOR ZERO-LEAKAGE CONNECTORS
FOR LAUNCH VEHICLES

Contract NAS 8-4012

VOLUME 4
DESIGN OF CONNECTORS

Edited by S. Levy

March 15, 1963

PREPARED FOR: Propulsion and Vehicle Engineering Division
George C. Marshall Space Flight Center
National Aeronautics and Space Administration
Huntsville, Alabama

PREPARED BY: Advanced Technology Laboratories
General Electric Company
Schenectady, New York

SPONSORED BY: Missile and Space Division
General Electric Company
Philadelphia, Pennsylvania

N.A.S.A. TECHNICAL MANAGER: C.C. Wood (M-P&VE-PT)

CONTENTS

CONTENTS (continued)

CONTENTS (continued)

40. INTERACTION OF FLANGE, GASKET, AND PIPE

by

S. Levy

40.0 Summary

This section presents a review of available design procedures for the many environmental factors affecting the performance of connectors. Novel and unusual effects are emphasized so that they may be correctly interpreted.

Later sections in this volume will discuss in more detail some of the specific design considerations introduced in this section.

6

40.1 Introduction

A fluid connector mechanically joins two sections of pipe and provides a seal against fluid leakage. It must perform these functions for a wide range of environmental conditions.

Ease in design suggests the use of separate parts of the connector for the "joining" and "sealing" functions with a minimum of interaction between them. Such a design approach avoids compromising the "sealing" function by changes intended to improve the reliability of "joining" and vice versa. The necessity to economize on weight and space does not ordinarily permit the complete separation of functions. As a result, it is found that many connectors in use today have constructions such that flange or bolt flexibility relaxes gasket pressure, while gasket creep may result in joint looseness.

As is pointed out in Ref. 1, the first step in the design of a bolted flanged connection, for example, is to select the seal or gasket material and its shape. Sufficient pressure must then be provided on the gasket to hold the joint tight at all times. The load required to do this, as well as overcome the internal fluid pressure, is provided by the bolts and determines their size. The flange dimensions must now be chosen to withstand the bolt load. Similar procedures can be described for other types of joints. After the initial design has been determined, it is necessary to evaluate its performance under the many other environmental conditions which may apply. Consideration must be given to tolerances, material availability, cost, LOX sensitivity, and many other factors.

Internal pressure has a major effect on connectors. In many designs it causes a reduction in gasket pressure and, therefore, in seal performance. A typical example is the conventional flange coupling shown in Fig. 40.1

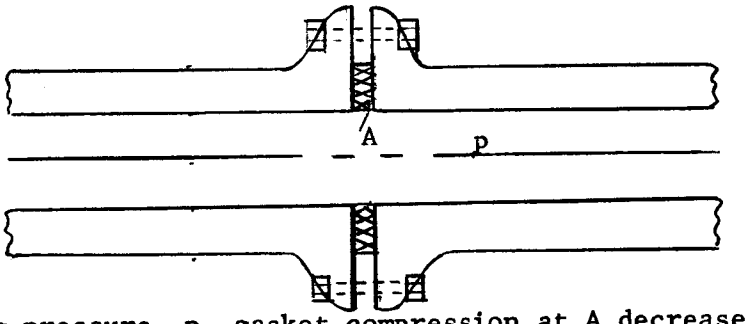

FIG. 40.1
Conventional flange coupling

With increasing pressure, p, gasket compression at A decreases. At a sufficiently high pressure, the gasket compression has decreased to be equal in magnitude to the internal pressure. Further increases in internal pressure find the gasket acting as a pressure relief valve with corresponding large-scale leakage. Recognition of the effect of internal pressure on gasket compression has led to many "pressure assisted" seals, a typical example of which is shown in Fig. 40.2. Such seals are based on Bridgman's "unsupported area" principle (Ref. 2). By allowing the internal pressure to "bulge" the U-shaped seal ring, it is possible to have the seal pressure (at A, for example) increase with internal pressure, p, rather than decrease.

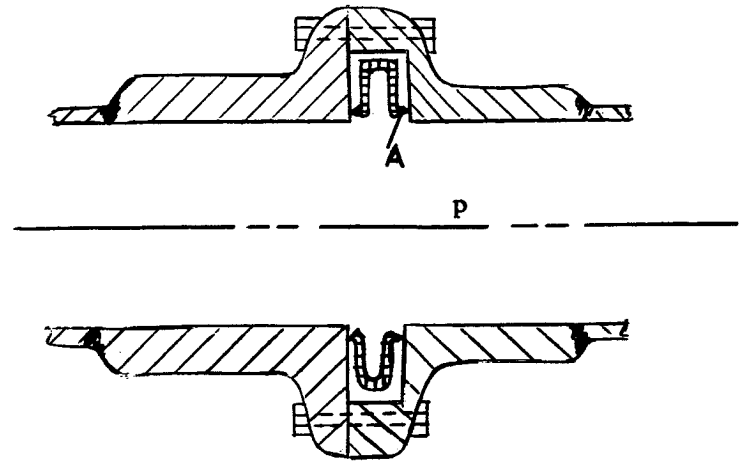

FIG. 40.2 - Pressure-assisted seals

Temperature changes and temperature transients also have a major effect on connectors. An example of an AN fitting is shown in Fig. 40.3. A cold fluid starting to flow through the pipe will cool the inside much more rapidly than the sleeve, A, or nut, B. As a result, the contraction of the sleeve and nut will be slower. The sealing pressure will thereby be lowered with increased possibility of leakage. Another example is the flanged connector shown in Fig. 40.4. Here the flange, A, could

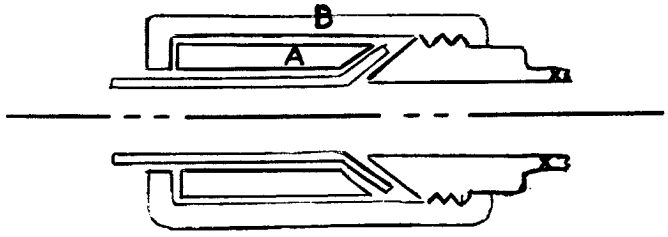

FIG. 40.3 - AN-type fitting

cool more rapidly than the bolts, B. As a result, the gasket load will be reduced and leakage made more likely. Again, recognition of the effect of temperature change in causing contraction or expansion has resulted in the design of "temperature-compensated" connectors. In Fig. 40.5 is shown

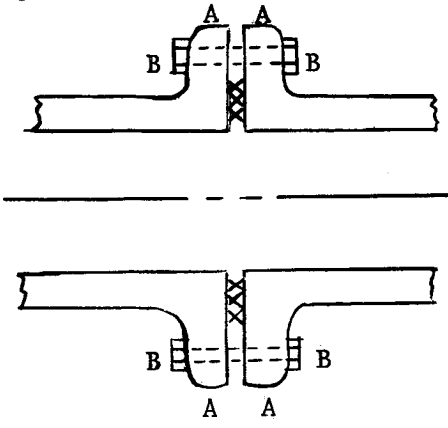

FIG. 40.4 - Flanged Connector

a flange connector with a sealant material confined between the flange and an invar ring (Ref. 3). During cooling the sealant contracts proportionately more than the flange material. The invar ring, since it contracts less, tends to compensate for this excess and keep the joint tight. Data on the effect of temperature on the elastic and expansion properties of materials are given in Refs. 4, 5, and 6. Since the coefficients of expansion may vary substantially with temperature, true compensation is seldom achieved.

Bending forces due to vibration or otherwise tend to open one side of the connector and close more tightly the other side.

Other environmental effects include radiation, erosion by the fluid flow, water-hammer, high vacuum, etc.

A successful connector must be capable of withstanding all environmental conditions without coming apart and with essentially zero leakage. To determine if a connector will be adequate, the methods given in other sections of this report and in the literature must be applied to determine deformations, stresses and leakage flow rates. In this section we will examine some of these methods and how the results thus obtained are combined to determine the overall connector performance.

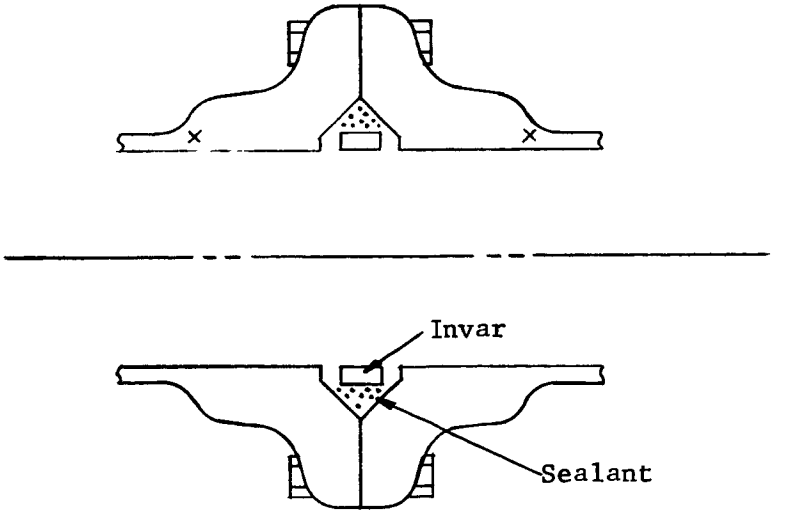

FIG. 40.5 - Temperature-Compensated Seal

40.2 Flange Deformation

An excellent discussion of the stresses and deformations of the flanges of connectors is given in Ref. 7. The flanges considered in Ref. 7 have the contact area between flanges entirely within the bolt circle (see also Section 42). This reference considers the elastic interaction of flange ring, tapered hub, and pipe. It presents charts which greatly increase the speed of computing maximum stresses. It also presents equations for determining flange rotation and radial expansion. It assumes an axisymmetric loading, with negligible "dishing" of the flange ring. It excludes all types of flange facings where the gasket or contacting flange surfaces have any contact outside of the bolt circle.

Flanges which are in bearing outside of the bolt circle are considered in Ref. 8 and in section 41. In this analysis it is assumed that radial force is resisted by hoop stress in the flange. Axial forces are considered to cause a bending moment in the flange which is resisted by bending stresses in the flange ring in a radial direction. It is assumed that the flange bends about the bolt center circle as if it were fixed there. The elastic interaction of flange ring, tapered hub, and pipe is then considered by requiring deflections and slopes to match at their junctures.

The effect of flange barreling due to pressure and temperature differences is considered in Ref. 9. Ref.9 presents a simplification of the approach in Ref. 7 by considering the flange and hub to move as a unit without cross-sectional distortion. This approach is a good approximation for sturdy flanges where the length and thickness are comparable.

40.3 Gasket Compression

From the point of view of mathematical analysis it would be most desirable if the gasket compressed as a linear spring. The actual relationship is much more complex, as is shown by Fig. 40.6 taken from Fig. 11 of Ref.10 for a

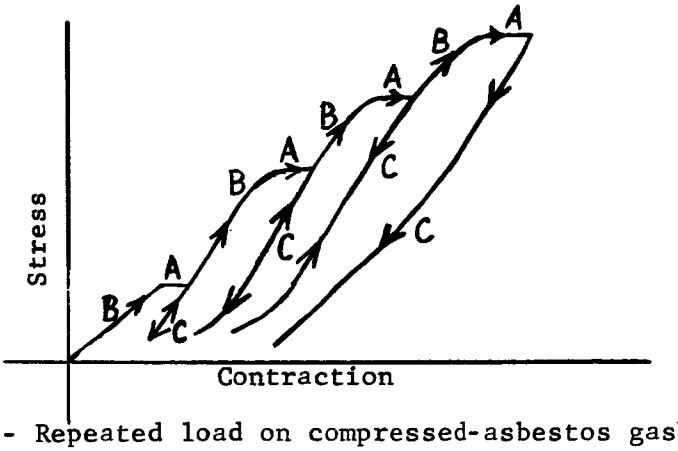

FIG. 40.6 - Repeated load on compressed-asbestos gasket material

compressed-asbestos gasket material. In the regions A we see creep under constant stress. At B we see the curved form of the initial load-shortening curve. At C we see that the curve for retraction differs from the loading curve B and in this case overlaps for reloading. (The overlapping is not always present. See, for example, Fig. 9 of Ref. 10.) Other gaskets may include metallic elements that improve the "springiness" and linearity and may include "soft" materials, such as teflon and rubber, that can be squashed substantially to improve the sealing effectiveness. Such gaskets are considered in detail in other sections of this report.

An important function of the gasket is to be soft enough to provide good sealing (see sections 22 and 33) while retaining adequate hoop strength to resist "blowing out."

An interesting characteristic of the interaction of flange and gasket is discussed in Ref. 11 for flanges whose contacting area is entirely within the bolting circle. It is pointed out that when pressure is applied "to our knowledge no increase in bolt stress has ever been observed. On the contrary, the bolt stress has been observed to reduce as internal pressure is applied both with solid metal and soft gaskets until the gasket precompression is lost and leakage begins. This effect is due to rotation of the ring flanges under the applied moments and far outweighs the effect of the hydrostatic end force." It seems likely that a similar phenomenon will be present when thermal transients heat the hub much more rapidly than the ring flange.

Creep in gaskets is treated most eloquently in Ref. 12. It is pointed out that one can observe "declines in gross gasket loads of ordinary 1/16-in. compressed-asbestos gaskets...of the order of 68 percent in 20 hours at a temperature corresponding to 350 psi steam." Such creep will have a marked effect on the stress and deformation distribution of a connector and must be considered where extended life is involved. In another comment,

W.R. Burrows, remarking on the paper in Ref. 13, stated that "very heavy exchange flanges with 1.25-in. SAE 4140 stud bolts, operating at 400 psi and 650°F, leaked after 24 hours on stream. Measured stud bolt stresses of 50,000 psi had relaxed to 12,000 psi owing to crushing of the soft-iron gaskets. These gaskets, following custom, had been designed for a bolt stress of 25,000 psi. The actual stress of 50,000 psi crushed the gaskets even at a temperature of 650°F."

At high pressures there is a tendency to use Bridgman-type closures, Ref. 14, which utilize the unsupported-area principle (see also Sections 51 and 52.) Many closures of this type have been devised and some are widely used. In some cases the gasket is a hard metal and sealing is accompanied by permanent deformation of either the gasket, the seat, or both. As pointed out in Ref. 14, "at present, even for the simplest types of gaskets, there is no completely reliable design criterion, based on anything other than experience."

In view of the nonlinear behavior of almost all good gasket materials, it would appear that reliable designs can best be achieved where the contribution of the gasket "stiffness" to the overall stiffness is small. In this way the uncertainty introduced by this analytically difficult portion of the design can be minimized.

12

40.4 Bolt Spacing

Proper bolt spacing depends on flange thickness and gasket flexibility as well as other factors (see Section 43). It is apparent that a given bolting load can be achieved by either a few large bolts or by a greater number of smaller bolts. Factors affecting bolt size and spacing, as pointed out in Ref. 1, are clearance necessary for socket wrenches; strength to withstand over-torquing; adequate spacing to avoid high stress-concentration; and close enough spacing to insure uniform gasket compression. Ref. 1 recommends a bolt spacing of 2-1/4 to 3-1/2 bolt diameters between centers. A somewhat more involved method of analysis is presented in Ref. 10. It considers the flange-gasket combination as a beam on an elastic foundation. In view of the questionable adequacy of neglecting the effect of the hub in increasing the flange ring bending stiffness, this refinement does not seem to have broad application. Bolt spacing is also considered in Ref. 8. It recommends a spacing less than 2.6 times the flange ring thickness to achieve good sealing between bolts. The variety of "rules" for choosing bolt spacing, all of which appear to be successful, indicates that bolt spacing is not a critical design consideration.

13

40.5 Interaction of Flange and Gasket

The effect of internal pressure on the interaction of flange and gasket is considered in detail in Ref. 13. Using the analysis for flange deformation in Ref. 7 and assuming the gasket behavior for decreasing load is adequately represented by a linear relationship, a method is provided for considering the loads when (a) assembling the joint, (b) at test pressure, and (c) in service. In Fig. 40.7, taken from Fig. 2 of Ref. 13, P_3 is the service pressure and P_2 is the test pressure. The line GJ is the limit of bolt load for flange yielding. It shows a decreasing permissible bolt load as the pressure increases. The line OA represents the bolt load to compensate the hydrostatic end force. Line OB represents line OA plus the gasket sealing force. (The required gasket sealing force is assumed to increase linearly with pressure.) The slope $-\alpha$ of the bolt load curves, CD, FB, MJ, and KL

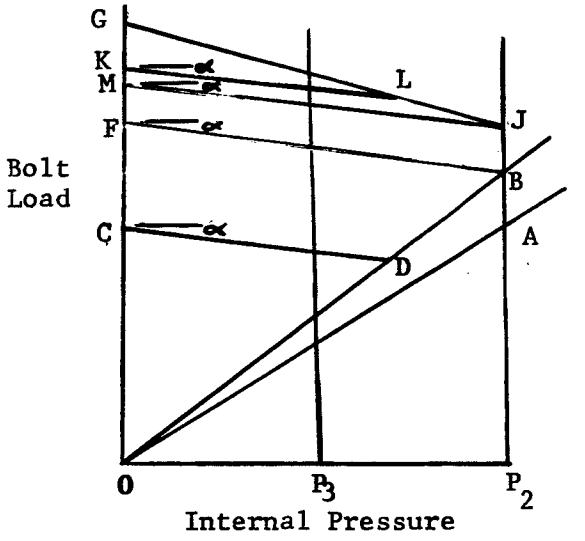

FIG. 40.7

Interaction of flange, bolts and gasket

is determined by the interaction of the various stiffnesses. If the bolts are initially tightened to C, leaking will occur at D at a pressure greater than P_3, the operating pressure, and less than P_2, the test pressure. With the bolts initially tightened to F, leaking will not occur, although at B the connection will be on the verge of leaking. With the initial bolt tightening to K, as pressure is increased, the flange begins to yield at L and continues to yield until J is reached. Upon removing load, the bolt tightness returns to M. It may be pointed out that the effect of gasket creep would be to lower the bolt-load curves, such as FB, with time so that they might leak after a short time in service.

40.6 Hydrostatic End Force

In most connectors one considers a "hydrostatic end force" to load the connector axially. Such a force is assumed in Ref. 7. In the case of a pipe having expansion joints, however, such as found in missile structures, it is not necessarily true that an axial force is present. Similarly, a pipe having closely spaced attachments to a supporting structure may have much reduced "end force" carried by the connector. In Ref. 15 it is pointed out that "in concentrating on the bolted-flange joint itself, it is easy to overlook the fact that there is little hydrostatic end force in pipe lines equipped with slip joints." The correct axial force to be considered in a connector, therefore, depends on interaction between piping and supporting structure and may be temperature dependent. In addition, it is reasonable to provide for a pipe bending moment to be transmitted across the connector. A rather extensive discussion of piping flexibility effects is given in Ref. 16.

15

40.7 Closures

Closures for pipes can be plugs in the case of small sizes but must be considered as heads for large sizes. A method for considering a "floating head" (see Fig 40.8) is given in Ref.17. The interaction of A and B is required to give equal radial displacement and rotation of their juncture J. Part A is considered to have no cross-sectional distortion. The analysis is well adapted for use with the flange analysis of Ref.13 to determine sealing performance as well as stresses and deformation.

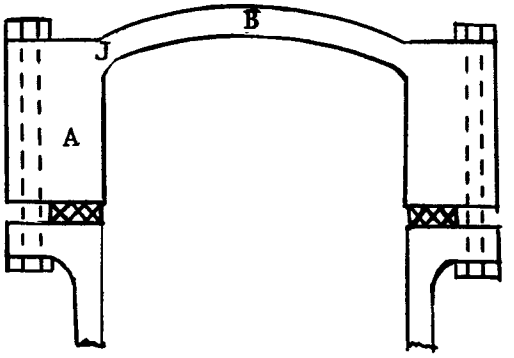

FIG. 40.8 - Pipe closure

16

40.8 Transient Thermal Stresses

During the initial flow through a connector of a fluid which is either hotter or colder than the connector walls, there will exist a transient temperature condition. The inner walls will change temperature more rapidly than the outer walls. In addition, the thinner sections will "heat through" more rapidly than the thicker sections. As a result of these temperature differences, there will be transient stresses and distortions which could initiate leakage. A discussion and general equations for some of the stress and temperature problems are given in Ref. 18. The author points out, however, that "clearly the stress and temperature formulas for hollow cylinders pose difficult problems in evaluation. The roots of the equation have not yet been evaluated. Also, the ratio of outer to inner radius is involved, and a general graphical presentation such as can be made for the case of plates is difficult because of the large number of graphs which would now be required." The results of an approximate solution for the transient temperatures in a cylinder are given in Section 61. This approximate solution is particularly adaptable to stress analysis, since it gives the temperature as a power function of the radius. The application of this solution to determining the distortion of flanges is given in Section 48. Figure 61.5 in Section 61 is particularly useful, since it gives the temperature difference from inner to outer wall at the time of maximum temperature difference. Additional information on stresses and temperature distributions is found in Ref. 19.

17

40.9 Warped Flanges

Initial lack of flatness in the flanges of connectors can result in leakage if the bolt loads are not sufficient to achieve positive gasket compression at all points on the circumference. The magnitude of permissible initial warping of the flanges is, therefore, governed by the available additional bolt strength and flange strength. Section 46 presents equations for computing flange warping displacements due to bolt load and gasket forces. The effect of the pipe in restraining the flange is included in the analysis. It is assumed that the deviation from uniformity of forces and displacements around the circumference of the flange can be adequately approximated by considering them to vary as cos 2θ. Ref. 9 considers warping also by developing the pipe shell as a flat plate. The adequacy of this approximation will depend on the flange and pipe hoop bending strengths and is questioned by Waters in his discussion of the paper.

18

40.10 Leakage Flow

The interface between gasket and flange forms a channel for leakage flow. The depth of this channel depends on surface finish, yield strength of the gasket and flange materials, and gasket compression. The interplay of these factors is considered in Sec. 33, using a statistical approach. Data are presented for typical surface asperities, and a method is presented for determining the effect of gasket compression on the effective flow channel. The magnitude of the flow through such a channel is considered in Sec. 33 making use of the method in Sec. 22. Sec. 22 considers the parameters affecting fluid flow and provides equations for the velocity, quantity, etc. The leakage flow may be turbulent, laminar, or molecular, depending on the flow parameters. An important result in Sec. 22 is that the mass rate of flow is proportional to the cube of the channel thickness in laminar flow and proportional to the square of the channel thickness in molecular flow. Thus, a reduction in clearance from 100 to 10 microinches reduces the flow by a factor of 100 to 1,000.

40.11 Fluid Momentum Effects

When the fluid in a pipe is caused to accelerate or decelerate, unbalanced forces are imposed on the piping system. Thus, in the pipe shown in Fig. 40.9, an acceleration in fluid flow in direction A causes a reaction of the pipe at B in the direction shown. The magnitude of the bending moment and axial force thus imposed on connectors in the piping system will depend on the restraint imposed on the piping system by the supporting structure C. When valves are suddenly opened or closed, these momentum changes are most severe and are described as "water hammer." A discussion of "water hammer" is given in Section 62.

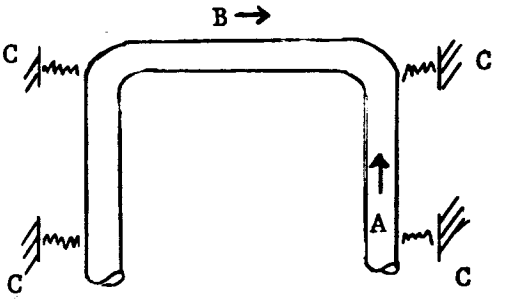

FIG. 40.9 - Effect of fluid flow

Even when the fluid flow is zero, momentum effects are present due to acceleration of the entire booster. (see Section 63).

40.12 Fatigue

In some instances the number of stress cycles at a particular connector may be sufficient to result in fatigue failure. A method for analyzing for fatigue damage is presented in Ref. 19. The method assumes that the stress condition is known versus time for a complete cycle of operation. It takes account of yielding and of the mean and alternating stresses.

40.13 Discussion

Many methods and considerations have been presented concerning the interaction of flange, gasket seal, and pipe. The optimum configuration of a connector varies widely depending on the service conditions. To consider all of the factors in any particular design requires a large amount of detailed computation. As a result of this, standard forms of connectors have evolved for particular applications in the past, and new forms can be expected to meet the requirements of new environments.

A large amount of careful work has been done in the field of connector design, and this provides a sound base from which to evolve new design methods and to develop and evaluate new materials for new environments.

The missile application of fluid connectors imposes much more severe design requirements because of the range of pressure, temperature and time over which performance is required and the limitations imposed by minimum weight, lox sensitivity, radiation and space environments in general.

When methods and applicable material properties have been assembled, it may be possible to combine them in one, or several, computer programs to yield optimum designs for specified load conditions.

21

40.14 References

1. E. O. Waters, D. B. Wesstrom, and F.S.G. Williams, "Design of Bolted Flanged Connections," Pressure Vessel and Piping Design Collected Papers 1927-1959, ASME, p. 58 (also published in Mechanical Engineering, 1934).

2. P. W. Bridgman, The Physics of High Pressure, 2nd Edition, G. Bell, London, 1949, Chapter II.

3. S. E. Logan, "Temperature-Energized Static Seal for Liquid Hydrogen," Advances in Cryogenics, Vol. 7 (Proceedings of Conference at Ann Arbor, Michigan, 1961), pp. 556-561.

4. R. Michel, "Elastic Constants and Coefficients of Thermal Expansion of Piping Materials Proposed for 1954 Code for Pressure Piping," Pressure Vessels and Piping Design Collected Papers 1927-1959, ASME, p. 442 (also in Trans. ASME, 1955).

5. J. R. Vinson, "Short-Time Properties of Materials as a Function of Temperature," General Electric TIS Report No. 60SD314, Feb. 8, 1960.

6. L. Mantell, Engineering Materials Handbook, McGraw-Hill Book Co., 1958, pp. 18-43 to 18-47, "Low-Expansion Alloys."

7. E. O. Waters, D. B. Wesstrom, D. B. Rossheim and F.S.G. Williams, "Formulas for Stresses in Bolted Flanged Connections," Pressure Vessel and Piping Design Collected Papers 1927-1959, ASME, p. 62 (also publ. in Trans. ASME, 1937, and in more extended form by the Taylor Forge and Pipe Works, "Development of General Formulas for Bolted Flanges").

8. C. K. Coombs, "Circumferential Flange Analysis," General Electric TIS Report No. R56AGT386, July 16, 1956.

9. W. M. Dudley, "Deflection of Heat Exchanger Flanged Joints as Affected by Barreling and Warping," Trans. ASME, Nov. 1961, pp. 460-466.

10. I. Roberts, "Gaskets and Bolted Joints," Pressure Vessel and Piping Design Collected Papers 1927-1959, ASME, p. 102 (also published in J. Appl. Mech., ASME, 1950).

11. D. B. Rossheim and J. J. Murphy, Discussion of paper by I. Roberts, Ref. 10, Pressure Vessels and Piping Design Collected Papers 1927-1959, ASME, p. 115.

12. F.C. Thorn, Discussion of paper by I. Roberts, Ref.10, Pressure Vessels and Piping Design Collected Papers 1927-1959, ASME, p. 117.

13. D.B. Wesstrom and S.E. Bergh, "Effect of Internal Pressure on Stresses and Strains in Bolted-Flanged Connections," Pressure Vessels and Piping Design Collected Papers 1927-1959, ASME, p. 121.

14. A.R. Freeman, "Gaskets for High Pressure Vessels," Pressure Vessels and Piping Design Collected Papers 1927-1959, ASME p. 165.

15. H.C. Boardman, Comment on paper, "Stress Conditions in Flanged Joints for Low-Pressure Service" by E.O. Waters and F.S.G. Williams, Pressure Vessels and Piping Design Collected Papers 1927-1959, ASME, p. 162.

16. A.R.C. Markl, "Piping Flexibility Analysis," Pressure Vessels and Piping Design Collected Papers 1927-1959, ASME, p. 419 (also in Trans. ASME, 1955).

17. J.E. Sochrens, "The Design of Floatingheads for Heat Exchangers," Pressure Vessels and Piping Design Collected Papers 1927-1959, ASME, p. 261 (also in ASME Paper 57-A-247).

18. M.P. Heisler, "Transient Thermal Stresses in Slabs and Circular Pressure Vessels," Pressure Vessels and Piping Design Collected Papers 1927-1959, ASME, p. 532 (also in J. Appl. Mech., 1953).

19. "Tentative Structural Design Basis for Reactor Pressure Vessels and Directly Associated Components," distributed by OTS, Dept. of Commerce, PB151987, 1 Dec. 1958 Revision with Addendum No.1 - 27 Feb. 1959 (see also NR-S-1 issued March 1961).

20. S. Timoshenko, Theory of Plates and Shells, McGraw-Hill, 1940.

21. S. Timoshenko, Strength of Materials, Part II, D. VanNostrand Co., 2nd Edition, 1941.

23

41. DESIGN OF LARGE-DIAMETER LIGHT-WEIGHT FLANGES HAVING CONTACT OUTSIDE THE BOLT CIRCLE

by

S. Levy

(Section 41.2 based on work of H.J. Macke)

41.0 Summary

This report presents a consolidation of light-weight flange design procedures for connector flanges having contact outside of the bolt circle. The specific equations presented in Sec. 41.2 apply in the case of flanges which have a slight lip so that they bear against each other only near the inner and outer radii of the flange. The equations in Sec. 41.3 apply in the case of flat flanges. The equations in Sec. 41.4 apply to dished flanges. Sec. 41.5 considers warping. The methods described should be considered as a design approach rather than a rigorous treatment of flanges. The objective is to provide a reasonably simple design tool for consistent design of light-weight flanges.

Flanges designed by this procedure may be compared with flanges designed by the procedure of Section 42 to determine which design is preferable for a particular application.

41.1 Nomenclature

		Units
A	Root cross-sectional area of bolts	$inch^2$
a	Radius to cylinder wall mid-thickness	inch
$\bar{a}$	Radius to flange mid-radius	inch
B	Bolt load per unit length of flange	lb/in
b	Distance from bolt circle to outer flange bearing circle, Fig. 41.2	inch
d	Diameter of bolt	inch
d_H	Diameter of bolt head	inch
e	Effective width of flange in bearing	inch
E	Young's modulus	lb/in^2
F	Axial tension in cylinder wall	lb/in
h	Cylinder wall thickness	inch
K=NAE/t	Bolt stiffness	(lb/in)/inch
K_A, K_B	Factors in Eq. (3)	
K_1, K_2	Factors in Eq. (7)	
ℓ	Distance from mid-thickness of cylinder wall to bolt circle	inch
L	Unsupported radial length of flange	inch
M	Moment per unit circumference at flange-cylinder junction	lb-in/inch
N	Number of bolts per inch	1/inch
p	Internal pressure	lb/in^2
Q	Shear per unit circumference at flange-cylinder junction	lb/in
R	Reaction force where flanges contact	lb/in
t	Flange thickness	inch
u	Radial outward deflection with suitable subscripts	inch
w	Warping deflection	inch
y	Axial deflection of flange	inch
ν	Poissons ratio	
σ_H	Hoop stress in flange	lb/in^2
σ_r	Radial bending stress in flange	lb/in^2
σ_R	Bearing stress between flanges	lb/in^2
σ_c	Axial stress in cylinder	lb/in^2

		Units
θ	Slope with suitable subscripts	radians
δ	Initial stretch in bolts	inch
β	Cylinder constant	1/inch

41.2 Flanges Having Lips at Edges

41.2.1. Introduction

The methods of designing flanged connectors where there is a gasket inside the bolt circle and no contact outside the bolt circle have received widespread consideration. Much of this work is collected in Ref. 1. A key element in this work is given in Ref. 2. Using Ref. 1, it is found that as the pipe radius increases relative to the pipe wall thickness, the flange cross-section becomes relatively heavier - primarily to resist flange twisting. Substantial weight saving is therefore possible by allowing the flanges to bear outside the bolt circle and thus resist twisting. When the flanges bear against each other near their inner and outer edges and are drawn together by the bolts, their behavior is well described by considering a radial strip between the two edges as a beam carrying the bolt load.

Quite a few assumptions and idealizations are involved. Some of the major ones are given in the list below.

a. The circumferential flange is considered flexible and bends in a radial direction as a beam simply supported at the flange inner and outer edges. It is realized that in some flanges the behavior may more nearly approximate a cantilever from the outer contact ring. The analysis for these cases is given in Section 41.3 and in Section 41.4. The flanges in this section resist load only by distortion of the cross-section, while those in Ref. 1 resist load primarily by twisting.

b. The difference between inner and outer flange radii is significantly less than the average flange radius.

c. The cylinder has uniform thickness and diameter.

d. The spacing between flanges is large enough so that flanges do not mutually affect each other.

e. The bolt load B is considered uniformly distributed across the bolt head width as shown in Fig. 41.1. The bearing force between flanges is R near the outer edge and zero at the inner edge corresponding to conditions just prior to separation at the inner edge. R is considered to act inboard of the outer flange edge at the center of pressure between flanges.

f. The cylinder is treated as if loaded axisymmetrically only, even though part of the load (due to vibration or maneuvers) may be antisymmetric.

g. Beam theory is used even though the flange thickness is comparable to the radial flange length.

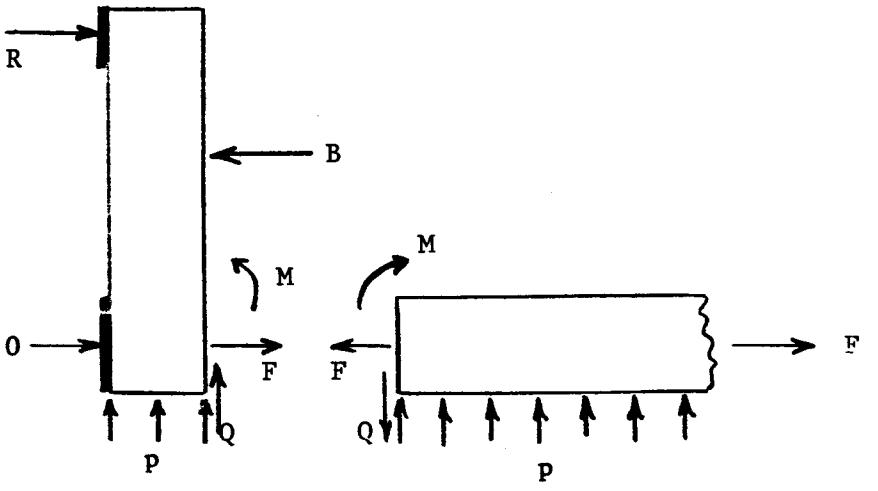

FIG. 41.1 - Loads on flange and pipe

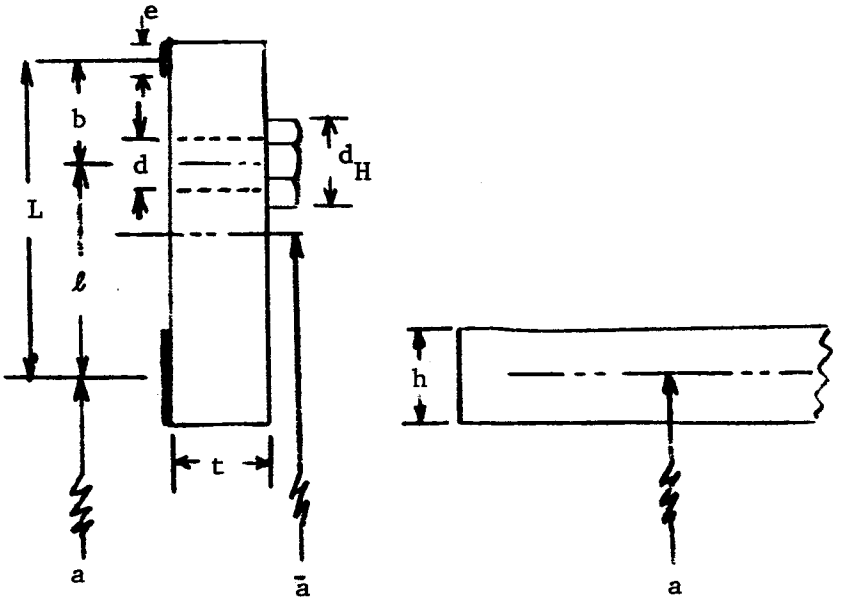

FIG. 41.2 - Flange and pipe dimensions

41.2.2. Analysis

41.2.2.1 Flange Deformation

The radial deflection of the flange is determined from the average hoop stress in the flange.

a. Hoop stress in the flange due to pressure is the product of pressure, inner flange radius, and flange width divided by flange cross-sectional area. It is approximately given by

$$pa/L$$

b. Hoop stress in the flange due to shear from the cylinder is the product of shear force and average pipe radius divided by flange cross-sectional area. It is approximately given by

$$Qa/tL$$

c. Total hoop stress in flange is

$$\sigma_H = \frac{pa}{L} + \frac{Qa}{tL} = \frac{u_1 E}{\bar{a}} \qquad (1)$$

where u_1 is the radial outward deflection of the flange. Solving Eq.(1)

$$u_1 = \frac{\bar{a}}{E}\left(\frac{pa}{L} + \frac{Qa}{tL}\right) = \frac{a\bar{a}}{EL}\left(p + Q/t\right) \qquad (2)$$

For simplicity, u_1 will be expressed as

$$u_1 = K_A + K_B Q \qquad (3)$$

where $K_A = pa\bar{a}/EL$

$K_B = a\bar{a}/tEL$

41.2.2.2. Cylinder Deflection due to Pressure and Axial Load

The radial deflection of the cylinder at a great distance from the flange is determined from the following stresses in the cylinder:

a. Hoop stress due to pressure = pa/h

b. Axial stress = F/h

The radial outward deflection of the cylinder at a great distance from the flange is then given by

$$u_2 = (a/Eh)\ (pa - \nu F) \tag{4}$$

41.2.2.3. Flange Slope at Junction of Flange and Cylinder

In the following analysis a radial strip of the flange between inner and outer radii is considered to be a simple beam on end supports at the two ends of L, Fig. 41.2. At the end attached to the cylinder a moment acts equal to M + Q t/2. Because the flange is not free to distort circumferentially the modulus of elasticity E is replaced by E / (1 - ν^2) in the beam equations. The flange is considered to have recessed faces between the edges so that bearing between flanges occurs only at the ends of L. The slope of the flange at the junction with the cylinder is then

$$\theta_1 = \frac{1-\nu^2}{2\ Et^3}\left[(4L^2 - 4b^2 - d_H^2)\ F + \frac{1}{L}\ (12L^2 - 4b^2 - d_H^2)\ (M + Qt/2)\right] \tag{5}$$

where the bolt load is given by

$$B = FL/b + (M + Qt/2)/b \tag{6}$$

We can write Eq. (5) in the form

$$\theta_1 = \frac{12(1-\nu^2)}{Et^3}\left[K_1 F + K_2\ (M + Qt/2)\right] \tag{7}$$

where,

$$K_1 = (1/24)\ (4L^2 - 4b^2 - d_H^2)$$

$$K_2 = (1/24L)\ (12L^2 - 4b^2 - d_H^2)$$

41.2.2.4. Cylinder Deflection due to Q and M

With cylindrical shell theory it can readily be shown that the slope and deflection of the cylinder due to an axisymmetric moment M and shear Q is

$$u_3 = (2a^2\beta^2/Eh)M - (2a^2\beta/Eh)Q \tag{8}$$

$$\theta_3 = -(4a^2\beta^3/Eh)M + (2a^2\beta^2/Eh)Q \tag{9}$$

where

$$\beta^4 = 3(1-\nu^2)/a^2h^2 \tag{10}$$

41.2.2.5. Calculation of M and Q

To determine the value of M and Q we equate the cylinder and flange deformations at their junction. From Eqs. (3), (4) and (8) we have

$$(a/Eh)\ (pa-\nu F) + (2a^2\beta^2/Eh)M - (2a^2\beta/Eh)Q = K_A + K_BQ \qquad (11)$$

From Eqs. (7) and (9) we have

$$\frac{12(1-\nu^2)}{Et^3}\left[K_1F + K_2\ (M + Qt/2)\right] = -(4a^2\beta^3/Eh)M + (2a^2\beta^2/Eh)Q \qquad (12)$$

which reduces to

$$K_1F = -M(t^3/\beta h^3 + K_2) + Q\ (t^3/2\beta^2h^3 - tK_2/2) \qquad (13)$$

Similarly Eq. (11) reduces to

$$p-\nu F/a - EhK_A/a^2 = -M(2\beta^2) + Q\ (2\beta + EhK_B/a^2) \qquad (14)$$

Equations (13) and (14) are readily solved for M and Q when p, F and the geometric constants are specified.

41.2.3. Important Stresses

41.2.3.1. Flange Stresses

Average hoop stress in flange is

$$\sigma_H = (a/L)\ (Q/t + p) \tag{15}$$

To obtain the maximum radial bending stress at the bolt circle we divide the usual beam stress by (1-Nd) to take account of the material removed for the bolt holes. We add no factor for stress concentration due to the bolt holes though this could be significant for fatigue. The maximum radial bending stress in the flange is then

$$\sigma_r = \left(\frac{6}{t^2}\right)\left(F\ell + M + Q\,\frac{t}{2} - Bd_H/8\right)\left(\frac{1}{1-Nd}\right) \tag{16}$$

The average bearing stress at the outer edge of the flange is

$$\sigma_R = (B - F)/e \tag{17}$$

where e is the effective width of the bearing area.

41.2.3.2. Cylinder Stresses

The maximum axial stress in the cylinder at the junction of the flange and cylinder is

$$_c = F/h + 6M/h^2 \tag{18}$$

41.2.3.3. Bolt Stresses

The bolt stress is

$$\sigma_B = B/NA \tag{19}$$

where N = number of bolts per inch

A = root cross-sectional area of bolts

41.2.4. Examples

41.2.4a. We consider a flange with

t	= 0.875 in.	d	= .438 in.
h	= 0.125 in.	d_H	= .610 in.
a	= 10.06 in.	b	= .270 in.
$\bar{a}$	= 10.66 in.	ℓ	= .844 in.
N	= 0.583 in^{-1}	L	= 1.114 in.
A	= 0.150 in^2	ν	= 0.3
E	= 28,000,000 lb/in^2	e	= .14 in.

With F = 1,000 lb/in and p = 200 lb/in^2 what are the stresses?

First evaluating Eq. (13) we need

$$K_1 = (1/24)\ (4L^2-4b^2-d_H^2) = 0.1792\ in^2 \tag{20}$$

$$K_2 = (1/24L)\ (12L^2-4b^2-d_H^2) = 0.532\ in. \tag{21}$$

$$\beta = \sqrt[4]{3(1-\nu^2)/a^2h^2} = 1.147\ in^{-1}$$

Then Eq. (13) becomes

$$179.2 = -299.5M + 130.6Q \tag{22}$$

To evaluate Eq. (14) we need

$$K_A = pa\bar{a}/EL = .000686\ in \tag{23}$$

$$K_B = a\bar{a}/tEL = .00000392\ in^2/lb \tag{24}$$

Equation (14) then becomes,

$$146.5 = -2.63M + 2.43Q \tag{25}$$

Solving (22) and (25) simultaneously gives

$$M = 48.6\ lb\text{-}in/in,\ Q = 112.4\ lb/in \tag{26}$$

We now evaluate the flange hoop stress from Eq. (15)

$$\sigma_H = (a/L)\ (Q/t + p) = 2960\ lb/in^2 \tag{27}$$

The maximum radial bending stress in the flange from Eq. (16) is

$$\sigma_r = 6{,}200 \text{ lb/in}^2 \tag{28}$$

where $B = 4{,}580$ lb/in (29)

from Eq. (6).

The average bearing stress at the outer edge of the flange is given by Eq. (17)

$$\sigma_R = (B-F)/e = 25{,}600 \text{ lb/in}^2 \tag{30}$$

The maximum axial cylinder stress (bending plus tension) at the junction of flange and cylinder is obtained from Eq. (18)

$$\sigma_c = F/h + 6\,M/h^2 = 26{,}620 \text{ lb/in}^2 \tag{31}$$

and the bolt stress from Eq. (19) is

$$\sigma_B = B/NA = 52{,}300 \text{ lb/in}^2 \tag{32}$$

41.2.4b We consider a flange with the same total cross-sectional area as that in 41.2.4a except that $t = 0.500$ in., $L = 1.952$ in., $b = 1.108$ in. and $\bar{a} = 11.07$ in. In that case

$$K_1 = .416 \text{ in}^2, \quad K_2 = .862 \text{ in} \tag{33}$$

$$\beta = 1.147 \text{ in}^{-1} \tag{34}$$

Equation (13) becomes,

$$416 = -56.8\,M + 24.2\,Q \tag{35}$$

We find,

$$K_A = .000407 \text{ in}, \quad K_B = .00000407 \text{ in}^2/\text{lb} \tag{36}$$

and Eq. (14) becomes,

$$156.2 = -2.63\,M + 2.43\,Q \tag{37}$$

Solving (35 and (37) simultaneously

$$M = 37.3 \text{ lb-in/in}, \quad Q = 104.6 \text{ lb/in} \tag{38}$$

Evaluating the stresses now,

$$\sigma_H = 2090 \text{ lb/in}^2 \tag{39}$$

$$\sigma_r = 24,700 \text{ lb/in}^2 \tag{40}$$

$$B = 1,820 \text{ lb/in} \tag{41}$$

$$\sigma_R = 5,800 \text{ lb/in}^2 \tag{42}$$

$$\sigma_c = 22,300 \text{ lb/in}^2 \tag{43}$$

$$\sigma_B = 20,800 \text{ lb/in}^2 \tag{44}$$

The radial stress, cylinder stress and bolt stress are in better balance here than they were in the first example.

41.2.5. Discussion

Equations have been presented in this section for computing the stresses in bolted flanges which have a slight lip so that they bear against each other only near the inner and outer radii of the flange. Similar equations are derived for flanges which are in contact in other ways in Sections 41.3, 41.4, and 41.5.

The examples in this section show that changes in the flange dimensions have a marked effect on the proportions of the different stresses. In the examples considered, the flange stresses are relatively unaffected by the cylinder restraint, while the cylinder stresses correspond nearly to full restraint by the flange. Assuming this to be true could even simplify the analytical approach further. The use of a short hub between flange and cylinder could ease the high cylinder stresses there.

Since the cylinder has only a minor effect on the flange stresses it would be a good approximation to use the same analytical approach even where F is not axisymmetric. In such a case the largest value of F around the circumference would be used in the equations.

41.3 Flat Flanges

41.3.1. Introduction

Frequently flat flanges are used with a spacer between them (or a small recess in their surfaces) to provide room for a seal. A sketch of such a flange is shown in Fig. 41.3. As load is applied, the bolt stretches slightly and the flange takes the shape shown in Fig. 41.4. The seal is ordinarily so flexible in comparison with the flange that its load can be neglected. (Where necessary its load can be considered as contributing to the load F.) The seal prevents the fluid pressure from acting on most of the flange face. The distance b from the bolt to the point of flange contact will ordinarily increase with load F. The bolt load will also increase with F. Both of these phenomena will be examined here.

The flange will again be considered to be adequately represented by treating a radial strip between inner and outer edge as a beam in bending. The bolt load, however, will be considered concentrated at the bolt circle and not distributed over the bolt head in computing deformations. The flanges will be considered to have no local flattening where they bear against each other. Beyond the point of flange contact, beam theory requires the bending moment and shear in a radial direction to be zero because the beam deflection is zero.

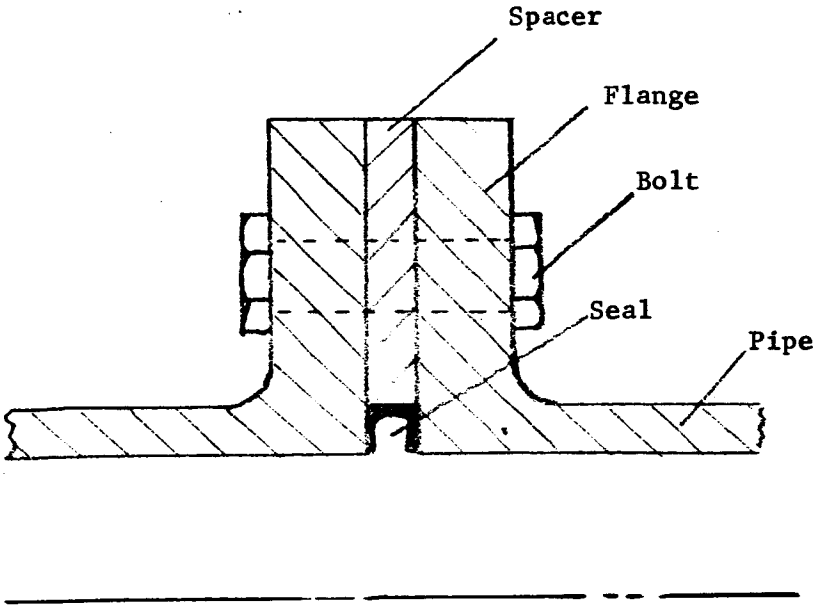

FIG. 41.3 Flanges with spacer

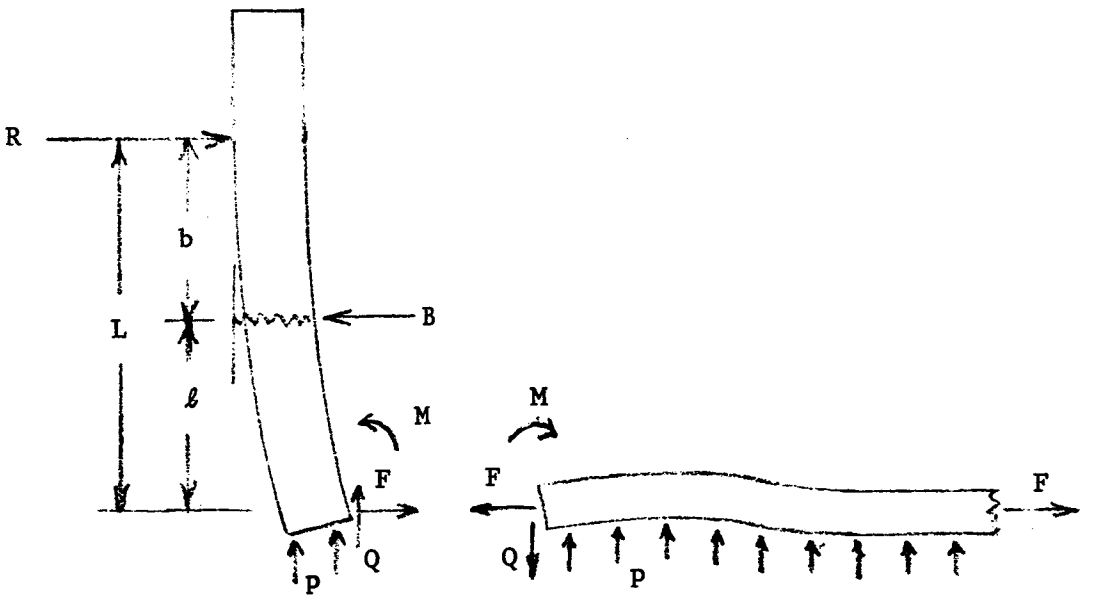

FIG. 41.4 Loads and dimensions

41.3.2. Analysis

The radial deflection of the flange due to hoop stress is adequately given by Eq. (3). The cylinder deflection due to pressure is given by Eq. (4). The cylinder deflection due to moment and shear is given by Eqs. (8) and (9). Equations are needed for the slope and axial displacement of the flange at the junction of flange and cylinder.

We find that the axial displacement of the flange is given by

$$y_1 = \left[\frac{F\ell^3}{3} \left(1 + \frac{b}{\ell}\right) \left(1 + \frac{b}{2\ell}\right) + \left(M + \frac{Qt}{2}\right) \left(\frac{\ell^2}{6} \right) \left(3 + 3\frac{b}{\ell} + \frac{b^2}{\ell^2} \right) \right] \frac{12(1-\nu^2)}{Et^3} \tag{45}$$

and the bolt load by

$$B = F\left(1 + \frac{\ell}{b}\right) + \left(M + \frac{Qt}{2}\right)(1/b) \tag{46}$$

Denoting the bolt stiffness by K (lb/in)/in of circumference and the initial bolt stretch by δ, we find for b

$$b^3 = \frac{Et^3}{2K(1-\nu^2)} \left[1 - \frac{(K\delta - F)\, b}{F\ell + (M+Qt/2)} \right] \tag{47}$$

where, K = NAE/t for a bolt completely through the flanges. A convenient nomogram for determining a solution of Eq. (47) is given in Fig. 41.5. In the example given in the figure, it is seen that a straight line joining the value of $Et^3/\left[2K\ell^3(1-\nu^2)\right]$ to the value of $\left[F + (M+Qt/2)\ell\right]/(K\delta - F)$ intercepts the b/ℓ curve at the correct value of b/ℓ. It is of interest to note that even for moderate values of F the value of b/ℓ is likely to exceed several tenths.

The slope of the flange at its junction with the cylinder is given by

$$\theta_4 = \frac{6(1-\nu^2)}{Et^3} \left[F\ell^2 (1+b/\ell) + (M+Qt/2)\ell(2+b/\ell) \right] \tag{48}$$

Using Eqs. (8) and (9) we can show that in the cylinder

$$M = -(Eh/2a^2\beta^2)(u_1 - u_2) - (Eh/2a^2\beta^3)\theta_4 \tag{49}$$

$$Q = -(Eh/a^2\beta)(u_1 - u_2) - (Eh/2a^2\beta^2)\theta_4 \tag{50}$$

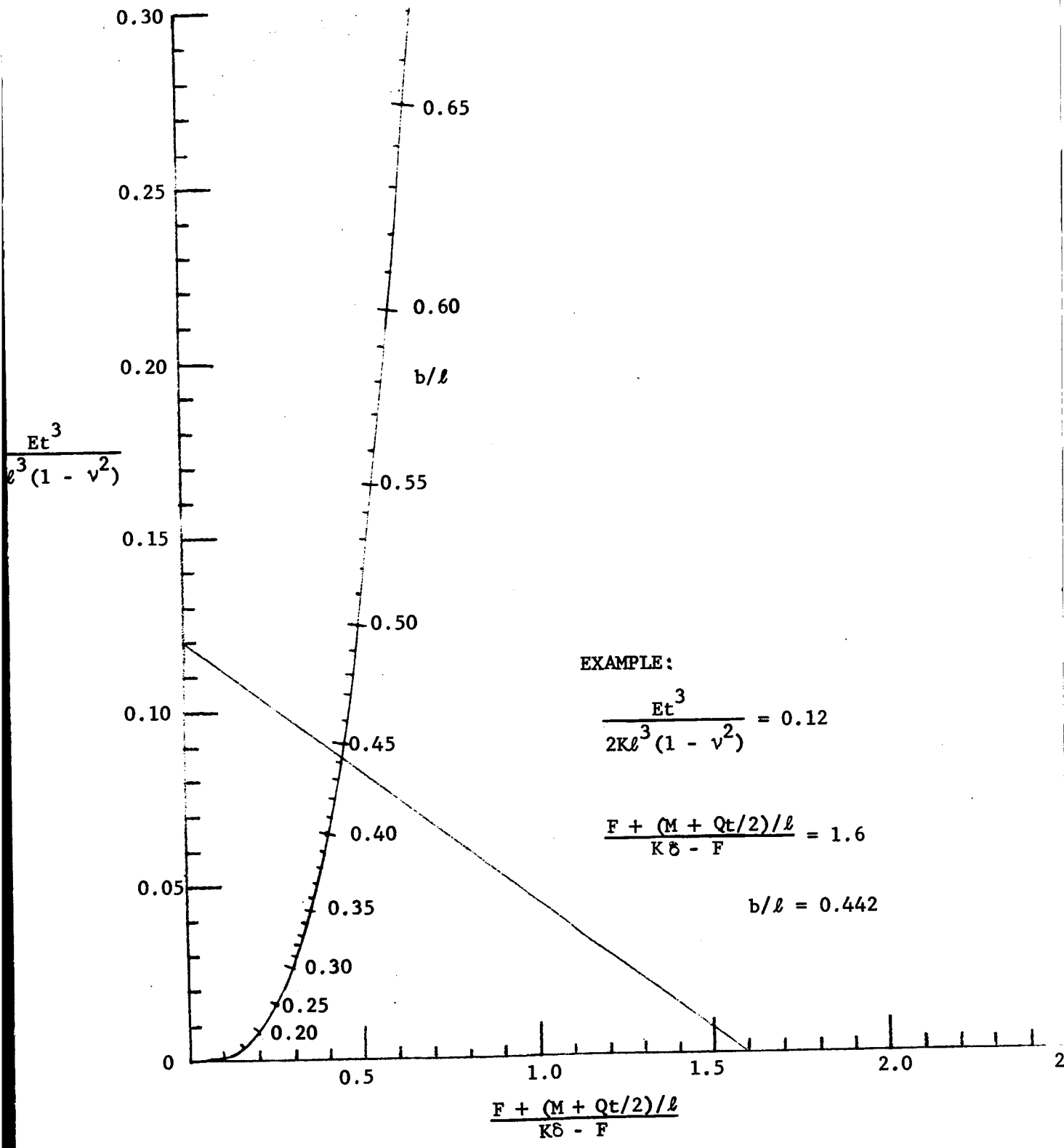

FIG. 41.5 Determination of b.

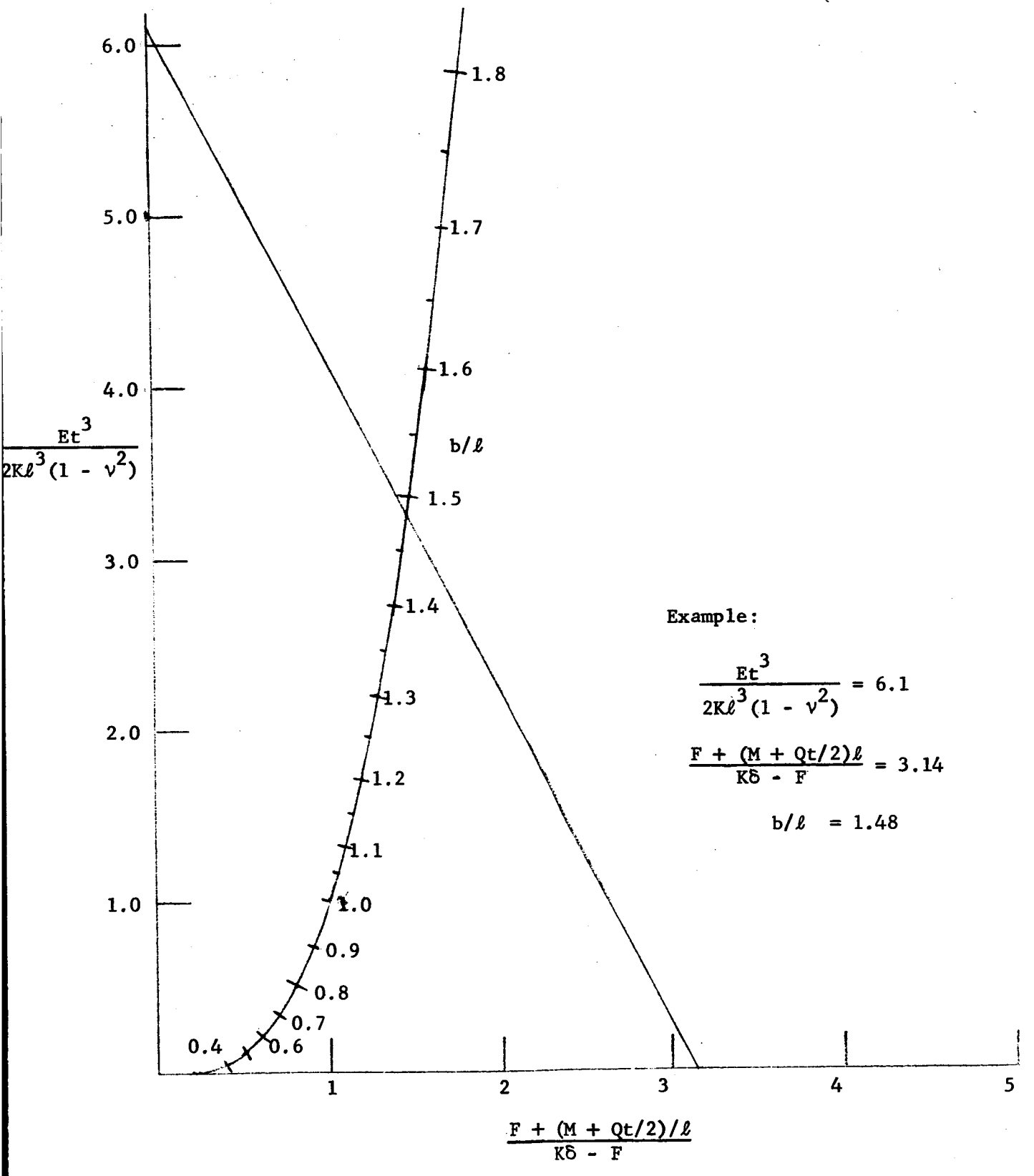

FIG. 41.5 (continued) - Determination of b.

To obtain a solution of the preceding equations we proceed as follows. First we approximate θ_4 as zero and u_1 as K_A from Eq. (3). Then using Eq. (4) to obtain u_2 we obtain approximate values of M and Q from Eqs. (49) and (50). Using these values of M and Q and the known values of F and δ, Eq. (47) or Fig.41.5 gives b and Eqs. (3) and (48) give improved values of u_1 and θ_4. The cycle can be repeated if necessary, however, convergence is very rapid.

In some instances we may find that the value of b exceeds the maximum possible value b_{max} due to flange height limitations. In that event there is initial slope θ_5 at the contact point between flanges and we use in place of Eq. (47) the equation

$$\left(\frac{b_{max}}{\ell}\right)^3 = \frac{Et^3}{2K\ell^3(1-\nu^2)} \left[1 - \frac{\left[K(\delta + \theta_5 b_{max}) - F\right] b_{max}/\ell}{F + (M + Qt/2)/\ell}\right] \qquad (51)$$

With a known value of (b_{max}/ℓ) Eq. (51) can be solved for θ_5, the slope at the reaction R(solution can also be done by use of Fig.41,5). In using Fig. 41.5 for this purpose we lay a straight edge on the value of (b_{max}/ℓ) on the (b/ℓ) scale and the value of $Et^3/\left[2K\ell^3(1-\nu^2)\right]$ on its own scale and read off the value of $\left[F + (M + Qt/2)/\ell\right] / \left[K(\delta + \theta_5 b_{max}) - F\right]$ on the $\left[F + (M + Qt/2)/\ell\right] / \left[K\delta - F\right]$ scale.

The slope of the flange at its junction with the cylinder is then given by

$$\theta_6 = \theta_4 + \theta_5 \qquad (52)$$

where θ_4 is obtained from Eq. (48) using b_{max} for b.

The axial displacement of the flange at its junction with the cylinder is given by

$$y_2 = y_1 + \theta_5 (b_{max} + \ell) \qquad (53)$$

where y_1 is obtained from Eq. (45) using b_{max} for b.

41.3.3 Important Stresses

Stresses in this case can be obtained from Eqs. (15) to (19). Equation (16) for the radial stress in the flange takes account of the bolt head diameter even though this was not included in Eqs. (45) and (48) for flange deformation. (In deriving Eqs, (45) and (48) it was felt that assuming the bolt load concentrated at the bolt circle was in part compensated for by neglecting the effect of the bolt holes on flexural stiffness.)

43

41.3.4 Examples

41.3.4a. We consider a flange with

t	= 0.875 in.	d	= 0.438 in
h	= 0.125 in.	d_H	= 0.610 in.
a	= 10.06 in.	ℓ	= 0.844 in.
$\bar{a}$	= 10.66 in.	b_{max}	= 0.336 in (edge of flange minus e/2)
N	= 0.583 in^{-1}	ν	= 0.3
A	= 0.150 in^2	e	= 0.14 in.
E	= 28,000,000	F	= 1000 lb/in
L	= 1.114 in. (flange height in Eq. 3)	p	= 200 lb/in^2
		δ	= 0.00163 in.

This is the same flange as we considered in 41.2.4a excepting for the absence of lips. Eqs. (23) and (24) still apply for K_A and K_B. The bolt stiffness

$$K = NAE/t = 2{,}800{,}000 \text{ lb/in}^2 \tag{54}$$

We determine

$$\frac{Et^3}{2K\ell^3(1-\nu^2)} = 6.1 \tag{55}$$

From Eq. (4)

$$u_2 = \left(\frac{a}{Eh}\right)(pa-\nu F) = 0.00491 \text{ in.} \tag{56}$$

As a first approximation we take

$$u_1(\text{approx 1}) = K_A = pa\bar{a}/EL = .000686 \text{ in.} \tag{57}$$

and

$$\theta_4(\text{approx 1}) = 0 \tag{58}$$

Using (53) to (55) in Eqs. (49) and (50) gives

$$M(\text{approx 1}) = -(Eh/2a^2\beta^2)(u_1-u_2) = 55.7(\text{lb-in})/\text{in} \tag{59}$$

and

$$Q(\text{approx 1}) = -(Eh/a^2\beta)(u_1-u_2) = 127.8 \text{ lb/in} \tag{60}$$

We form

$$\frac{F + (M+Qt/2)/\ell}{K\delta - F} \quad (\text{approx } 1) = 0.319 \tag{61}$$

The values in Eqs. (52) and (58) are beyond the range of the first chart in Fig. 41.5 but within the range of the second chart. They give $b/\ell = 0.317$.

$$b(\text{approx } 1) = \ell(b/\ell) = 0.267 \text{ in} \tag{62}$$

Since this value is less than b (max) we may proceed. Using Eq. (3) we get

$$u_1(\text{approx } 2) = K_A + K_B Q(\text{approx } 1) = 0.00119 \text{ in.} \tag{63}$$

From Eq. (48) we get with (62), (59) and (60)

$$\theta_4(\text{approx } 2) = .000325 \text{ radians} \tag{64}$$

Then Eqs. (49) and (50) give

$$M(\text{approx } 2) = -\left(\frac{Eh}{2a^2\beta^2}\right)\left(u_1(\text{approx } 2) - u_2\right) - \left(\frac{Eh}{2a^2\beta^3}\right)\theta_4(\text{approx } 2)$$

$$= 45.4 \text{ (lb-in)/in} \tag{65}$$

$$Q(\text{approx } 2) = -\left(\frac{Eh}{a^2\beta}\right)\left(u_1(\text{approx } 2) - u_2\right) - \left(\frac{Eh}{2a^2\beta^2}\right)\theta_4(\text{approx } 2)$$

$$= 108.5 \text{ lb/in} \tag{66}$$

The changes in M and Q from approximation 1 to approximation 2 are small enough to proceed with the value of b in Eq. (62).

We compute the axial displacement at the flange-cylinder junction from Eq. (45)

$$y_1 = 0.000205 \text{ in.} \tag{67}$$

and from Eq. (46)

$$B = 4510 \text{ lbs.} \tag{68}$$

The stresses are nearly the same as those in 41.2.4a since b, Eq. (62), has nearly the value that was used there.

41.3.4b This flange is the same as 1.2.4b except without lips. It differs from that in Example 1.3.4a only in having t = 0.500 in, L = 1.952 in, b_{max} = 1.174 in, $\bar{a}$ = 11.07 and δ = 0.00037 in.

We find,

$$K = NAE/t = 4{,}900{,}000 \text{ lb/in}^2 \tag{69}$$

$$\frac{Et^3}{2K\ell^3(1-\nu^2)} = 0.633 \tag{70}$$

$$u_2 = 0.00491 \text{ in.} \tag{71}$$

$$u_1(\text{approx 1}) = K_A = pa\bar{a}/EL = 0.000406 \text{ in.} \tag{72}$$

$$\theta_4(\text{approx 1}) = 0 \tag{73}$$

$$M(\text{approx 1}) = -(Eh/2a^2\beta^2)\ (u_1-u_2) = 59 \text{ (lb-in)/in} \tag{74}$$

$$Q(\text{approx 1}) = -(Eh/a^2\beta)\ (u_1-u_2) = 136 \text{ lb/in} \tag{75}$$

$$\frac{F + (M + Qt/2)/\ell}{K\delta - F}(\text{approx 1}) = 1.37 \tag{76}$$

From Fig. 41.5 and Eq. (47) we get

$$(b/\ell)\ (\text{approx 1}) = 0.683,$$

$$b\ (\text{approx 1}) = 0.576 \text{ in.} \tag{77}$$

This is less than b_{max} so we proceed. Using Eq. (3) we get

$$u_1(\text{approx 2}) = K_A + K_B\ Q(\text{approx 1}) = 0.000957 \tag{78}$$

From Eq. (48) we get

$$\theta_4(\text{approx 2}) = 0.00220 \text{ radians} \tag{79}$$

Eqs. (49) and (50) give

$$M(\text{approx } 2) = 26.8 \text{ (lb-in)/in} \tag{80}$$

$$Q(\text{approx } 2) = 90.5 \text{ lb/in} \tag{81}$$

The changes in M and Q in going from the first to second approximation are substantial, however, not enough to indicate a need for a third approximation in so far as the value of b and the major stresses are concerned. We therefore proceed with the computation of axial displacement at the flange-cylinder junction from Eq. (45)

$$y_1 = 0.00151 \text{ in.} \tag{82}$$

and from Eq. (46)

$$B = 2550 \text{ lbs.} \tag{83}$$

The stresses will be nearly the same as those obtained in Example 41.2.4b except for the bolt stress.

$$\sigma_B = B/NA = 29{,}100 \text{ lb/in}^2 \tag{84}$$

41.4 Dished Flanges

A dished flange is essentially the same as the flange with lips discussed in Section 41.2, excepting that the lip is quite shallow. From a design point of view it is desirable to have an equation for the necessary flange clearance under the bolts. This equation is obtained with the same assumptions used in deriving Eq. (45).

$$y_b = \frac{-2(1-\nu^2)}{Et^3}\left[2b\ell^2 F + (M+Qt/2)b\ell\left(\frac{3\ell + 2b}{\ell + b}\right)\right] \tag{85}$$

For most flanges this will be a small deflection.

Example 41.4a. Consider the flange in Example 41.2.4b and determine the necessary clearance to provide for springing under the bolt. The values of that example when substituted into Eq. (85) give

$$y_b = 0.00090 \text{ in.} \tag{86}$$

41.5 Warped Flanges

In some cases a flange may be somewhat warped out of a plane at the junction of flange and cylinder. In that case additional local bolt force will be required to bring mating flanges together. We can determine the relation between cylinder tension F and displacement for a warped-end cylinder from Sec. 46 when the warping can be adequately described by considering it to vary as cos 2θ around the circumference. In that reference it is shown that in order to correct a warping of amplitude

$$w = w_{max} \cos 2\theta \tag{87}$$

an additional force

$$F_{variable} = F_{v.max} \cos 2\theta \tag{88}$$

is required, where,

$$F_{v.max} = E\, w_{max} \Big/ \left[0.681\sqrt{a/h}(1 + 0.670\ a/h)\right] \tag{89}$$

Example 41.5a. Determine the additional force $F_{v.max}$ to flatten a warping of 0.01 inch = w_{max} in the cylinder of Example 41.2.4a.

$$F_{v.max} = 840 \text{ lb/in} \tag{90}$$

It is seen that this additional force is comparable to the uniform force of 1000 lb/in in Example 41.2.4a and therefore results in proportionate increases in stress.

41.6 References

1. ASME, Pressure Vessel and Piping Design Collected Papers 1927-1959.

2. E. O. Waters, D. B. Wesstrom, D.B. Rossheim and F.S.G. Williams, "Formulas for Stresses in Bolted Flanged Connections" Trans. ASME, vol. 59, Paper No. FSP-59-4. (Also published in more extended form by the Taylor Forge and Pipe Works, "Development of General Formulas for Bolted Flanges.")

3. H. J. Macke, Private Communication.

42. FLANGE JOINTS WITHOUT CONTACT OUTSIDE THE BOLT CIRCLE

by

S. Levy

42.0 Summary

The more frequently used basic equations applicable to the design of flanged joints without contact outside the bolt circle are assembled here. For a more extensive treatment the reader is referred to Refs. 1, 7, 9, 10, and 13 of Section 40.

Equations are also presented for axisymmetric pipe deformation. For thin-wall pipes these agree with those usually found in books on shell theory. For thick-wall pipes, however, they include the increased flexibility resulting from shear deformation of the pipe wall. This increase is minor for most pipes of interest in missile piping systems.

Flanges designed by this procedure may be compared with flanges designed by the procedure of Section 41 to determine which design is preferable for a particular application.

42.1 Introduction

Flanged joints have been extensively considered in the literature as described in Section 40. The treatment can be considered as involving:

(1) the determination of the deformation of the flange, treated as a ring

(2) the determination of the deformation of the pipe

(3) the interaction between pipe and flange

We will present here the equations which are applicable when the flange is considered sturdy enough to be free of cross-sectional distortion. For the pipe we will present equations for the thin-wall case and for the case where the wall is so thick that shear deformation in the wall must be considered. An example of the use of these equations is given in Section 44.4 and in Section 13.3.5.

The question of whether to use a flange which contacts outside the bolt circle, as described in Section 41, or to use a flange which does not, as described here, must be answered on the basis of overall design considerations. It seems likely that a weight saving can be achieved by using flanges which contact outside the bolt circle whenever the pipe is of relatively large diameter. Use of such flanges, however, affects the choice of gasket, the outer flange diameter, machining costs, and perhaps other factors such as assembly procedures. The final choice must therefore be made after all factors have been given full consideration.

42.2 Twisting of Flange by Couples Uniformly Distributed Along Its Centerline

For the flange we will follow closely the theory presented by Timoshenko on pages 177 to 180 of Ref. 1. We consider here a flange which is sturdy enough to be free of cross-sectional distortion. The flange may include the hub in those cases where the hub length is less than about half $\sqrt{a_{av}h_{av}}$ where a_{av} is the average hub radius and h_{av} is its average thickness.

The behavior of the flange ring is illustrated by Fig. 42.1. Taking half the ring (upper figure) as a free body, from the condition of equilibrium of moments about the diameter ox, there must be a bending moment on each cross-section m and n of

$$M_T = M_t \bar{a} \tag{1}$$

where $\bar{a}$ is the radius to the center of gravity of the cross-section and M_t is the twisting couple per unit length of the center of gravity circle due to bolt force, internal pressure, gasket force, and pipe forces. The pipe forces include a moment and a shear as well as axial tension due to hydrostatic pressure or other axial forces on the pipe.

We consider now the deformation of the ring. From the condition of symmetry, each cross-section rotates in its own plane through the same angle θ. Let C (lower figure in Fig. 42.1) be the center of rotation (center of gravity) of the cross-section and B a point in the cross-section at a distance ρ from C. As the cross-section rotates, the point B describes a small arc $\overline{BB_1} = \rho\theta$. Due to this displacement the annular fiber of the ring, which is perpendicular to the cross-section at the point B, increases its radius by $\overline{B_2B_1}$. If the coordinate axes are taken as indicated, we have from the similarity of triangles BB_1B_2 and BDC

$$\overline{B_1B_2} = \overline{BB_1}\frac{\overline{DB}}{\overline{BC}} = \rho\theta\,\frac{y}{\rho} = \theta y \tag{2}$$

Let us consider first the case in which the cross-sectional dimensions of the ring are small in comparison with the radius $\bar{a}$ to the center of gravity of the cross section. Then the radii of all ring fibers may be taken equal to $\bar{a}$ without great error and the unit elongation of the fiber B, due to the displacement given by Eq. 2, is

$$\epsilon = \theta y/\bar{a} \tag{3}$$

The corresponding stress is

$$\sigma = E\theta y/\bar{a} \tag{4}$$

Now from the equilibrium of the half ring, the moment of all the normal forces acting on the cross-section of the ring about the x-axis must be equal to M_T (see Eq. 1). If dA denotes an elemental area of the cross-section, the equation of equilibrium becomes

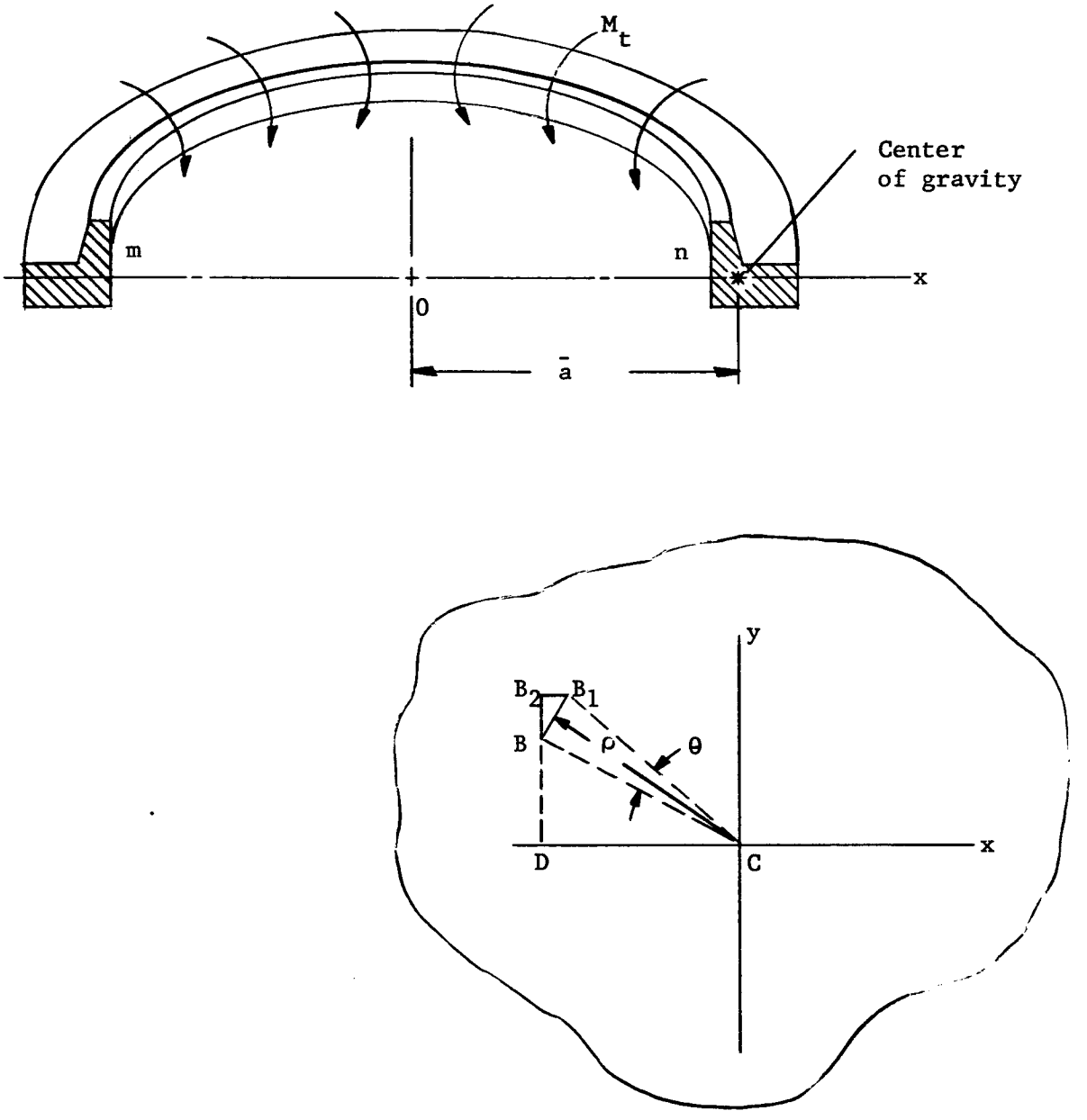

FIG. 42.1 - Flange ring showing moments and rotation

$$M_T = \int_A \sigma y dA = \int_A (E\theta y^2/\bar{a}) dA = \frac{E\theta I_x}{\bar{a}} \tag{5}$$

where the integration is extended over the cross-sectional area A and I_x is the moment of inertia of the cross-section of the ring with respect to the x-axis. Combining Eqs. (5) and (1)

$$\theta = (M_T\bar{a}/EI_x) = (M_t\bar{a}^2/EI_x) \tag{6}$$

Substituting Eq. (6) into Eq. (4)

$$\sigma = M_t\bar{a}y/I_x \tag{7}$$

The distribution of the normal stresses over the cross-section of the ring is the same as in the case of bending of straight bars; the stress is proportional to the distance from the neutral axis x and the maximum stress occurs at the points most remote from this axis.

Considering a flange ring of rectangular cross-section (Fig. 42.2) whose width b is not small in comparison with the radius a of the centroid of the cross-section and assuming that the deformation consists of rotations of the cross-section without cross-sectional distortion, let θ be the angle through which the cross-section rotates. The elongation of a fiber at radius r and the corresponding stress are

$$\epsilon = \theta y/r; \quad \sigma = E\theta y/r \tag{8}$$

The equation of equilibrium analogous to Eq. (5) is

$$\int_{-t/2}^{t/2} dy \int_c^d (E\theta y^2/r) dr = M_T \tag{9}$$

Integrating gives

$$M_T = (E\theta t^3/12)\log_e(d/c) \tag{10}$$

from which

$$\theta = \frac{12M_T}{Et^3\log_e(d/c)} = \frac{12\bar{a}M_t}{Et^3\log_e(d/c)} \tag{11}$$

With Eq. 8,

$$\sigma = \frac{12M_T y}{rt^3\log_e(d/c)} \tag{12}$$

The maximum stress is at the inner corner of the flange where r=c and y=t/2

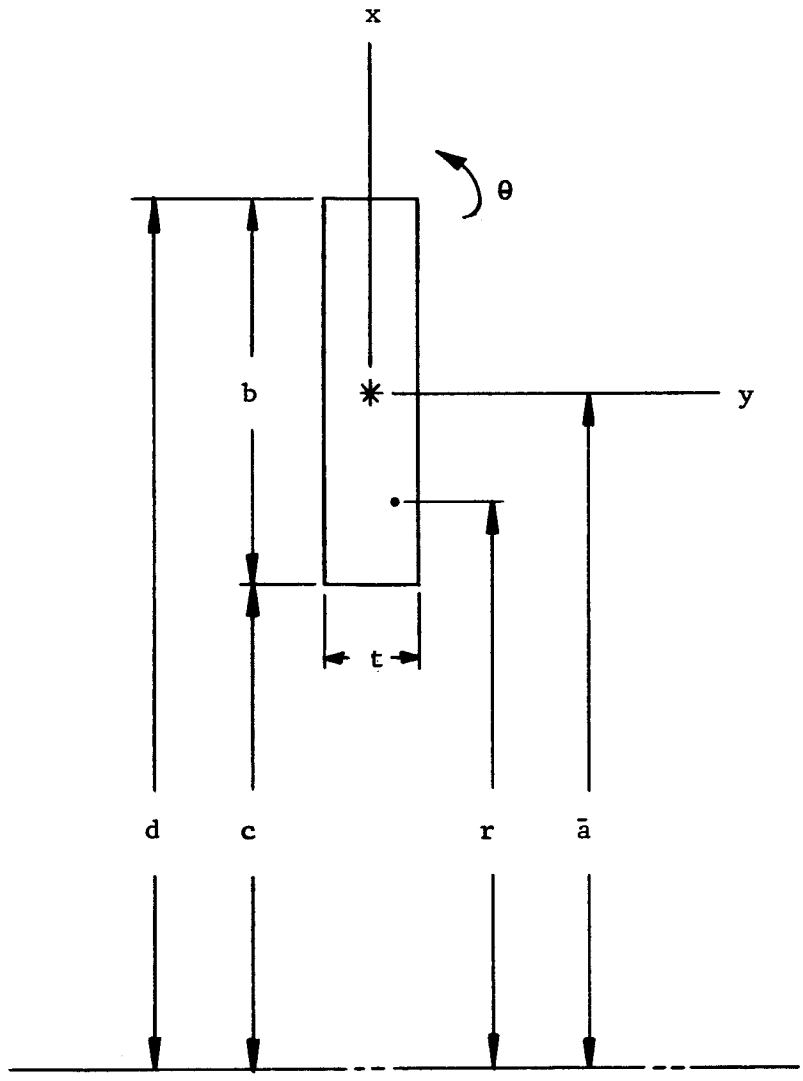

FIG. 42.2 - Flange ring of rectangular cross-section

$$\sigma_{max} = \frac{6M_T}{ct^2 \log_e(d/c)} = \frac{6aM_t}{ct^2 \log_e(d/c)} \qquad (13)$$

If b/c is small, Eqs. (11) and (12) reduce to Eqs. (6) and (7).

The radial displacement of the flange at its point of attachment to the pipe results from the combined action of internal pressure, shear from the pipe, and rotation of the cross-section. Referring to Fig. 42.3, the radial outward deflection of the flange is given by

$$u_1 = (\bar{a}cp\ell_f/EA_f) + (a\bar{a}Q/EA_f) + \theta\ell_{fp} \qquad (14)$$

where A_f is the area of the flange cross-section and p is the internal pressure.

57

42.3 Deformation of Pipe

With cylindrical shell theory it can readily be shown that the slope and deflection of the wall at the end of a long pipe due to pressure and an axisymmetric moment M, shear Q and tension F per inch at the mid-thickness (Fig. 42.3) is

$$u_3 = (2a^2\beta^2/Eh)M - (2a^2\beta/Eh)Q + (a/Eh)(pa-\nu F) \qquad (15)$$

$$\theta_3 = -(4a^2\beta^3/Eh)M + 2(a^2\beta^2/Eh)Q \qquad (16)$$

where

$$\beta^4 = 3(1-\nu^2)/a^2h^2 \qquad (17)$$

In the case of a thick-walled pipe the deflections given by Eqs. (15) and (16) are somewhat less than the actual deflections (Ref. 2). The corrected equations are

$$u_3 = (2a^2\beta^2/Eh)M - \sqrt{1.0 + .59\ h/a}\ \ (2a^2\beta/Eh)\ Q + (a/Eh)(pa-\nu F) \qquad (18)$$

$$\theta_3 = -\sqrt{1 + .59\ h/a}\ (4a^2\beta^3/Eh)\ M + (2a^2\beta^2/Eh)\ Q \qquad (19)$$

for Poisson's ratio $\nu = 0.3$. It is seen that as h/a approaches zero the equations reduce to Eqs. (15) and (16). The ratio h/a is approximately equal to the ratio of internal pressure p to material allowable stress σ_a. For a pressure p of 5,000 psi and an allowable stress σ_a = 50,000 psi, h/a is approximately 0.1. In this case the correction term, $\sqrt{1+.59h/a} = 1.03$, has a negligible effect.

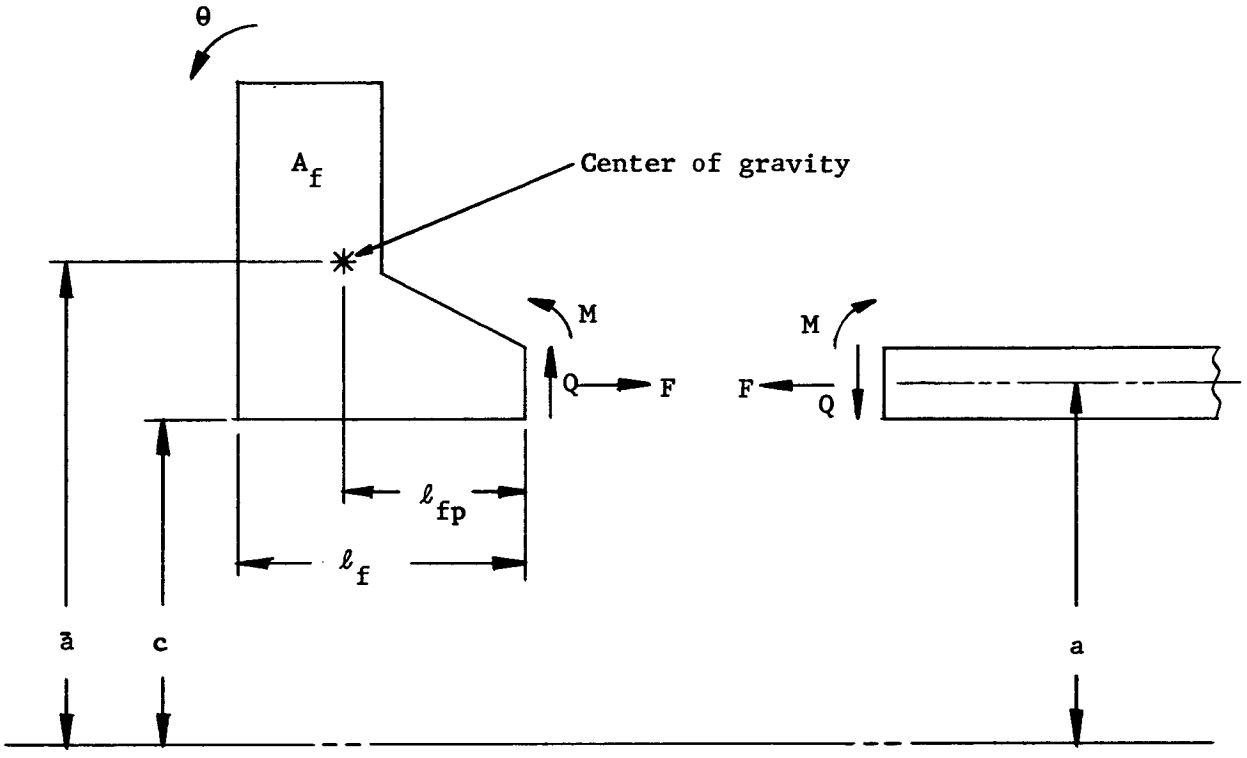

FIG. 42.3 - Flange cross-sectional dimensions and loads related to interaction with pipe

42.4 Interaction of Flange and Pipe

The forces and moment arms for determining the twisting couple, M_t, per unit length of the center of gravity circle are shown in Fig. 42.4. From this diagram

$$M_t = M\left(\frac{a}{\bar{a}}\right) + Q\ell_{fp}\left(\frac{a}{\bar{a}}\right) + p\left(\frac{c}{\bar{a}}\right)\ell_f(\ell_{fp}-\ell_f/2) + B\left(\frac{\bar{a}+f}{\bar{a}}\right)f + G\left(\frac{\bar{a}-g}{\bar{a}}\right)g + F\left(\frac{a}{\bar{a}}\right)(\bar{a}-a)$$

$$+ pe\left(\frac{c+e/2}{\bar{a}}\right)(\bar{a}-c-e/2) \qquad (20)$$

In this diagram

B is the bolt load per unit length at the bolt circle
G is the gasket force per unit length at the gasket circle
and e is the distance over which direct pressure can act on the flange below the gasket

Using Eqs. (20), (11) and (14) gives the flange displacement, u_1, and the flange rotation, θ, at the junction of pipe and flange as a function of M and Q. Likewise using Eqs. (15) and (16), or (18) and (19) if applicable, gives the pipe wall displacement u_3 and pipe wall rotation θ_3 as a function of M and Q. Equating

$$u_1 = u_3 \qquad (21)$$

and $$\theta = \theta_3 \qquad (22)$$

gives the two equations from which M and Q are determined. Having these and the given loads permits the determination of all deformations and stresses.

60

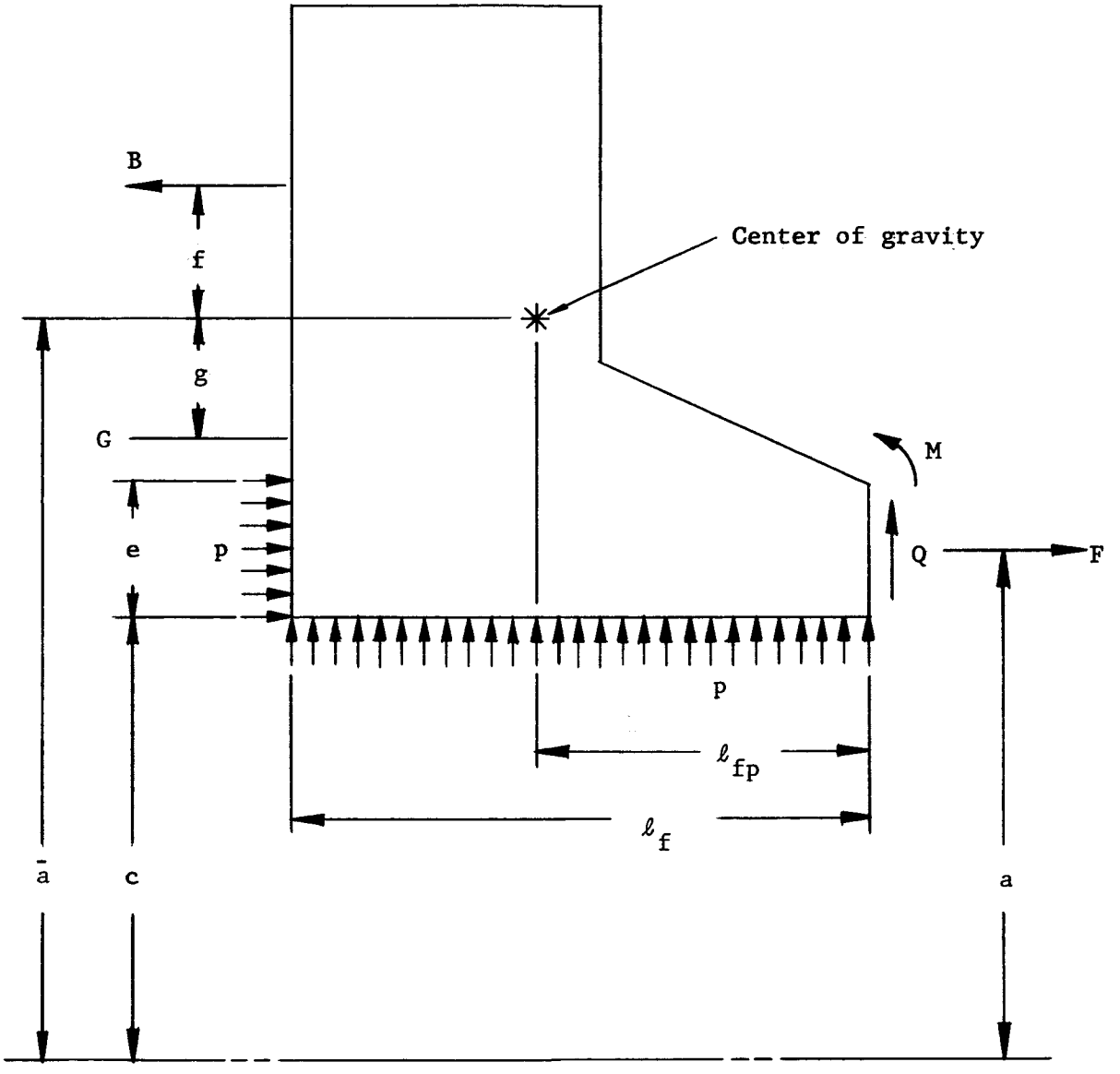

FIG. 42.4 - Forces and moment arms for determining flange moment M_t

42.5 Discussion

Equations have been presented for determining the behavior of the flange and pipe and their interaction. These equations permit the design of flanges which are not in contact beyond the bolt circle when the required gasket load, internal pressure, and pipe load are specified.

62

42.6 References

1. S. Timoshenko, Strength of Materials - Part II - Advanced Theory and Problems. Second Edition, Aug. 1941, D. Van Nostrand Co. Inc., New York.

2. S. Levy, "Shear and Bending of the Walls of Short Cylindrical Shells" (To Be Published)

63

43. BOLT SPACING

by

J. Wallach

43.0 Summary

The optimum design is to have a uniform contact pressure between bolts. This condition is approximated by making the contact pressure half way between two bolts equal to the maximum contact pressure which occurs at the bolt hole edge. Using the curves in Figures 43.1, 43.2, and 43.3 and applying the above rule a bolt spacing of 1.6 to 2.7 times the bolt hole diameter is obtained. These numbers are in the same range as those stated in Section 40.4. This criterion suggests a bolt spacing smaller than that permitted by wrench clearance in nearly all the cases considered. It would appear optimum, therefore, to place bolts as closely together as wrench clearance permits insofar as uniformity of clamping is concerned.

43.1 Introduction

Any analysis of, or design procedure for, bolted flanges has concerned itself with bolt spacing. However, very little analytical or experimental work on the subject is available in the literature. Most articles on flange design offer "rules of thumb" for bolt spacing. These usually call for a close bolt spacing allowing sufficient space for wrenching the bolts.

C.R. Soderberg analyzed the effect of the distance between bolts on the flange-to-flange contact pressure, Ref. 1. The model he chose was a point load on an infinitely long beam on an elastic foundation. The analysis in this section goes a step further and considers a uniformly distributed load on an infinite circular plate with a hole in the center and on an elastic foundation. The flat plate

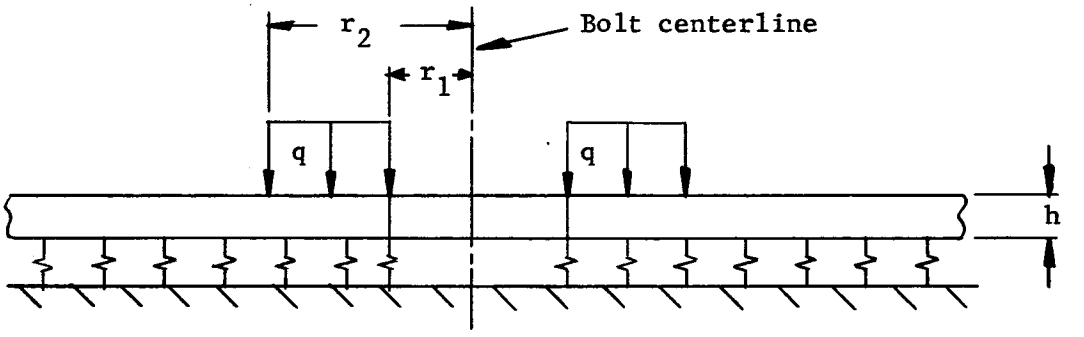

is assumed thin, the elastic foundation approximates the compressibility of the flat plate and the flange interface remains flat. r_1 and r_2 are the inside and outside radii of the contact area between the bolt and flange. The loading and geometry are symmetric about the bolt centerline.

This approach includes many simplifying assumptions. By assuming an infinite plate, the pipe structure and loads, and the finiteness of the outside flange diameter are neglected. Also not included are: flexibility of the bolt head; deformations of the flange due to shear in the vicinity of the bolt; and the fact that the flanges are not ordinarily in contact under the bolts because of the presence of gaskets. Nevertheless it seems reasonable that a good bolt spacing for the simplified problem considered in this section may also be good for other cases.

The usual flanged joint analysis considers only axisymmetric geometry and loading. No consideration is given to the finiteness of the bolt spacing. From the flanged joint analysis it is possible to calculate the bolt load per inch of circumference and the load per bolt. Also the amount of flange separation may be determined. Then using these results with the analysis contained in this section it may be possible to determine the variation in flange separation between bolts.

43.2 Discussion

The flange-to-flange contact pressure is given by equations (9) and (10) in terms of arbitrary constants which are obtained from equations (11). The contact pressure is a function of the load intensity (q), inside and outside radii of the loaded area (r_1 and r_2), plate thickness (h) and Poisson's ratio (ν). The metals of interest have a Poisson's ratio of about .3. Therefore, this parameter may be considered constant. Also, from the equations it is obvious that the contact pressure varies directly as the load intensity. However, the effect of changes in r_1, r_2 or h on p are not so obvious. Therefore, a set of calculations of p versus the radial distance from the bolt centerline (r) were made. A one-pound bolt load is used throughout, but r_1, r_2 and h are varied.

The results of the calculations are presented as three sets of curves. Fig. 43.1 shows that increasing the inside bolt radius, r_1, and head radius, r_2, simultaneously increases the area of contact between the bolt and flange and results in a lower contact pressure under the bolt. However, the increase in radius increases the area of contact pressure (between the flange faces) only slightly. As a result the contact pressure at a particular radius increases as the inside radius is increased. In contrast increasing the head radius, r_2, while holding the bolt radius, r_1 constant, Fig. 43.2, shows a decrease in the contact pressure close to the bolt and an increase at larger radial distances. The effect is a wider distribution of the contact pressure as the outside radius, r_2, is increased. A similar, but more pronounced, effect is obtained by increasing the flange thickness, h, Fig. 43.3. The results of the three sets of curves may be summarized by stating that by designing for the required inside radius, r_1, a large outside radius, r_2, and thick flange, h, the maximum distance between bolts may be obtained.

FIGURE 43.1 Flange Interface Pressure as a function of Radial Distance from the Bolt Centerline for a One-Pound Bolt Load. Difference between outside and inside radius of bolt-to-flange contact area and flange thickness are held constant while inside radius is varied.

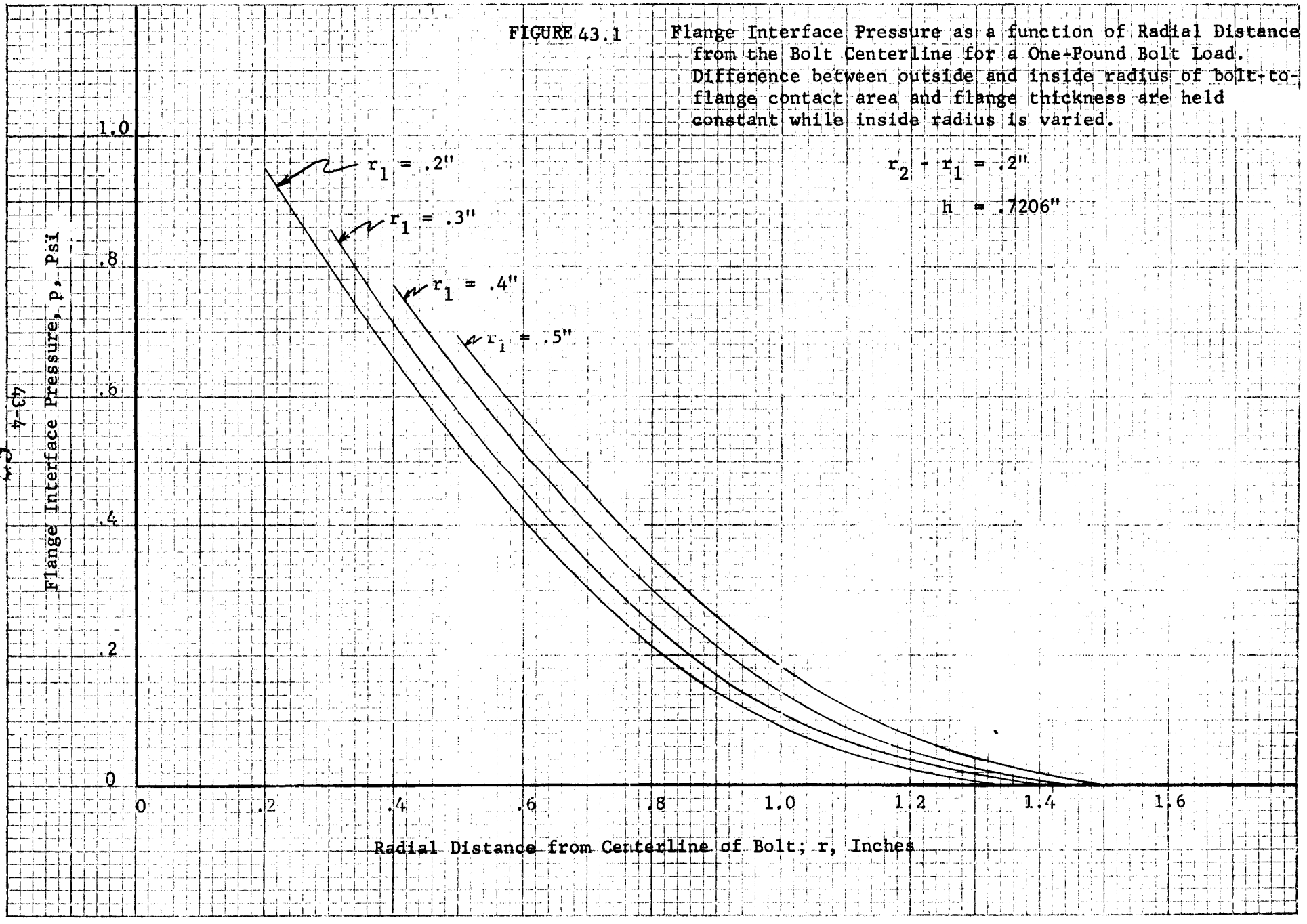

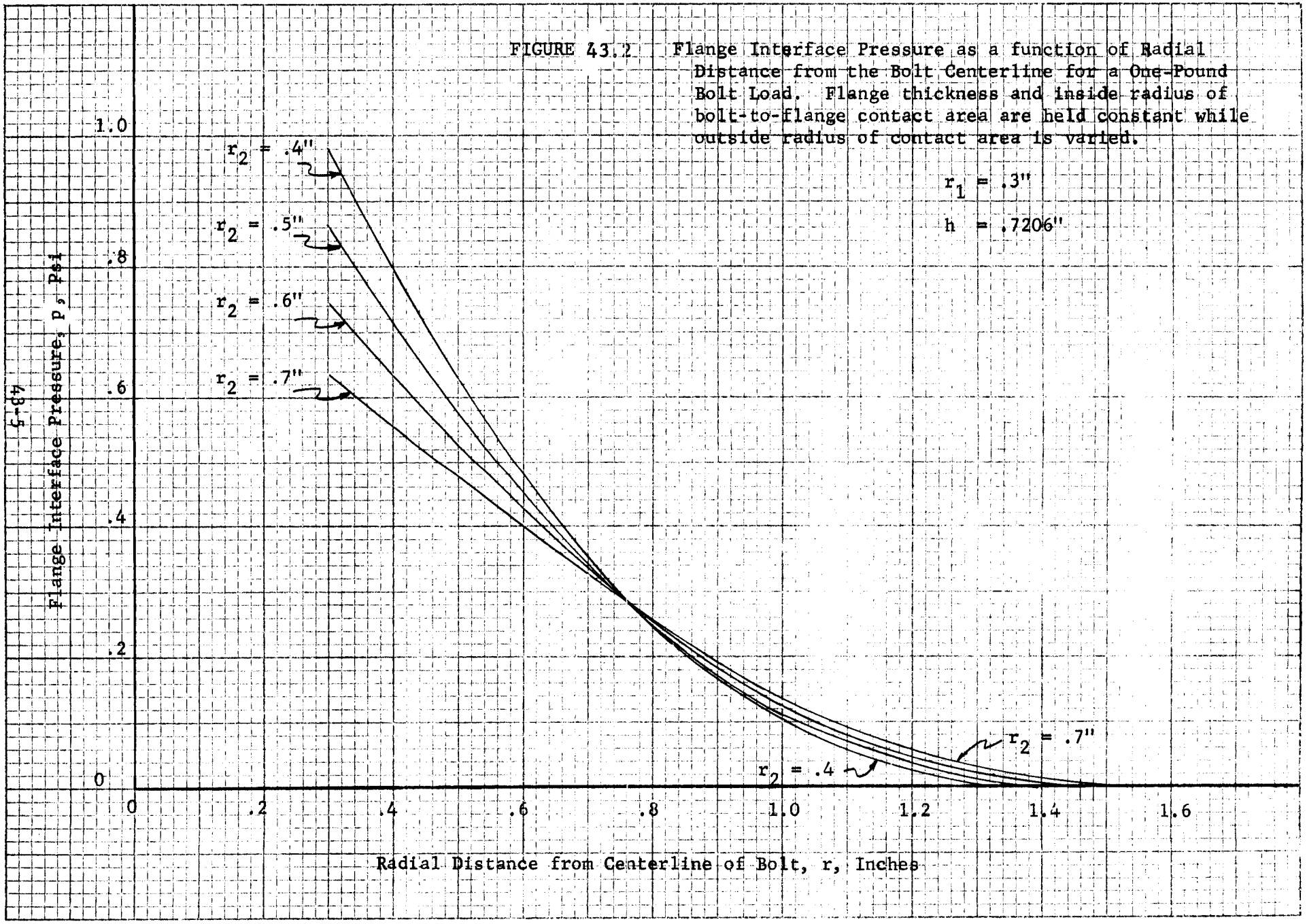

FIGURE 43.2 Flange Interface Pressure as a function of Radial Distance from the Bolt Centerline for a One-Pound Bolt Load. Flange thickness and inside radius of bolt-to-flange contact area are held constant while outside radius of contact area is varied.

FIGURE 43.3 Flange Interface Pressure as a function of Radial Distance from the Bolt Centerline for a One Pound Bolt Load. Inside and outside radius of bolt-to-flange contact are held constant and flange thickness is varied.

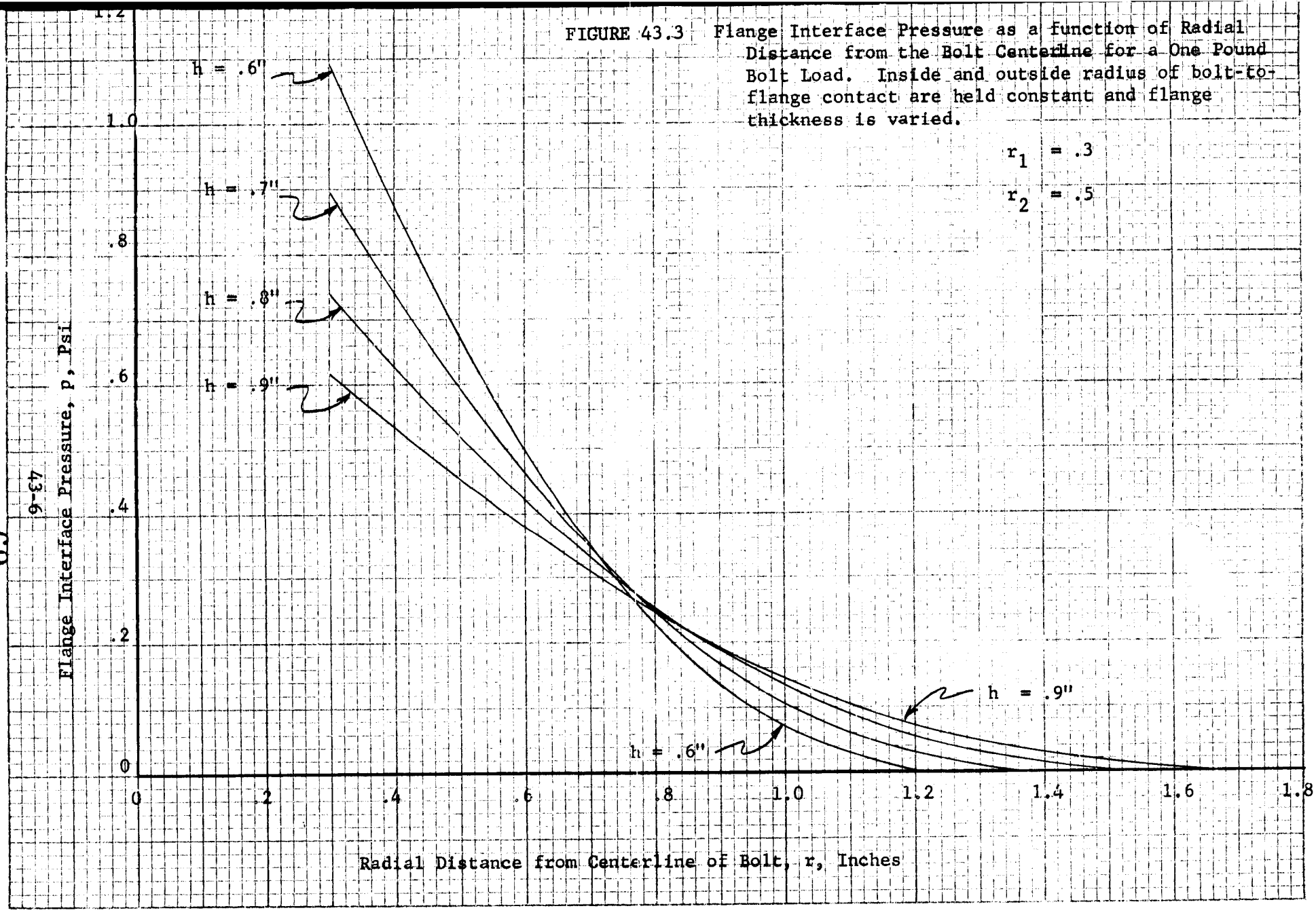

43.3 Analysis

The contact pressure between the two flanges is determined by an analysis of a plate on an elastic foundation. The load is due to the bolt and is applied uniformly over the area of contact between the bolt and flange. This area of contact is a ring. The plate is a thin circular plate with the bolt hole in the center and an infinite outside radius. The elastic foundation is uniform and is determined from a consideration of the compressibility of one-half the plate thickness. One-half the plate thickness is used, because the plate equations are for the deflection of the mid-plane of the plate. The flanges are assumed symmetric about the plane of contact of the flanges and, therefore, this plane of contact remains plane.

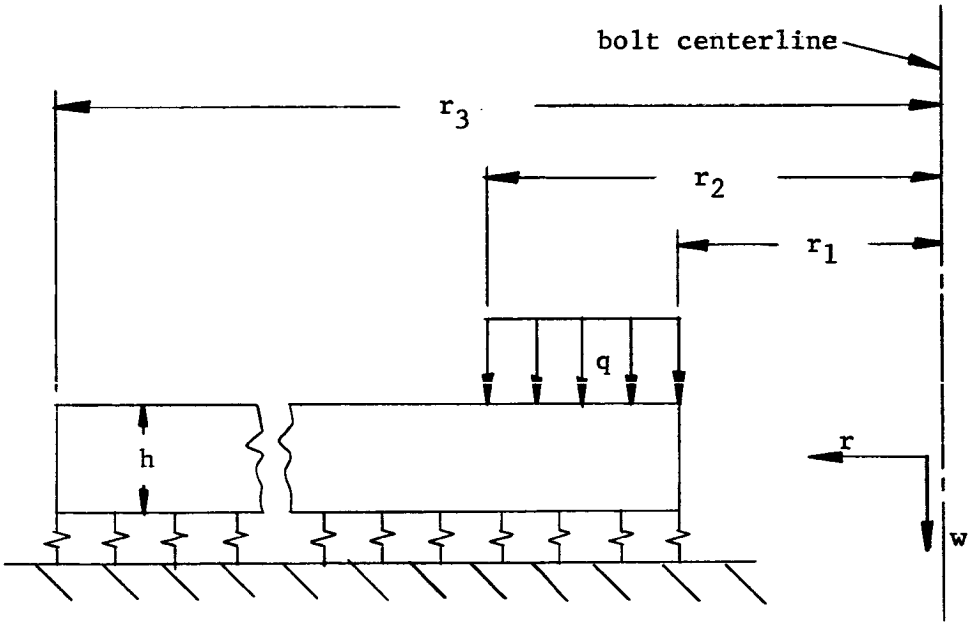

Nomenclature:

C	Constant of integration	
D	Flexural rigidity of plate	inch lb
E	Modulus of Elasticity	psi
$F_1, F_2 .. F_8$	Arbitrary constants	
h	Plate thickness	inch
K	Spring constant of foundation	$lb/inch^3$
M	Bending moment	inch lb/inch
q	Bolt head to flange contact pressure (assumed uniform)	psi

p	Flange-to-flange contact pressure	psi
Q	Shear	lb/inch
r	Radius	inch
w	Deflection	inch
x	Argument of Z function	
Z	Functions defined in Ref. 2	
ν	Poisson's ratio	

The differential equation for a plate on an elastic foundation is derived and solved in Section 30 of Ref. 2. The differential equation is:

$$\frac{d^4w}{dr^4} + \frac{2}{r}\frac{d^3w}{dr^3} - \frac{1}{r^2}\frac{d^2w}{dr^2} + \frac{1}{r^3}\frac{dw}{dr} + \frac{Kw - q}{D} = 0 \qquad (1)$$

where

$$D = \frac{E\,h^3}{12\,(1 - \nu^2)} \qquad (2)$$

$$K = \frac{2E}{h} \qquad (3)$$

The solution to equation (1) is:

$$w = \frac{q}{K} + C_1 Z_1(x) + C_2 Z_2(x) + C_3 Z_3(x) + C_4 Z_4(x) \qquad (4)$$

where

$$x = (K/D)^{1/4}\, r \qquad (5)$$

and the Z functions are given by equation (79), page 103, Ref. 2.

The plate is separated into two parts.

I $\quad r_1 \leq r \leq r_2 \qquad q$ finite

II $\quad r_2 \leq r \leq r_3 \qquad q = 0$

This means two solutions of the form of equation (4) with eight arbitrary constants. The boundary conditions are:

$$\text{Bending moment: } M_r = -D\left(\frac{d^2w}{dr^2} + \frac{\nu}{r}\frac{dw}{dr}\right) = 0, \text{ when } r = r_1$$

$$\text{Shear: } Q_r = -D\left(\frac{d^3w}{dr^3} + \frac{1}{r}\frac{d^2w}{dr^2} - \frac{1}{r^2}\frac{dw}{dr}\right) = 0, \text{ when } r = r_1 \qquad (6a)$$

Deflection: $w_I = w_{II}$, when $r = r_2$

Slope: $\frac{dw_I}{dr} = \frac{dw_{II}}{dr}$, when $r = r_2$

Bending moment: $\left(M_r\right)_I = \left(M_r\right)_{II}$, when $r = r_2$ (6b)

Shear: $\left(Q_r\right)_I = \left(Q_r\right)_{II}$, when $r = r_2$

Deflection: $w_{II} = 0$, when $r \to \infty$

Slope: $\frac{dw_{II}}{dr} = 0$, when $r \to \infty$ (6c)

The deflection equations for each part of the plate are then written in the following form:

$$w_I = \frac{q}{k}\left\{1 + F_5 Z_1 + F_6 Z_2 + F_7 Z_3 + F_8 Z_4\right\} \tag{7}$$

$$w_{II} = \frac{q}{k}\left\{F_3 Z_3 + F_4 Z_4\right\} \tag{8}$$

where F_1 and F_2 are zero because of conditions (6c).

The flange-to-flange contact pressure is equal to the plate deflection times the spring constant of the foundation.

$$p_I = q\left[1 + F_5 Z_1 + F_6 Z_2 + F_7 Z_3 + F_8 Z_4\right] \tag{9}$$

$$p_{II} = q\left[F_3 Z_3 + F_4 Z_4\right] \tag{10}$$

The F's are determined by applying the boundary conditions at r_1 and r_2 to equations (7) and (8). The resulting set of linear simultaneous equations may be solved for the constants by any standard method of solution. The equations are:

$$Z_3(x_2)F_3 + Z_4(x_2)F_4 - Z_1(x_2)F_5 - Z_2(x_2)F_6 - Z_3(x_2)F_7 - Z_4(x_2)F_8 = 1$$

$$\frac{dZ_3(x_2)}{dx}F_3 + \frac{dZ_4(x_2)}{dx}F_4 - \frac{dZ_1(x_2)}{dx}F_5 - \frac{dZ_2(x_2)}{dx}F_6 - \frac{dZ_3(x_2)}{dx}F_7 - \frac{dZ_4(x_2)}{dx}F_8 = 0$$

$$\frac{dz_4(x_2)}{dx} F_3 - \frac{dz_3(x_2)}{dx} F_4 - \frac{dz_2(x_2)}{dx} F_5 + \frac{dz_1(x_2)}{dx} F_6 - \frac{dz_4(x_2)}{dx} F_7 + \frac{dz_3(x_2)}{dx} F_8 = 0$$

$$\left[z_4(x_2) - \frac{1-\nu}{x_2} \frac{dz_3(x_2)}{dx}\right] F_3 + \left[-z_3(x_2) - \frac{1-\nu}{x_2} \frac{dz_4(x_2)}{dx}\right] F_4$$
$$+ \left[-z_2(x_2) + \frac{1-\nu}{x_2} \frac{dz_1(x_2)}{dx}\right] F_5 + \left[z_1(x_2) + \frac{1-\nu}{x_2} \frac{dz_2(x_2)}{dx}\right] F_6$$
$$+ \left[-z_4(x_2) + \frac{1-\nu}{x_2} \frac{dz_3(x_2)}{dx}\right] F_7 + \left[z_3(x_2) + \frac{1-\nu}{x_2} \frac{dz_4(x_2)}{dx}\right] F_8 = 0$$

(11)

$$\frac{dz_2(x_1)}{dx} F_5 - \frac{dz_1(x_1)}{dx} F_6 + \frac{dz_4(x_1)}{dx} F_7 - \frac{dz_3(x_1)}{dx} F_8 = 0$$

$$\left[z_2(x_1) - \frac{1-\nu}{x_1} \frac{dz_1(x_1)}{dx}\right] F_5 + \left[-z_1(x_1) - \frac{1-\nu}{x_1} \frac{dz_2(x_1)}{dx}\right] F_6$$
$$+ \left[z_4(x_1) - \frac{1-\nu}{x_1} \frac{dz_3(x_1)}{dx}\right] F_7 + \left[-z_3(x_1) - \frac{1-\nu}{x_1} \frac{dz_4(x_1)}{dx}\right] F_8 = 0$$

Note that the F's are a function only of r_1, r_2, h and ν. As $\nu = .3$ for aluminum and is a good approximation for steel, ν may be held constant.

In order to show the effect on the contact pressure of changes in r_1, r_2 and h, a set of calculations were made of contact pressure versus radius for various values of these parameters given in Table I.

TABLE I - Parameters used in analysis

Case	r_1 inch	r_2 inch	h inch
1	.2	.4	.7206
2	.3	.5	.7206
3	.4	.6	.7206
4	.5	.7	.7206
5	.3	.4	.7206
6	.3	.5	.7206
7	.3	.6	.7206
8	.3	.7	.7206

TABLE I (continued)

Case	r_1 inch	r_2 inch	h inch
9	.3	.5	.6
10	.3	.5	.7
11	.3	.5	.8
12	.3	.5	.9

A one-pound bolt load was used, so

$$q = \frac{1}{\pi(r_2^2 - r_1^2)} \tag{12}$$

The results are presented in Figures 43.1, 43.2 and 43.3 in the form of three sets of curves. In each set, two parameters are held constant and one is varied.

In Table 2, the results are summarized. The radius r at which the flange contact pressure is half its value at r_1 is also given as well as the ratio $(2r/2r_1)$. For a bolt spacing of 2r it seems likely that the contact pressure between flanges will be nearly uniform. The ratio $(2r/2r_1)$ varies from 1.61 to 2.65 for the cases considered. It should be noted, however, that in most cases this criterion would place the bolts too close together for use of a wrench. Wrench clearance is, therefore, the governing criterion.

TABLE II

Radius r where p(r) is one-half $p(r_1)$, bolt spacing 2r, ratio $(2r/2r_1)$ and difference between r and r_2 for a range of bolt head dimensions and plate thicknesses.

h	r_1	$p(r_1)$	r	p(r)	2r	r_2	$2r/2r_1$	$r-r_2$
.7206	.2	.95	.53	.475	1.06	.4	2.65	.13
.7206	.3	.85	.615	.425	1.23	.5	2.05	.115
.7206	.4	.77	.715	.385	1.43	.6	1.79	.115
.7206	.5	.69	.805	.345	1.61	.7	1.61	.105
.7206	.3	.980	.59	.49	1.18	.4	1.97	.19
.7206	.3	.85	.615	.425	1.23	.5	2.05	.115
.7206	.3	.74	.66	.37	1.32	.6	2.20	.06
.7206	.3	.64	.71	.32	1.42	.7	2.36	.01
.6	.3	1.09	.57	.545	1.14	.5	1.90	.07
.7	.3	.90	.61	.45	1.22	.5	2.03	.11
.8	.3	.74	.65	.37	1.30	.5	2.16	.15
.9	.3	.62	.70	.31	1.40	.5	2.33	.20

43.4 References

1. C. Richard Soderberg, Discussion of "Practical Aspects of Turbine Cylinder Joints" by C.B. Campbell, Journal of Applied Mechanics, March 1939, p. A-31.

2. M. Hetenyi, Beams on Elastic Foundation, The Univ. of Michigan Press, 1946.

44. CRYOGENIC CONNECTOR CONSIDERATIONS

by

S. Levy

44.0 Summary

The effect of seal and bolt length on relative expansion effects is presented. It is shown that differential expansion between bolts and flanges is a primary cause of gasket load changes. The "elastic springback" available in a connector to moderate relative expansion effects is shown to be directly proportional to the amount of material used and the level of stress achieved during bolting. It is found that high "elastic springback" is not necessarily desirable since it may be desirable to have the gasket load increase substantially at low temperatures. Transient temperature conditions during cooling are shown to give rise to somewhat increased temporary leakage possibilities. Pertinent mechanical-property data on materials which might be used in connectors are provided.

Bolted flange connectors are considered in some detail and it is shown for the cases chosen that the gasket load does not change much even when the bolts and flanges are made of material with substantially different expansion properties. For heavier flanges the effect would be greater since the "elastic springback" in the flanges could be kept lower.

It is concluded that an important secondary cause of cryogenic leakage is a failure to increase the gasket load in proportion to the increase in hardness of the gasket material. Aluminum bolts in steel flanges are indicated as one way of increasing the gasket load during cooling. A more substantial increase is shown to be attainable with invar rings.

77

44.1 Introduction

Connectors which perform satisfactorily at room temperature may leak when suddenly cooled by cryogenic fluid. The leakage is usually due to differences in relative expansion. Where different parts of the connector do not have identical shrinkage, a release of sealing pressure may occur. In addition, a transient condition arises initially. Due to the high rate of cooling by the cryogenic fluid, the inner walls of the connector are cooled more rapidly than the outer portions. In particular, the bolts in the case of a flanged connector, or the outer nut in the case of an AN fitting, will cool more slowly. As a result the inner portions of the connector tend to shrink away from each other and thus release pressure on the seal during the initial stages of rapid cooling.

An additional difficulty in designing connectors which will stay tight as the temperature changes is that the mechanical properties vary with temperature. Thus the expansion of copper per unit length in going from 100°R to 200°R is about 0.0005; while from 400°R to 500°R it is .0009. Similarly for Teflon from -400°F to -300°F the unit expansion is 0.0030, while from 0°F to 100°F it is 0.0088. Conductivity and specific heat also have marked non-linearities. Strength and modulus of elasticity rise with reduction in temperature while elongation at failure tends to be lower as the temperature drops.

Elastomers have been shown, Refs. 1 and 2, to perform well as O-rings at temperatures in the 76° to 300°K range. Materials used include Viton-A(R), Hypalon (R) and neoprene. In Ref. 2 both O-rings between tongue-and-groove flanges and O-rings between flat flanges are considered. These references show that when the initial compression exceeds 70 to 90% it is possible to achieve tight seals. The seal material tends to shrink about three times as fast as the metal as the temperature goes down but the high pre-compression maintains an adequate sealing pressure. With proper flange design it is suggested that it may be possible to use flange flexing to reduce the rate of force decay during cooldown. The authors point out the importance of keeping the final gasket thickness to a minimum in order to minimize shrinkage effects. In this connection they suggest a seal in which a raised ring (.042" radius) on one flange presses into a 10-mil mylar film on the flat opposite flange. The initial compression is sufficient to reduce the mylar thickness to 3 mils.

In Ref. 3 the use of Teflon O-ring vacuum seals is described. The O-ring is contained in a groove in one flange and is initially compressed to achieve a 10 to 15 percent volume reduction. Lock-washers are used under the bolts in this connector design and may provide some "follow-up" as the gasket shrinks - at least until the flanges bottom against each other. The authors observe that when leakage occurred in this oonnector it was usually during warm-up of the test assembly.

The concept of "temperature energizing" seals is considered in Refs. 4 and 5. It is pointed out that the excessive shrinkage of the seal can be partially compensated for by containing the seal between an inner invar ring and the flanges. Because the invar ring contracts much less than the

flange material during cooling, the space available to the seal decreases at about the same rate as the seal shrinks. In the design described by the author, either stainless steel or aluminum is suggested for the flanges. Adiprene C polyurethane rubber or neoprene W is suggested for the gasket with additives giving a hardness of 70 durometer A. Either invar or titanium is suggested for the inner ring. The author points out that near room temperature such a design has pressure-compensating characteristics also.

The temperature distribution in a joint will be non-uniform during the initial transient cooling period. As pointed out in Ref. 6, however, it may be non-uniform even after a steady-state condition is achieved. At temperatures below the freezing point of air, the outside of a pipe carrying liquid hydrogen is coated by a slushy condensate consisting of solid air, ice, and liquid air. With a 15 mph wind only the dry solid air is visible. Heat transfer rates of 3500 and 6000 BTU/hr-ft^2 were observed by the author for zero wind and 15 mph wind respectively when there was enough pressure in the pipe to maintain single-phase flow (about 100 psi). With heat flows of this magnitude, a temperature difference through the connector of about 50°F is possible in the case of stainless steel and somewhat less for aluminum alloy.

LOX compatibility is of primary importance. The behavior of materials in this regard is discussed in Ref. 7. It appears that all of the elastomers which are found in Refs. 1, 2 and 4 to be good low-temperature gasket materials are also lox sensitive. Where LOX compatibility is vital, it appears that there is a need for additional materials that are relatively soft at low temperatures.

79

44.2 Thermal and Mechanical Properties

Typical thermal and mechanical properties taken from Refs. 8 and 9 are shown in Tables 44.1 to 44.4. An outstanding characteristic of these tables is the large variation in properties with temperature.

Expansion properties, Table 44.1, are about five times as great for the "seal" materials as for the metals. In addition the change in length per 100°F is approximately twice as great near room temperature as it is at very low temperatures for all the materials listed.

Conductivity, Table 44.2, is more than twice as high at room temperatures as it is at very low temperatures. In addition the conductivity of the metals is many times more than that of the "seal" materials.

Both Young's modulus, Table 44.3, and strength, Table 44.4, are almost an order of magnitude greater at very low temperatures than they are at room temperatures.

In Tables 44.5 and 44.6 from Ref. 10 are given the modulus and stress relaxation values for Allpax 500. The effect of thickness on modulus at -320°F is so different from that at room temperature that additional tests seem to be needed. The effect of cycling is shown and indicates an increase in modulus of about 10 percent with cycling - the major increase occurring in the first cycle. The effect of cycling on stress relaxation is essentially to decrease the relaxation after the first few cycles. The relaxation after 20 minutes at -100°F and at -320°F is negligible, while that at room temperature is about 10 percent on the first cycle.

TABLE 44.1

TYPICAL VALUES OF THERMAL EXPANSION
(Change from 70°F length per unit length)

Temp °R	0		100		200		300		400		500
°F	-460	-400		-300		-200		-100		0	
Material											
Teflon	-.022	-.0215		-.0185		-.0165		-.0123		-.007	
Nylon	-.014	-.0135		-.0125		-.0096		-.0068		-.003	
Kel-F	-.0115	-.0108		-.0094		-.0075		-.0052		-.0022	
Copper	-.0033		-.0032		-.0027		-.0020		-.0011		-.0002
Aluminum	-.0042		-.0041		-.0036		-.0026		-.0016		-.0003
Iron	-.0020		-.0020		-.0018		-.0013		-.0008		-.0002
Nickel	-.0022		-.0022		-.0019		-.0015		-.0009		-.0002

TABLE 44.2

TYPICAL VALUES OF CONDUCTIVITY
(BTU/hr ft ^{o}F)

Temp ^{o}R / ^{o}F	10	20	40	60	80	120	160	200	300	400	500
Material											
Teflon	.036	.055	.088	.110	.120	.140	.140				
Nylon	.011	.027	.070								
Stainless	.21	.55	1.3	2.2	2.8	4.3	5.2	5.8	7.0	7.7	8.2
Aluminum(2024)	2.5	5.5	12.0	18.0	20	28	35	40	51	62	68

TABLE 44.3

TYPICAL VALUES OF YOUNG'S MODULUS
(10^6 psi)

Temp ^oR								
^oF	-460	-400	-300	-200	-100	0	100	200
Material								
Teflon	1.00	.80	.45	.30	.15	.10	.06	
Nylon	1.40	1.30	1.10	.80	.55	.30	.15	.08
Mylar			1.7	1.3	1.2	1.1		
Kel-F			.85	.73	.61	.45		

TABLE 44.4

TYPICAL VALUES OF STRENGTH (psi)

Temp ^{o}R / ^{o}F	-460	-400	-300	-200	-100	0	100	200
Material								
Teflon	22,000	18,000	12,600	8,500	5,000	3,200	1,500	1,000
Nylon						13,000	8,000	5,000
Mylar			30,000	28,000	27,000	23,000		
Kel-F			16,300	15,500	13,700	10,800	4,000	

TABLE 44.5

MODULUS OF ALLPAX 500

Thickness	Temp.	Modulus at 1500 psi stress 1st Cycle	2nd Cycle	10th Cycle
1/32"	RT	29,400	33,400	33,400
		28,500	32,800	33,900
		25,800	31,900	35,000
1/16"	RT	24,400	43,400	50,500
		27,400	44,200	49,200
		24,300	34,300	48,100
1/8"	RT	38,400	52,700	56,200
		31,500	53,400	60,000
		38,700	57,600	60,800
1/32"	-320°F	35,200	38,700	49,400
		47,400	51,700	66,200
		34,000	45,200	60,300
1/16"	-320°F	83,600	108,500	114,000
		103,000	108,000	135,000
		94,600	98,600	128,000
1/8"	-320°F	175,000	190,000	199,000
		190,000	190,000	199,000
		155,000	175,000	182,000

TABLE 44.6

STRESS RELAXATION OF ALLPAX 500 AT RT, -100°F and -320°F

Original Stress Each Cycle (psi)	Temp.	Stress psi (thousands) after 20 minutes each cycle									
		1	2	3	4	5	6	7	8	9	10
2250	-320°F	2.245	2.245	2.240	2.240	2.245	2.245	2.248	2.250	2.250	2.250
	-100°F	2.200	2.230	2.230	2.230	2.225	2.225	2.225	2.235	2.225	2.220
	RT	2.000	2.125	2.175	2.175	2.185	2.200	2.200	2.200	2.200	2.200
1500	-320°F	1.490	1.495	1.500	1.500	1.500	1.500	1.500	1.500	1.500	1.500
	-100°F	1.480	1.490	1.490	1.490	1.480	1.490	1.490	1.495	1.495	1.480
	RT	1.350	1.420	1.425	1.440	1.450	1.455	1.455	1.460	1.455	1.470
750	-320°F	0.730	0.740	0.745	0.750	0.750	0.750	0.750	0.750	0.750	0.750
	-100°F	0.725	0.743	0.742	0.747	0.742	0.742	0.748	0.742	0.748	0.747
	RT	0.615	0.685	0.705	0.710	0.715	0.720	0.722	0.725	0.725	0.730

44.3 O-Rings between Flat Flanges (Contacting outside the bolt circle)

The Cryogenic Engineering Laboratory of the National Bureau of Standards has had good results using an O-ring seal between flat flanges, Ref. 1. The O-ring was stretched slightly over a short stainless steel retaining sleeve which fit snugly inside the flange and prevented inward extrusion during the flange tightening. A flange design which they found gave good sealing with 55 to 70% compression of the O-ring is shown in Fig. 44.1. Designed for use with a 2.5-in. pipeline, the flanges were made in 321 stainless steel with flange faces 0.200 in. thick. Ten 1/4 in. steel bolts equally spaced on a 3.345 in. bolt circle drew the flanges together. The O-ring was 1/16 in. thick prior to compression.

We will now examine the stresses and deformations in this connector:

1) at room temperature
2) at 76°K (137°R)
3) at transient conditions to 137°R from room temperature

We make use of the analysis procedure for flanges contacting outside the bolt circle, Section 41. We know that the initial bolt tightening is sufficient to compress the 1/16 in. O-ring to about 0.02 in. Equations (45) and (53) of Section 41 show that

$$y_2 = \left[\frac{F\ell^3}{3}\left(1+\frac{b_{max}}{\ell}\right)\left(1+\frac{b_{max}}{2\ell}\right) + \left(M+\frac{Qt}{2}\right)\left(\frac{\ell^2}{6}\right)\left(3+3\frac{b_{max}}{\ell}+\frac{b_{max}^2}{\ell^2}\right)\right]\frac{12(1-\nu^2)}{Et^3}+\theta_5(b_{max}+\ell) \qquad (1)$$

where y_2 = axial displacement of flange of gasket = 0.02/2 = 0.01 in.

F = sum of axial force on flange from pipe and gasket (lb/in)

θ_5 = slope of flange at contact with other flange (rad)

ℓ = distance from bolt circle to gasket circle (assumed same as pipe circle here) 1.672 - 1.240 = 0.432 in.

b_{max} = maximum value of b. We take it as 0.04 in less than the distance from bolt circle to outer edge = (2-1.672)-.040 = 0.288 in. to allow for some local crushing

M = moment between pipe and flange (lb-in)/in

Q = shear between pipe and flange (lb/in)

E = Young's modulus = 30,000,000 lb/in^2

ν = Poisson's ratio = 0.3

t = flange thickness = 0.200 in.

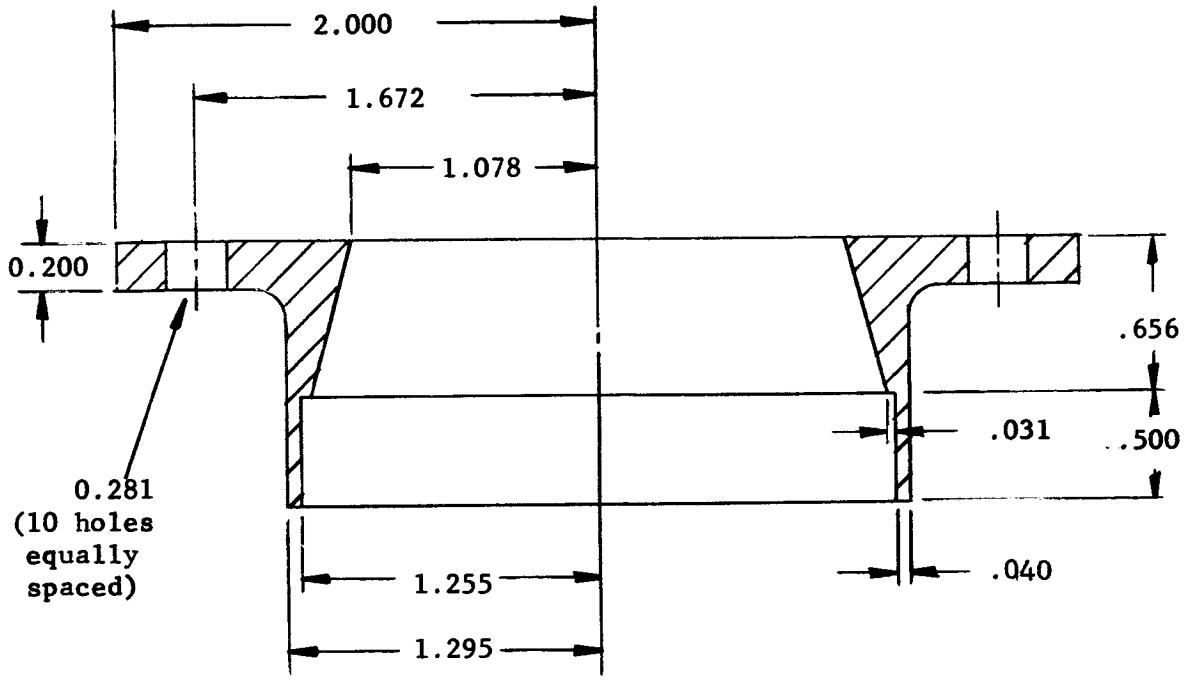

FIG. 44.1 - NBS Flange Dimensions (Ref. 1)

We have assumed that when the flange deflection y_2=0.01 in. (half the available 0.02 in. for each flange) the applicable equations of Section 41 correspond to bearing between flanges near their outer edge. It is assumed that the flange thickness is such that the contribution of its hoop stretch in resisting rolling is negligible. (This assumption is confirmed in 44.8, Appendix A.) Then Eq. (51) of Section 41 gives,

$$\left(\frac{b_{max}}{\ell}\right)^3 = \frac{Et^3}{2K\ell^3(1-\nu^2)}\left[1 - \frac{\left[K(\delta+\theta_5 b_{max}) - F\right](b_{max}/\ell)}{F + (M+Qt/2)/\ell}\right] \qquad (2)$$

where

b_{max} = maximum value of b. We take it as 0.04 in less than the distance from bolt circle to outer edge = (2-1.672)-.040 = 0.288 in. to allow for some local crushing

K = bolt stiffness per unit circumference = NAE/t = $10/(\pi x 3.345)\ (\pi/4)(.25)^2(30,000,000)/0.2 = 7,000,000$ lb/in.^{2}

δ = initial bolt stretch (in the absence of flange separation) = $0.003x0.2-\Delta$ = $.0006-\Delta$ in. (assuming an initial bolt strain of 0.003 corresponding to a bolt stress of 90,000 lb/in^2 and an unstretched lack of bolt bottoming Δ, to be determined)

The relation between bolt load and axial force is given by Eq. (46) of Section 41 as

$$B = F(1+\ell/b) + (M+Qt/2)(1/b) \qquad (3)$$

where

B = bolt force per unit circumference = $10x(\pi/4)(.25)^2$ x $90,000/(3.345\pi)$ = 4200 lb/in

The slope of the flange at its junction with the cylinder is given by Eq. 52 of Section 41 as

$$\theta_6 = \frac{6(1-\nu^2)}{Et^3}\left[\ell^2 F(1+b/\ell) + (M+Qt/2)(2+b/\ell)\right] + \theta_5$$

Values of M and Q can be obtained from Eqs. (49) and (50) of Section 41 with θ_4 replaced by θ_6. It will be assumed here that the wall is thin enough to approximate M and Q as zero. (In 44.9, Appendix B, a check is given on the assumption that M and Q have a negligible effect.) Then from Eq. (3)

$$4200 = F(1+0.432/0.288);\ F = 1680 \text{ lb/in.} \qquad (5)$$

From Eq. (2)

$$\left(\frac{.288}{.432}\right)^3 = \frac{30,000,000(0.2)^3}{2x7,000,000(.432)^3(.91)}\left[1 - \left(\frac{7,000,000(0.0006-\Delta+.288\theta_5)-1680}{1680}\right)\left(\frac{.288}{.432}\right)\right]$$

$$\theta_5 = 3.47\Delta - .00160$$

Substituting values into Eq. (1) gives

$$y_2 = \left[\frac{1680(.432)^3}{3}(1.667)(1.333)\right]\left(\frac{12(.91)}{30\text{x}10^6\text{x}.2^3}\right) + (3.47\Delta - .00160)(.288 + .432)$$

$$= .00457 + 2.50\Delta - .00115$$

$$\text{but } y_2 = .01 \text{ so } \Delta = .00263 \text{ in., } \theta_5 = .00752 \text{ radians} \qquad (7)$$

Thus the unstretched lack of bolt bottoming is 0.00263 in per flange and the bolt stretch is 0.0006 in per flange when the flange separation at the gasket is 0.01 in per flange. The initial bolt tightness develops stresses of 90,000 lb/in^2 in the bolts. This is the condition at room temperature.

We now consider the state of affairs at 137°R. We have no values of thermal contraction for the steel bolt material; however, for the purpose of this example we will consider it to be .0002 less per unit length than for the flange. Since the flange thickness is 0.2 inch this results in a decrease in δ by 0.2 x .0002 = .00004 in. to .00056 - Δ = -.00207. We have no value of thermal contraction for the gasket material used; however, for the purpose of this example we take it as 0.02 in per inch. The new value of y_2 is therefore 0.01 x 0.98 = 0.0098 in.

Equation (1) is then (subscript c denotes cold value)

$$0.0098 = \left[\frac{F_c(.432)^3}{3}(1.667)(1.333)\frac{12(.91)}{30\text{x}10^6\text{x}.2^3} + \theta_{5c}(.720)\right] \qquad (8)$$

and Equation (2) becomes

$$\left(\frac{.288}{.432}\right)^3 = \frac{30\text{x}10^6\text{x}.2^3}{2\text{x}7\text{x}10^6\text{x}.91\text{x}.432^3}\left[1 - \left(\frac{7\text{x}10^6(-.00207 + .288\theta_{5c}) - F_c}{F_c}\right)\left(\frac{.288}{.432}\right)\right] \qquad (9)$$

Solving Eqs. (8) and (9) simultaneously, F_c = 1573 lb/in. and θ_{5c} = .00764 radians. These values are not greatly different from the room temperature values in Eqs. (5) and (7). Since the stiffness of the gasket material is so much greater at the cold temperature it is not certain that the gasket could "reseat" with the force F_c = 1573 lb/in. Assuming the O-ring has squashed to a width of 0.15 in., the sealing pressure is 1573/.15 = 10,500 psi. This may not equal the cold yield strength so sealing would not be good. Nevertheless if the "seating" is not disturbed during cooling a good seal might be maintained. This is likely where the pair of flanges use the same materials.

The flange stress is obtained from Eq. (16) of Section 41 as

$$\sigma_r = \frac{6}{t^2}(F\ell + M + Qt/2 - Bd_H/8) \Big/ (1 - Nd) \qquad (10)$$

where

σ_r = radial stress in flange (lb/in.^{2})

N = number of bolts per unit circumference = $10/3.345\pi = 0.95$/in.

d = diameter of bolt hole = 0.281 in.

d_H = diameter of bolt head = 0.392 in.

Substituting values in Eq. (10) we find the room temperature stress is

$$\sigma_r = 106{,}000 \text{ psi} \tag{11}$$

and the cold temperature stress

$$\sigma_r = 100{,}000 \text{ psi} \tag{12}$$

These values are high enough to suggest the possibility of some flange yielding with correspondingly lower stresses and lower flange "spring back". Increasing the b, ℓ, and t of the flange in proportion would give a proportionate decrease in stress without affecting the available springback; or if the bolt load were increased to give the same stress in the flange, the available springback would be proportionately increased. The higher bolt load in this case would provide greater sealing pressure but would require an increase in the bolt area.

During the transient temperature condition there will be somewhat more rapid cooling of the flanges than of either the O-ring or the bolts. It is possible that the bolt contraction might lag that of the flanges by as much as 0.001 per unit length or 0.0002 in for its 0.2-in. length. This corresponds to a decrease in δ from the -0.00203 to -0.00223 with a corresponding reduction in load to $F_{cTran.}$=1440 lb/in. This is only a bit lower than the cold value but does increase the possibility of leakage.

44.4 Flat Gasket Between Flat Flanges (not contacting outside the bolt circle)

Flat Allpax 500 gaskets have been used successfully between flat flanges for cryogenic temperatures. In Fig. 44.2 is shown such a flange made of 321 stainless steel and having a flange thickness selected to give the same flange stress and gasket force as was found in Section 44.3. In this case, where the flanges do not contact beyond the bolt circle, the flange thickness is 0.246 in. rather than the 0.200 in. used in Section 44.3. Ten 1/4-in. steel bolts draw the flanges together. The gasket is initially 1/4-inch wide and 1/16-inch thick. The gasket load is the same 1680 lb/in. as was found at room temperature in Section 44.3 in Eq. 5.

The bolt and gasket loads are in equilibrium, therefore

$$1.672B = 1.406F \text{ giving } B = 1410 \text{ lb/in.} \tag{13}$$

The moment M_t per unit length of the mid-flange circle (radius a) in Ref. 11, page 179, or Figure 42.2 is given by

$$aM_t = 1410(1.672)(1.672-1.406) = 627 \text{ lb in} \tag{14}$$

The corresponding angle through which the flange twists (neglecting the tube restraint as was done in Section 44.3) is given by Eq. 11 of Section 42 as

$$\theta = \frac{12aM_t}{Et^3 \log_e(d/c)} \tag{15}$$

where d = outer flange radius = 2.000 in.

and c = inner flange radius = 1.250 in.

Substituting values into Eq. (15) gives

$$\theta = 0.0357 \text{ radians} \tag{16}$$

With this much flange roll, the outside of the flanges will be drawn together with respect to the gasket by

$$\theta(d-1.406) = .0212 \text{ in per flange}$$

$$\text{or } .0424 \text{ in. for a pair of flanges} \tag{17}$$

This exceeds the initial gasket thickness of 1/16 inch by so little that there is some possibility that the flanges could come into contact due to initial set in the gasket material.

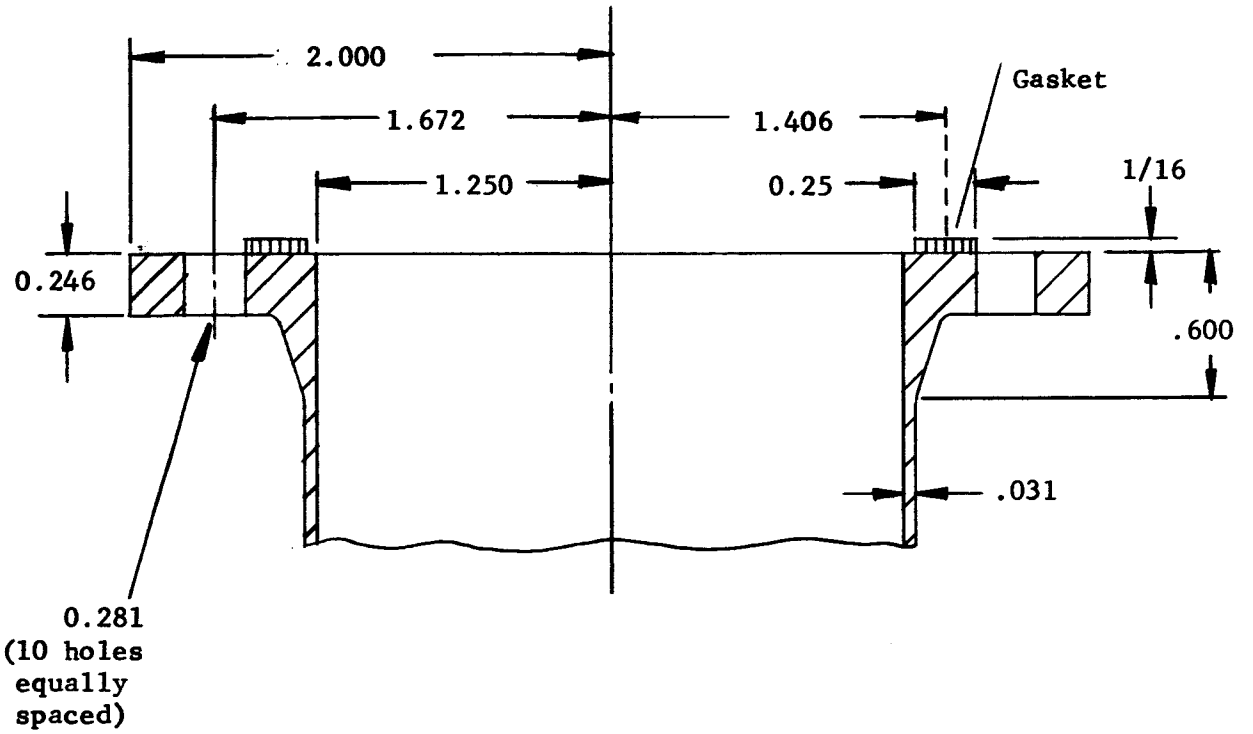

FIG. 44.2 - Flange Which Does Not Contact Outside Bolt Circle

From Eq. 13 of Section 42 the maximum flange stress is

$$\sigma_f = \frac{6aM_t}{t^2 c \log_e(d/c)} = 106{,}000 \text{ lb/in}^2 \qquad (18)$$

This is equivalent to the stress obtained in Eq. (11), as was desired, however, it should be noted that the stress in Eq. (11) was in a radial direction and was maximum at the bolt circle; while the stress in Eq. (18) is in a circumferential direction and is a maximum at the inner radius.

The bolt stress is given by

$$\sigma_B = B/NA \qquad (19)$$

where N = number of bolts per inch = 0.95/in.

A = cross-sectional area of bolt = 0.049 in.^{2}

With Eq. (13) this gives

$$\sigma_B = 1410/(0.95\text{x}0.049) = 30{,}300 \text{ lb/in.}^2 \qquad (20)$$

The bolt stretch is the strain times the length per flange. This length is about 0.246 in. + 1/32 in. = 0.277 in. per flange

$$\delta_b = \frac{\sigma_B}{E}(0.277) = 0.000279 \text{ in.} \qquad (21)$$

The gasket squash, using a modulus of 50,000 lb/in.^{2} from table 5 and a thickness of 1/32 inch per flange, is

$$\delta_g = \frac{\sigma_G}{E_G}(.031) = \frac{1680}{0.25\text{x}50{,}000}(0.031) = .00417 \text{ in.} \qquad (22)$$

In the above we have considered the room temperature condition of this connector. We would now like to consider it at 137°R. We take the contraction of the bolt as 0.0002 less per inch than for the flange, as was done in Section 44.3. We take the contraction of the bolt as about the same per inch as that of the gasket, based on the limited information in Ref. 12, page 35-19. The primary effect of cooling then is a relative lengthening of the bolt by 0.0002x0.246 = 0.0000492 in. This must be accommodated by a combination of flange twisting and bolt contraction and gasket expansion.

From Eqs. (13) and (16) we see that

$$\Delta B/\Delta\theta = 1410/.0357 = 39500 \text{ (lb/in.)/radian} \qquad (23)$$

for the flange (neglecting the effect of temperature on flange material modulus). From Eqs. (13), (21) and (22) we see that (neglecting the effect of temperature on flange material modulus)

$$\Delta F/\Delta\delta_g = 1680/.00417 = 403{,}000 \text{ (lb/in.)/in.}$$

$$\Delta B/\Delta\delta_b = 1410/.000279 = 5{,}050{,}000 \text{ (lb/in.)/in.} \qquad (24)$$

where $\Delta\delta_b$ is the increase in bolt length due to an increase in bolt load, and $\Delta\delta_g$ is the decrease in gasket height due to an increase in gasket load. But,

$$\Delta\theta/(\Delta\delta_b + .0000492 + \Delta\delta_g) = -1/(1.672-1.406) = -3.76 \text{ rad/in.} \qquad (25)$$

Combining (23), (24) and (25) and using $\Delta B/\Delta F = 1410/1680 = 0.84$,

$$\Delta\delta_b = -0.99 \times 10^{-6} \text{ in.}, \quad \Delta\delta_g = -14.7 \times 10^{-6} \text{ in.} \qquad (26)$$

and

$$\Delta B = -5.0 \text{ lbs.}, \quad \Delta\theta = -126.2 \times 10^{-6} \text{ rad} \qquad (27)$$

These changes are negligibly small.

As was true in Section 44.3, the transient temperature condition could result in bolt contraction of 0.001 inch per inch of length less than that of the flanges. This is five times as much as resulted in the increments given in Eqs. (26) and (27). As a result the bolt load might drop to 1410-5x5 = 1385 lb/in. with a corresponding gasket load of 1680 (1385/1410) = 1650 lb/in. This is nearly the same as was there before and indicates little increase in the possibility of leakage.

44.5 AN Fittings

AN fittings and tubes made of the same materials can be expected to show very little change in leakage characteristics at uniform low temperatures since the relative contractions should be nearly equal and the changes in modulus and strength should also be nearly equal.

During the transient conditions accompanying a rapid cool down (as for a high velocity flow of cryogenic fluid through the connector), there may be a lag in cooling for the outer portions of the connector. This could result in a temporary decrease in sealing load; however, since the heat flows rapidly, it is not likely to have a duration of more than a half minute.

In the case of a hydrogen or helium line which is condensing liquid air on its outer surface, it is possible that a steady-state condition might develop where the outer surface is not as cold as the inner. The sealing load would then be lower. To counterbalance this effect, a nut with greater coefficient of contraction might be used as compensation.

44.6 Invar Rings

In Ref. 4 a seal using an invar ring between the gasket and the flanges is described. The seal is claimed by the author to contain LH_2 at 1800 psi. A drawing is shown in Fig. 44.3. A compressive stress of about 100 to 300 psi is attained in the gasket at assembly. The seal is pressure energized at room temperatures. At low temperatures the outer flange shrinks more rapidly than the invar ring, thus creating extra sealing pressure.

An estimate of the additional pressure can be attained from the formula

$$\Delta p = (E_i t_i / a_i)\Delta\epsilon \qquad (28)$$

where

E_i = modulus of the invar

t_i = thickness of invar (in.)

a_i = invar ring radius (in.)

$\Delta\epsilon$ = differential contraction per unit length between ring and flange

For example in the ring of Ref. 4, $t_i = 0.235$ in. and $a_i = 2.03$ in. For shrinkage $\Delta\epsilon$ of .001 and an assumed $E_i = 28{,}000{,}000$ lb/in.^{2}, Eq. (28) gives $\Delta p = 3470$ lb/in.^{2}. This is a very substantial increase compared with the sealing pressures of about 200 psi used in Ref. 4 at room temperature. For high-pressure service a heavier invar ring might be needed.

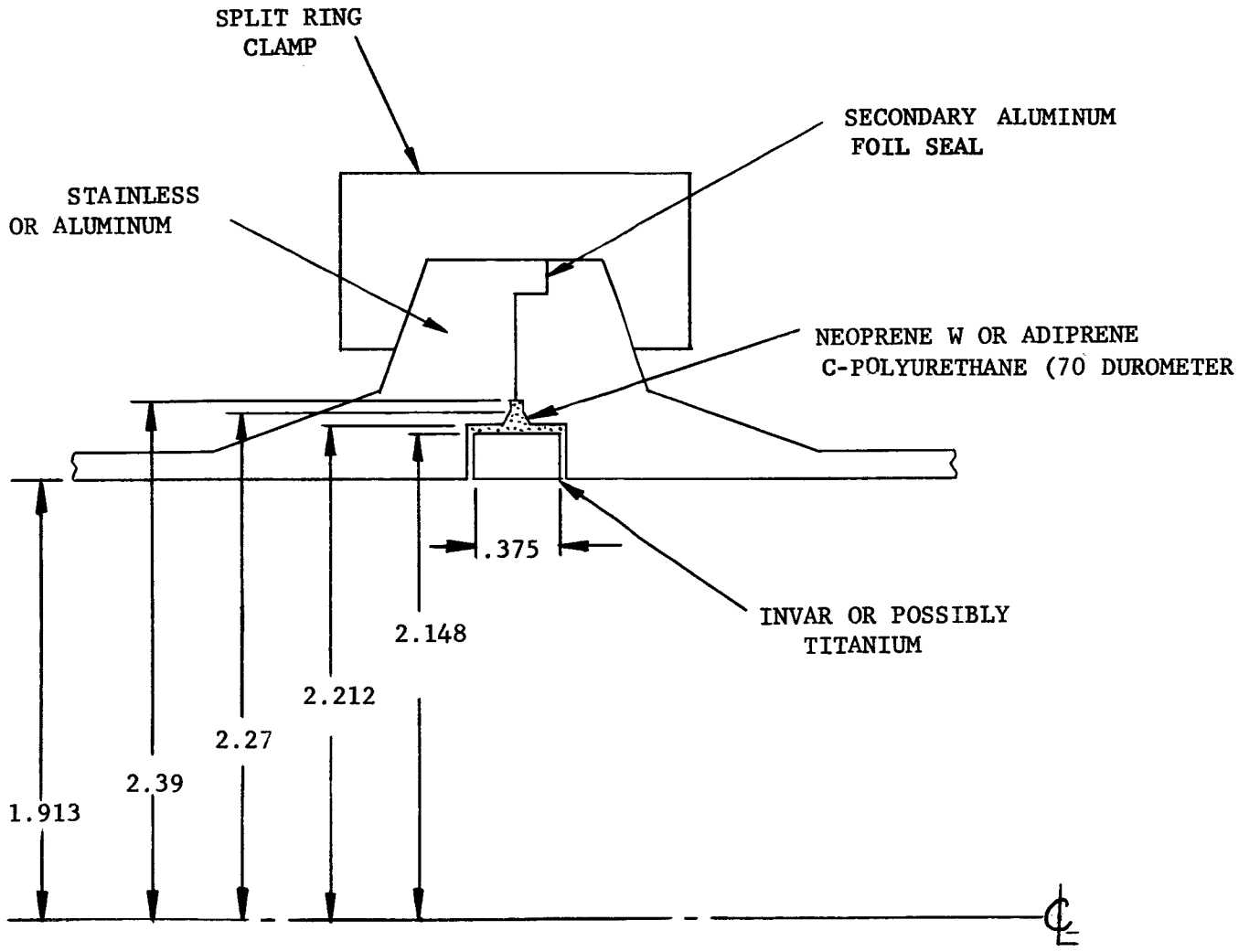

FIG. 44.3 Temperature-Energized LH_2 Seal for 1800 psi.

44.7 Discussion

It has been shown in Sections 44.3 and 44.4 that, although there is a decrease in gasket load with a drop to cryogenic temperatures, it is relatively moderate in magnitude. For flanges which are thicker and have longer bolts, it would be proportionately greater. The generally observed increase in leakage is therefore not only due to a decrease in gasket load but also must result from an increase in hardness of the gasket material. We see from Table 44.3 that there is indeed an order-of-magnitude increase in modulus. If the gasket requires any reseating as it cools, it is therefore likely that intimate contact between gasket and flange surfaces would require gssket forces that are an order of magnitude larger. It is believed that this need for greatly increased gasket forces with cooling is an important cause of low temperature leakage.

Various ways have been conceived for increasing gasket forces. Perhaps the simplest would be to use bolts having a higher rate of shrinkage with temperature than the flanges. The bolt length could be increased if necessary to achieve the proper squeeze. It would then be necessary to design the flanges somewhat heavier so that the increased bolt and gasket loads at low temperature would not cause failure.

If the bolts in the flanges of Sections 44.3 and 44.4 had been aluminum of three times the cross-sectional area, they might have shortened as much as 0.002 more per unit length than the flange material. Using the same analysis procedure as was used in those Sections, we find an increase in gasket force from 1680 to 1950 lb/in. for Section 44.3 and from 1680 to 1740 lb/in. in Section 44.4. These might help somewhat on sealing, however, more effective designs seem to be indicated. It should be pointed out that with stiffer flanges these load increases could be substantially more.

"Elastic springback" in a connector tends to reduce the effects of relative expansion in changing the gasket load. The "elastic springback" is larger as the elastic energy stored in the flange increases. Thus for a given gasket load, increasing the bulk of flange material and the stress level increases the springback. This is not necessarily a desirable design objective, since to avoid low-temperature leakage it may be desirable to increase the gasket load substantially.

An invar ring, with the gasket sandwiched between it and the flange, appears to be a promising method for increasing gasket loads during cooling. For the case considered, the increase in sealing pressure was about an order of magnitude. For higher-pressure service and harder gasket materials, the increase would be smaller but still substantial.

44.8 Appendix A: Check on Neglect of Flange Rolling

In connection with Eq. (2) it has been tacitly assumed that flange rolling of the type conventionally present in ASME-type flanges is so small that the effect on the load is negligible. To check on this we refer to Eq. 11, Section 42. The moment accompanying flange twisting is

$$M_t = \left(\theta_5 E t^3 \log_e \frac{d}{c}\right)/(12a) \qquad \text{(A-1)}$$

where d = outer flange radius = 2.000 in.

c = inner flange radius = 1.078 in.

a = mean flange radius = 1.539 in.

Substituting values from Eqs. (11) and (7) into Eq. (A-1) gives

$$M_t = 64(\text{lb.-in.})/\text{in.} \qquad \text{(A-2)}$$

For comparison the moment of the bolt force B about the flange contact point is

$$M_b = B(b_{max}) = 4200(+0.288) = 1210(\text{lb.in.})/\text{in.} \qquad \text{(A-3)}$$

The moment M_t from flange twisting is about one twentieth of that due to bolt load, so neglecting it is justifiable.

44.9 Appendix B: Check on Neglect of Pipe Restraint

In obtaining Eq. (5) it has been assumed that M and Q are negligibly small. As a check on this we refer to Eq. (h), page 181 of Ref. 11. We see there that

$$M = 2\beta D\theta_6;\ Q = 2\beta^2 d\theta_6 \tag{B-1}$$

where h = tube wall thickness taken as 0.031"

$$\beta = \sqrt[4]{\frac{3(1-\nu^2)}{c^2h^2}} = 7.32 \text{ in.}^{-1}$$

$$D = \frac{Eh^3}{12(1-\nu^2)} = 81.8 \text{ lb.-in.}$$

Using the value of θ_5 given in Eq. (7) we have with Eq. (4)

$$M = 14(\text{lb.-in.})/\text{in.} \tag{B-2}$$

and

$$Q = 100 \text{ lb./in.} \tag{B-3}$$

It is apparent that M is negligible in comparison with the moment of 1210 (lb/in.)/in. due to gasket force, Eq. (A-3). The moment due to Q is

$$\frac{Qt}{2} = 10 \text{ (lb.in.)/in.} \tag{B-4}$$

It is apparent that this is also negligible.

44.10 References

1. R.F. Robbins, D.H. Weitzel, and R.N. Herring, "The Application and Behavior of Elastomers at Cryogenic Temperatures," Advances in Cryogenic Engineering, Vol. 7, Conference at Ann Arbor, 1961, Plenum Press, 1962.

2. D.H. Weitzel, R.F. Robbins, G.R. Bopp, and W.R. Bjorklund, "Elastomers for Static Seals at Cryogenic Temperatures," Advances in Cryogenic Engineering, Vol. 6. Plenum Press, 1961.

3. J.E. Harlow, E.L. Murley, and H.L. Laquer, "Vacuum Gaskets for Use at 20°K," Advances in Cryogenic Engineering, Vol. 5, Plenum Press, 1960.

4. S.E. Logan, "Temperature-Energized Static Seal for Liquid Hydrogen," Advances in Cryogenic Engineering, Vol. 7, Plenum Press, 1962.

5. S.E. Logan, "Static Seal for Low Temperature Fluids," Jour. American Roc. Soc., Vol. 25, July 1955.

6. R.J. Richards, W.G. Steward and R.B. Jacobs, "Transfer of Liquid Hydrogen Through Uninsulated Lines," Advances in Cryogenic Engineering, Vol. 5, Plenum Press, 1960.

7. J.E. Curry and W.A. Riehl, "Compatibility of Engineering Materials with Liquid Oxygen," Rep. No. MTP-M-S and M-M-61-7, Mar. 21, 1961, by Eng. Matls. Br., Structures and Mechanics Division, Marshall Space Flight Center, NASA.

8.. A Compendium of the Properties of Materials at Low Temperatures, Phase 1, Part II, Properties of Solids, WADD TR 60-65, Oct. 1960.

9. Cryogenic Materials Data Handbook, PB171809, Office of Technical Services, U.S. Department of Commerce.

10. R.B. Gosnell, "Elastomeric Gasket Materials Development for Cryogenic Applications, Fourth Monthly Progress Report, Period Ending 15 November 1962," NARMCO Research and Development Division of Telecomputing Corporation.

11. S. Timoshenko, Strength of Materials, Part II, D. Van Nostrand, Second Edition, 1941.

12. C.L. Mantell, Engineering Materials Handbook, McGraw-Hill Book Co., 1958.

45. EFFECT OF CREEP ON FLANGE CONNECTORS

by

B. T. Fang

45.0 Summary

Creep of the components in a fluid connector will cause the undesirable relaxation of gasket compression. In this section, previous work on this subject is briefly reviewed first. A more general theory is then formulated together with a suggested method of solution using high-speed digital computers. A simple numerical example is given without taking into consideration the creep bending of the flanges.

It appears that the weakest link in the analysis of the creep problem is the lack of material creep data. In addition the creep of materials is very sensitive to the temperature at elevated temperatures. Therefore temperatures of the components of a connector have to be determined in order to predict their creep behavior accurately. Because of these uncertainties, it seems desirable to make an order-of-magnitude study of the equations formulated in this section and make some drastic simplifications. The contribution of the bolts to relaxation of flanged connectors should always be considered. Some other members of the connector may be neglected, depending on their geometrical and material properties. Some criteria are given for assessing the relative importance of the components of the connector.

45.1 Introduction

Creep is the slow deformation of solid materials over extended periods under load. It is usually more pronounced at elevated temperature and under high stress. Fig. 45.1 shows a typical creep strain-time relation as obtained in a constant-load tensile test at a given temperature.

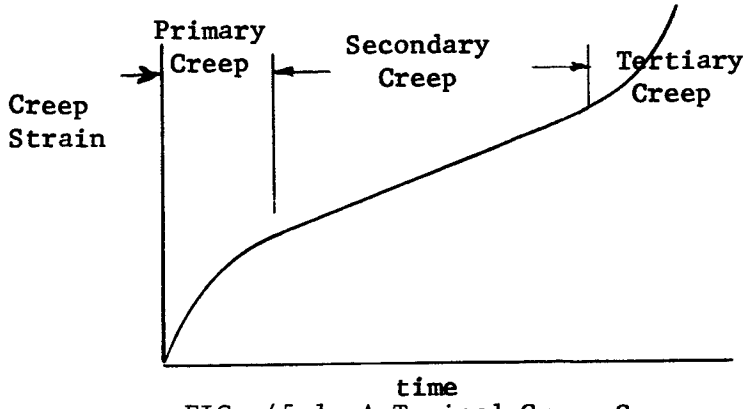

FIG. 45.1 A Typical Creep Curve

Intimately related to creep is the slow relaxation of stress in a body under strain. In a flange connector the relaxation in gasket compression may lead to leakage. This was among the earliest problems studied on creep. As representative investigations on the subject we may refer to the work of Baumann (Ref. 1), Waters (Ref. 2) and Marin (Ref. 3). Baumann's result is presented in a very attractive simple form. One of the major conclusions is that it is desirable to have the other members of the flange assembly very flexible in comparison with the bolts. This has led to the use of bolt collars to reduce the relaxation of bolt stress. Unfortunately Baumann's result is not applicable when the bolts, flanges and gasket obey different creep laws and when rolling of the flange is included. The former does not add much to the complexity of the problem but the latter presents considerable difficulty because of the continuous redistribution of stresses in the flange during creep. For "long time" creep behavior the stress redistribution is complete, the problem again becomes simpler and solutions are available (Refs. 3,4). The transient period of stress redistribution has been neglected by most investigators on account of its difficulty. A notable exception is the work of Waters (Ref. 2). It is believed that the transient behavior is important because

1. The time duration of interest is much shorter for launch vehicles than for steam power plants, with which most previous investigators are concerned.

2. Weight consideration calls for less conservative designs for connectors used on launch vehicles. The higher stresses involved cause severe creep.

3. Knowledge of the transient behavior would furnish us an optimum time for the retightening of the connector.

In Waters' paper the transient behavior of the creep of bolts and the rolling of flanges is treated. Even though many important factors are not considered, still the governing equations become very much complicated and solution of these equations is quite beyond the computing facilities available at that time.

In all these works mentioned, the primary creep (see Fig. 45.1) is not considered and particular forms are chosen for the creep law governing the secondary creep of flange connectors. An exception is the work of Popov (Ref. 5). But again only axial creep of the bolts and flanges are included.

In the following sections we shall make a general study of the creep of flange connectors. Very general forms of flange loading, flange cross-section, and creep laws shall be considered. We shall formulate the problem in a form which is conceptually clear, easy for generalizations, and best suited for machine calculations.

45.2 Nomenclature

A	Total cross-sectional area
B	Inside diameter of flange
C	Bolt circle diameter
D	Bending rigidity, $= \frac{Eg_o^3}{12(1-\mu^2)}$
E	Young's modulus
e	Elastic strain
ϵ	Creep strain
F	Total force per unit length of pipe circumference, $= \frac{\sigma A}{2\pi r_o}$
F_D	$\frac{B^2P}{8r_o}$
F_R	$\frac{PBx}{2r_o}$
F_T	$\frac{P(G^2-B^2)}{8r_o}$
G	Gasket circle diameter
g_o	Pipe thickness
h_G	$\frac{C-G}{2}$
L	Length
M_o	Pipe reaction moment, per unit length of pipe circumference
M_t	Twisting moment, per unit length of pipe circumference
M_y	Bending moment about y-y axis
P	Internal pressure
Q_o	Pipe reaction shear force, per unit length of pipe circumference
r_c	Distance from flange axis to centroid of flange cross section
r_o	Pipe radius

106
~~107~~

r_T	$\frac{G^2 + G_B + B^2}{3(G + B)}$
W_o	radial deflection at junction of pipe and flange
x, z, ξ	axial distances (Fig. 45.2)
y	radial distance from centroid
σ	stress
θ	rotation of flange (Fig. 45.2)
μ	Poisson's ratio
T	Temperature

Subscripts

B	Bolt
F	Flange
G	Gasket
K	Collar
c	Centroid

Superscript

$\cdot$	Derivative with respect to time

107

45.3 Creep Law

Our present knowledge of the physical process does not allow us to formulate a satisfactory creep law from the structure-of-matter point of view. Instead we have to rely upon phenomenological laws derived from test results. The majority of the creep tests performed have been carried out in tensile creep test machines under constant load and at a given temperature. A typical test curve is shown in Fig. 45.1. Immediately after the application of load, in primary creep, the creep strain increases very fast. Gradually the creep slows down until finally the creep rate remains practically constant (secondary creep). Finally, in the tertiary period, the creep rate increases sharply until fracture occurs. At high temperatures and high stresses creep proceeds faster. In particular the primary creep often extends over a large time interval and cannot be overlooked.

Many different creep laws have been suggested on the basis of test results (Ref. 6,7,8). The effort is hampered by the meagerness of test results, and because most of these tests have been constant-stress tests. For our purpose it is immaterial which creep law is used as long as we have the information about the creep rate at each instant under consideration. Since it is not possible to have tests which duplicate every stress-strain-time history, generally we shall not have this information. To get around this difficulty we shall neglect the possible history dependence of creep rate and adopt the postulate for the existence of a functional relationship

$$\phi\ (\sigma,\ \epsilon,\ \dot{\epsilon},\ T) = 0 \tag{1}$$

among the stress σ, creep strain ϵ, creep strain rate $\dot{\epsilon}$ and temperature T. This is the so called "strain hardening" theory of creep (Ref. 8). With this postulate the constant-stress, constant temperature test results would give us the functional form of 'ϕ', or the creep rate is known when the stress, creep strain and temperature is given. It is by no means to say that Eq. (1) is the correct general creep law. Specifically this does not include the well-known creep recovery effect. It is believed to be the most reasonable postulate to extend the applicability of the present available test results. Conceivably with the accumulation of more experimental data we may very well revise this postulate. The method we are going to describe shall be very general so that it will be adaptable to these changes.

Most of the time we shall deal with constant-temperature conditions and Eq. (1) can be written in the alternate form

$$\dot{\epsilon} = f(\sigma,\ \epsilon) \tag{2}$$

For secondary creep the creep rate is almost independent of creep strain and we have

$$\dot{\epsilon} = \pi(\sigma) \tag{3}$$

45.4 Formulation of Equations

A flange connector assembly consists of the gasket, bolt and collars, flanges and the adjoining pipes. The behavior of the gasket, bolts and collars are comparatively simple because they can be treated approximately as members under uniform axial tension or compression. The adjoining pipes interact with the flanges. The loads transmitted from the flanges to the pipes are essentially axi-symmetric. Solutions are available for their behavior if creep bending of the pipes is neglected (Ref. 9). The difficulty of analyzing the creep behavior of a flange connector lies in the flanges. Since creep under uni-axial stress condition is much simpler than under multi-axial stress condition we shall use the simplified approach of treating the flange as the small twisting of a ring under uniformly distributed couples. This approach in the elastic analysis of flanges was initiated by Timoshenko (Ref. 4) and elaborated recently by Dudley (Ref. 10). An additional simplification shall be made that the dimensions of the flange cross section is small compared with the radius of the pipe. The consequence is that the deformation of the flange can be approximately represented as the sum of a "hoop extension" of the centroid of the flange cross section and a uniform twist of the flange cross section about the centroid.

Fig. 45.2 is a cross sectional view of a typical flange and the adjoining pipe. Nomenclature used shall follow that of Ref. 10 whenever possible.

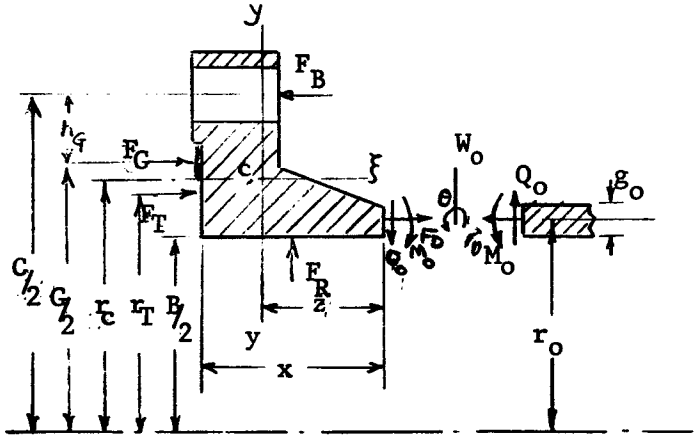

FIGURE 45.2

Cross Section of a Typical Flange, Showing Forces and Moments

The forces on the flange are bolt load F_B, gasket compression F_G, internal pressure loads F_T, F_D, F_R and the pipe reaction M_o and Q_o. All these loads are taken per circumferential length at the pipe radius r_o. Notice that the pressure loads F_T, F_D and F_R do not change with the creep of the flange connector.

Equilibrium in the axial direction gives us

$$F_G = F_B - F_T - F_D$$

or, in terms of stresses

$$\sigma_G = \frac{A_B}{A_G}\,\sigma_B - \frac{2\pi r_o}{A_G}(F_T + F_D) \tag{4}$$

In creep problems we shall most often make use of the "time-rate" equations. Differentiating Eq. (4) with respect to time, we obtain

$$\dot{\sigma}_G = \frac{A_B}{A_G}\,\dot{\sigma}_B \tag{5}$$

The resultant moment of the forces about the centroid C is

$$M_t = F_B(\tfrac{G}{2} - r_c) - F_G(\tfrac{G}{2} - r_c) + F_T(r_c - r_T) + F_R(z - \tfrac{x}{2}) + F_D(r_c - r_o) - Q_o z - M_o \tag{6}$$

The moment M_o and shear Q_o due to the pipe reaction are related to the rotation of the flange and the radial deflection at the junction of pipe and flange W_o by (Ref. 9)

$$\theta = \frac{1}{2\beta^2 D}(2\beta M_o - Q_o) \tag{7}$$

$$W_o = \frac{1}{2\beta^3 D}(-\beta M_o + Q_o) \tag{8}$$

where

$$\beta = \frac{\sqrt[4]{3(1-\mu^2)}}{\sqrt{r_o g_o}}$$

The radial deflection is the result of the flange rotation and hoop extension, i.e.

$$W_o = z\theta + (e_c + \epsilon_c - e_p - \epsilon_p) r_c \tag{9}$$

where e_c and ϵ_c are elastic and creep hoop strains of the flange and e_p and ϵ_p are elastic and creep hoop strains of the pipe. Solving for M_o and Q_o from Eqs. (6), (7), and (8) we obtain

$$Q_o = 2\beta^2 D\left\{\theta(1+2z\beta) + 2\beta r_c\,(e_c + \epsilon_c - e_p - \epsilon_p)\right\} \tag{10}$$

$$M_o = 2\beta D\left\{\theta(1+z\beta) + \beta r_c(e_c + \epsilon_c - e_p - \epsilon_p)\right\} \tag{11}$$

The elastic hoop strains are related to the hoop stress by Hooke's law, i.e.

$$e_c = \frac{\sigma_c}{E_F} \tag{12}$$

$$\simeq \frac{(F_R - Q_o)}{E_F A_F} r_o r_c \tag{12a}$$

and

$$e_p = \frac{\sigma_p}{E_p} = \frac{PB}{2E_p g_o} \tag{13}$$

From Eqs. (10) and (12a) we obtain the following relation between the rotation θ and the hoop stress σ_c

$$\theta = \frac{1}{1+2z\beta} \left\{ - c \left[\frac{A_F}{2\beta^2 D r_o r_c} + \frac{2\beta r_c}{E_F} \right] + \frac{F_R}{2\beta^2 D} - 2\beta r_c (\epsilon_c - e_p - \epsilon_p) \right\} \tag{14}$$

Alternatively the angle of rotation θ can be related to the stresses and strains in the flange. On account of rotational symmetry, the flange cross section will remain in its diametral plane during deformation. Therefore the strain at any point can be written as the sum of a "twisting" part and a "hoop extension" part, or

$$(e_F + \epsilon_F) = \frac{\xi}{r_c} \theta + (e_c + \epsilon_c) \tag{15}$$

Using Hooke's law, we can rewrite Eq. (15) as

$$\theta = \frac{r_c}{\xi} \left[\frac{1}{E_F} (\sigma_F - \sigma_c) + (\epsilon_F - \epsilon_c) \right] \tag{16}$$

111

Notice that the angle of rotation θ, and therefore the left-hand side of Eq. (15), is independent of the location at which σ_F and ϵ_F^* are evaluated. From Eqs. (14) and (16) we obtain the following relation between σ_F and σ_c.

$$\sigma_F = \sigma_c \left\{1-\frac{\xi/r_c}{1+2z\beta}\left[\frac{E_F A_F}{2\beta^2 D r_o r_c} + 2\beta r_c\right]\right\} - E_F\epsilon_F + E_F\epsilon_c\left\{1 - \frac{\xi/r_c}{1+2z\beta}(2\beta r_c)\right\}$$
$$+ \frac{E_F \xi/r_c}{1+2z\beta}(2\beta r_c)(e_p+\epsilon_p) + \frac{E_F \xi/r_c}{1+2z\beta}\frac{F_R}{2\beta^2 D} \qquad (17)$$

or

$$\dot{\sigma}_F = \dot{\sigma}_c \left\{1 - \frac{\xi/r_c}{1+2z\beta}\left[\frac{E_F A_F}{2\beta^2 D r_o r_c} + 2\beta r_c\right]\right\}$$
$$-E_F\dot{\epsilon}_F + E_F\dot{\epsilon}_c\left[1 - \frac{\xi/r_c}{1+2z\beta}(2\beta r_c)\right] \qquad (18)$$
$$+ \frac{E_I \xi/r_c}{1+2z\beta}(2\beta r_c \dot{\epsilon}_p)$$

The resultant moment of the stresses in the flange cross section about the y axis is

$$M_y = \int_{-x+z}^{z} \int_{y=y(\xi)} \sigma_F \xi dy d\xi \qquad (19)$$

which should balance the external moment. It can be easily shown from equilibrium that

$$M_t = \frac{M_y}{r_o} = \frac{1}{r_o}\int_{-x+z}^{z} \int_{y=y(\xi)} \sigma_F \xi dy d\xi \qquad (20)$$

Differentiating Eq. (6) with respect to time and making use of Eqs. (10), (12), (14) and (20) we obtain

$$\int_{-x+z}^{z} \int_{y=y(\xi)} \dot{\sigma}_F \, \xi \, dy d \, \xi = \dot{\sigma}_B \frac{A_B(\frac{C}{2}-r_c)}{2\pi} - \dot{\sigma}_G \frac{A_G(\frac{G}{2}-r_c)}{2\pi}$$

$$+ \dot{\sigma}_c \left\{ \frac{A_F}{r_c} \left[z + \frac{1}{2\beta}\left(1 + \frac{1}{(1+2z\beta)}\right)\right] + \frac{2\beta^2 D r_o r_c}{E_F(1+2z\beta)} \right\} \qquad (21)$$

$$+ \frac{2\beta^2 D r_o r_c}{1+2z\beta} (\dot{\epsilon}_c - \dot{\epsilon}_p)$$

Eqs. (5), (18) and (21) are three equations for the four unknown stress rates, $\dot{\sigma}_B$, $\dot{\sigma}_G$, $\dot{\sigma}_c$ and $\dot{\sigma}_F$. Another equation involving these unknowns can be obtained from the compatibility condition that the length of the bolt is equal to the length of the compressed flange assembly at all times, i.e.,

$$L_B(1+e_B+\epsilon_B) = L_K(1+e_K)+L_G(1+e_G+\epsilon_G)+2L_F-2h_G\theta \qquad (22)$$

We shall assume the thickness of the flange L_F remains unchanged. Differentiating with respect to time, and making use of Hooke's law and Eq. (14), we obtain

$$\frac{\dot{\sigma}_B}{E_B} + \dot{\epsilon}_B = \frac{L_K}{L_B}\left[\frac{\dot{\sigma}_K}{E_K} + \quad\right] + \frac{L_G}{L_B}\left[\frac{\dot{\sigma}_G}{E_G} + \dot{\epsilon}_G\right]$$

$$+ \frac{2h_G}{L_B} \frac{1}{1+2z\beta} \left\{ \dot{\sigma}_c \left[\frac{A_F}{2\beta^2 D r_o r_c} + \frac{2\beta r_c}{E_F} \right] - 2\beta r_c(\dot{\epsilon}_c - \dot{\epsilon}_p) \right\} \qquad (23)$$

Equation (23) introduces one more unknown, the rate of change of stress in the collars, $\dot{\sigma}_K$. But we have one additional condition that the bolt loads are transmitted through the collars, i.e.

$$\sigma_K = \frac{A_B}{A_K} \sigma_B$$

or

$$\dot{\sigma}_K = \frac{A_B}{A_K} \dot{\sigma}_B \qquad (24)$$

Equations (5), (18), (21), (23) and (24) are the five basic equations for the five rates of change of stresses, $\dot{\sigma}_B$, $\dot{\sigma}_G$, $\dot{\sigma}_K$, $\dot{\sigma}_c$ and $\dot{\sigma}_F$. In addition we have the following auxiliary equations for the determination of the strain rates:

$$\begin{aligned}
\dot{\epsilon}_B &= f_B(\sigma_B, \epsilon_B) \\
\dot{\epsilon}_F &= f_F(\sigma_F, \epsilon_F) \\
\dot{\epsilon}_c &= f_F(\sigma_c, \epsilon_c) \\
\dot{\epsilon}_G &= f_G(\sigma_G, \epsilon_G) \\
\dot{\epsilon}_K &= f_K(\sigma_K, \epsilon_K)
\end{aligned} \tag{25}$$

and the equations

$$\begin{aligned}
\sigma &= \int \dot{\sigma}\, dt \\
\epsilon &= \int \dot{\epsilon}\, dt
\end{aligned} \tag{26}$$

for obtaining the stresses and strains from the stress and strain rates.

45.5 Method of Solution

In general the system of equations formulated in the preceding section has to be solved using step-by-step integration starting from zero time. Even so the integration is still difficult because we do not know the distribution of the stress rate $\dot{\sigma}_F$ in the flange cross section. Should we know the distribution at any instant, we would be able to carry out the double integration in Eq. (21). Then we would be able to eliminate four unknown stress rates and obtain a single equation relating one of the stress rates to the known stresses, creep strains, and creep strain rates. From the now known stress rate we could determine the stresses, strains and strain rates at an immediate future time and the step-by-step integration could be carried out smoothly. This difficulty of not knowing the stress distribution in the flange was encountered in the early investigation by Waters (Ref. 2). Waters suggested a simple approximate method by replacing the actual stress distribution in the flange during creep by a trapezoidal distribution. It is believed that this is not an unreasonable assumption when evaluating the bending moment in Eq. (19). The trapezoidal assumption, however, violates the requirement that the right-hand side of Eq. (16) should be invariant with respect to ξ. Waters' scheme would enforce the satisfaction of Eq. (16) only at the extreme fibres of the flange cross section. The validity of this procedure seems to be rather questionable. In particular, Waters' method predicts a vanishing rate of change of bending moment at the beginning (Eq. 18, Ref. 2), which does not seem to be reasonable at all. A more reasonable method would be to require that Eq. (16) be satisfied approximately at several points in the flange cross section. But then the simplicity of Waters' method may become lost. We shall not go into this further, but shall describe a method of solution based on step-by-step integration with iteration at each step. The detailed procedure for use on a high-speed digital computer is outlined as follows:

1. Find the elastic solution, i.e., the stresses and strains at zero time. This involves the simultaneous solution of Eqs. (4), (6), (10), (11), (12), (13), (17), (20), and (22) with the creep strains equal to zero. The solution can be found easily without use of the computer.

2. Store in the memory the functional form of the creep laws $\dot{\epsilon} = f(\sigma, \epsilon)$ for the gasket, bolts, collars, flange, and pipe, either

   a. formulate subroutines for the assumed analytical expression $\dot{\epsilon} = f(\sigma, \epsilon)$, or

   b. store in the computer memory tabulated data of $\epsilon = f(\sigma, \epsilon)$ obtained from tests. If each dependent variable takes on 20 different values, the dependent variable ϵ will occupy 20x20=400 memory spaces. We shall also need to devise an interpolation formula to find the functional relation $\dot{\epsilon} = f(\sigma, \epsilon)$ at intermediate points.

3. Step-by-step integration from zero time and iteration at each step.

   a. Proceed from zero time, at each time step, assume a rate of change of bolt stress $\dot{\sigma}_B$. Substitute in Eq. (23) and find $\dot{\sigma}_C$. Then Eq. (18) gives us the variation of $\dot{\sigma}$ in the flange cross section. Substitute $\dot{\sigma}_C$ and $\dot{\sigma}_F$ thus found in Eq. (21) and solve for $\dot{\sigma}_B$. If the calculated $\dot{\sigma}_B$ agrees with the $\dot{\sigma}_B$ assumed, we have the correct solution. In general they will not agree. Then assume a new rate of change of bolt stress $\dot{\sigma}_B$ which is related in some way to the previously assumed $\dot{\sigma}_B$ and previously calculated $\dot{\sigma}_B$. Repeat the process until finally the calculated $\dot{\sigma}_B$ and assumed $\dot{\sigma}_B$ converge.

   b. From the physics of creep we should expect the rate of change of bolt stress $\dot{\sigma}_B$ to be large at first. Therefore the time step at the beginning should be small.

   c. Initial iteration may take longer, since we have no idea about the order of magnitude of $\dot{\sigma}_B$ at the very beginning.

45.6 A Numerical Example

The previous sections show that the difficulty with the creep problem lies in the bending of flanges. As a result, a high-speed computer has to be resorted to for its solution. As a relatively simple numerical example which can be solved by hand calculations we shall consider flanges as rigid and shall concern ourselves only with the creep of the bolts and the gasket. This will illustrate the effect of primary creep on stress relaxation which has been neglected by most investigators.

Let us consider the bolts used in the connector have effective length of L_B = 8 in. and are initially tightened to 40,000 psi. The gasket has 1/8 in. thickness and has four times the cross-sectional area of the bolts. The bolts are made of alloy steel obeying the following empirical creep law:

$$\epsilon_B = 10^{-5}(at^m + bt) \tag{27}$$

where t is time in hours

a, b, m are parameters having the values given in the following table:

Stress, psi	a	b	m
40,000	40.8	0.15	0.38
25,000	14.1	0.11	0.33
15,000	5.2	0.03	0.33
7,500		0.01	0.33

The gasket is made of copper obeying the following creep law (Ref. 5)

$$\epsilon_G = \begin{cases} 6.10\times10^{-8} t \sinh\frac{\sigma_G}{4150} + 5.68\times10^{-5} t^{0.21} \sinh\frac{\sigma_G}{6000}, \\ \qquad 0 \le t \le 1400 \text{ hours}, \quad \text{and} \\ 6.10\times10^{-8} t \sinh\frac{\sigma_G}{4150} + 2.6\times10^{-4} \sinh\frac{\sigma_G}{6000}, \\ \qquad t > 1400 \text{ hours}. \end{cases} \tag{28}$$

The relaxation of gasket compression due to creep can be found from the equilibrium equation

$$\sigma_G A_G = \sigma_B A_B \tag{29}$$

and the modified form of the compability equation (22)

$$L_B\left(1 + \frac{\sigma_B}{E_B} + \epsilon_B\right) = 2L_F + L_G\left(1 + \frac{\sigma_G}{E_G} + \epsilon_G\right) \tag{30}$$

where L_F is the thickness of the rigid flange. Initially the creep strain vanishes. Eq. (30) becomes

$$L_B\left(1 + \frac{\sigma_B^o}{E_B}\right) = 2L_F + L_G\left(1 + \frac{\sigma_G^o}{E_G}\right) \tag{31}$$

where σ_B^o and σ_G^o are the initial stresses in the bolts and the gasket. Therefore Eq.(30) can be written as

$$\frac{L_B}{L_G}\left[\epsilon_B - \left(\frac{\sigma_B^o - \sigma_B}{E_B}\right)\right] = \epsilon_G - \frac{\sigma_G^o - \sigma_G}{E_G} \tag{32}$$

Substituting in the dimensions and material properties of the bolts and gaskets, we obtain the following equations for Eqs. (29) and (32):

$$\sigma_B = 4\,\sigma_G \tag{29a}$$

$$64\left[\epsilon_B - \frac{\sigma_G^o - \sigma_G}{7.5\text{x}10^6}\right] = \epsilon_G - \frac{\sigma_G^o - \sigma_G}{14.1\text{x}10^6} \tag{32a}$$

Notice that in this particular example, because the bolts are long compared with the gasket thickness, while Young's modulus of bolt and gasket material are comparable, the elastic strain of the gasket is negligible. Therefore Eq. (32a) becomes approximately

$$64\left[\epsilon_B - \frac{\sigma_G^o - \sigma_G}{7.5\text{x}10^6}\right] = \epsilon_G \tag{32b}$$

where σ_G^o = 10,000 psi is the initial stress in the gasket. Eqs. (27),(28), (29a) and (32b) can be solved using step-by-step integration starting from zero time. The result of the gasket stress relaxation with time is presented in the following table.

Gasket Stress, psi	Time, hours
10,000	0
8,350	1
8,000	2
7,500	10
6,800	100
4,000	1000

During the first ten hours most of the stress relaxation occurs because of primary creep. It is somewhat unfortunate that because of the unavailability of gasket creep data, Eq. (28) for the creep of the copper gasket is chosen more or less arbitrarily. As a result, the creep resistance of the bolts and the gasket are comparable. Because the bolt length is much greater than the gasket thickness, the relaxation of gasket compression is almost entirely the result of the creep of bolts.

45. 7 Discussion

In the preceding Sections a general formulation of the creep of a flanged connector is presented. The creep laws of the components are assumed to be known. As a rule, however, only very limited material creep data are available, and they were obtained under constant-load and constant-temperature conditions. In addition the creep properties of materials are very sensitive to the temperature at elevated temperatures. Therefore, temperatures of the components of a connector have to be determined in order to predict the creep behavior accurately. Because of these uncertainties, it appears that oftentimes it is superfluous to solve the complicated complete equations using inadequate creep data while just as plausible results can be obtained based on simplified models. Some of the possible simplifications are as follows:

1. If the connector is designed for long-time service, the primary creep can be neglected. This underestimates the stress relaxation, particularly in the beginning, but becomes more accurate as time goes on. The large error in the beginning does not matter, since if there is still sufficient gasket compression at the end of the designed life, there would certainly be enough compression at the beginning.

2. As shown by our previous numerical example, because of the small thickness and lower stress of the gasket, the gasket can be neglected in calculating the relaxation of the connector if the creep and elastic properties of the gasket do not differ very much from those of the bolts.

3. In flange connectors with contacting outside the bolt circle, bending of the flange can be neglected. Since the bolt load is carried by a much larger area of the flange, the stresses in the flanges are much lower than those in the bolts. If the material of the flanges has comparable elastic and creep properties to those of the bolts, the contribution of the flange to the stress relaxation of the connector can be neglected.

4. For flanges contacting inside the bolt circle, bending of the flange is of importance. The flange contributes to both creep deflection and elastic recovery. It is known (Ref. 11) that for some cases the elastic recovery may even be more than the creep deflection so that the flange deformation actually retards the stress relaxation. Since bending of the flange is a somewhat different mechanism from the tension and compression of bolts and other members of the connector, it is not obvious how its contribution to stress relaxation compares with that of the bolts. An estimate of their relative importance can be made by the following method. Assume that the bolts and flange obey creep laws of the following form:

$$\epsilon = K\sigma_n t \tag{33}$$

A modified form of the compatibility equation (22) can be written as:

$$L_B\left[2\pi r_o \frac{F_B - F_B^o}{E_B A_B} + K_B t\left(\frac{2\pi r_o F_B}{A_B}\right)^{n_B}\right] + 2h_G(\theta - \theta_o) = 0 \tag{34}$$

The additional rotation of the flange $\theta-\theta_o$ for a simple ring flange is given by Eq.(11) of Ref. 3. Therefore, Eq. (34) becomes

$$L_B\left[\frac{W_B - W_B^o}{E_B A_B} + K_B t\left(\frac{W_B}{A_B}\right)^{n_B}\right] + 2h_G K_F t\left[\frac{W_B h_G (2)^{(1 + 1/n_F)}(1 - 1/n_F)(2 + 1/n_F)}{\left\{(d)^{(1 - 1/n)} - (c)^{(1 - 1/n)}\right\}(h)^{(2 + 1/n_F)}}\right]^{n_F} = 0 \tag{35}$$

where

L_B	=	bolt length
W_B^o	=	initial total bolt load
W_B	=	total bolt load
E_B	=	Young's modulus of bolt
A_B	=	total bolt area
K_B, n_B	=	constants in the creep law for bolts, see Eq. (33)
K_F, n_F	=	constants in the crrep law for flanges, see Eq. (33)
h_G	=	distance from gasket radius to bolt radius
t	=	time
d	=	outside radius of flange
c	=	inside radius of flange
h	=	flange thickness

If the last term in the above equation is smaller than either of the first two terms then the contribution of the flange to stress relaxation is negligible. For hubbed flanges the last term should even be smaller.

In conclusion we may state that for very critical applications the complete equations formulated in the preceeding sections shall be solved to determine the relaxation of a flanged connector with time. In most other cases the complete equations can be simplified. The contribution of bolt relaxation should always be considered. But some other members of the connector may be neglected. A judgement based on the knowledge of the geometrical and material properties is needed. For members subjected to simple tension and compression, the judgement is comparatively easy. However, care should be exercised that it is not only the creep but also the elastic recovery that controls the relaxation of a connector. The relative importance of the bending of flanges is more difficult to judge. Eq. (35) furnishes us a means to determine whether flange bending is of importance to the relaxation of a fluid connector.

45.8 References

1. K. Baumann, "Some Considerations Affecting the Future Development of the Steam Cycle," Engineer, Vol. 130, Nov. 7, 1930, p. 600. See also, G. H. MacCullough, "Applications of Creep Tests," Trans. ASME, Vol. 55, 1933, p. APM 55-12

2. E. O. Waters, "Analysis of Bolted Joints at High Temperature," Trans. ASME, Vol. 60, 1938.

3. J. Marin, Discussion of "Formulas for Stresses in Bolted Flanged Connections," Trans. ASME, Vol. 60, 1938, p. 271.

4. S. Timoshenko, Strength of Materials, Part II, 3rd Edition, 1958, Van Nostrand. p. 527-533.

5. E. P. Popov, "Correlation of Tension Creep Tests with Relaxation Tests," J. of Applied Mechanics, Vol. 14, No. 2, 1947, p. A-135 - A-142.

6. A. M. Freudenthal, The Inelastic Behavior of Engineering Materials and Structures, Wiley, 1950.

7. I. Finnie and W. R. Heller, Creep of Engineering Materials, McGraw-Hill, 1959.

8. Y. N. Rabotnov, "Some Problems of the Theory of Creep," NACA TM 1353, April 1953.

9. S. Timoshenko and S. Woinowsky-Kreiger, Theory of Plates and Shells, 2nd Edition, McGraw-Hill, 1959.

10. W. M. Dudley, "Deflection of Heat Exchanger Flanged Joints as Affected by Barreling and Warping," J. of Eng. for Industry, Nov. 1961, pp. 460-465.

11. R. W. Bailey, "Flanged Pipe Joints for High Pressures and Temperatures," Engineering, 1937.

46. BOLT FORCE TO FLATTEN WARPED FLANGES

by

S. Levy

46.0 Summary

Initial lack of flatness of the flanges of pipe connectors can result in leakage if the bolt loads are not sufficient to achieve positive gasket compression at all points on the circumference. Equations are presented for computing the magnitude of the bolt load necessary to flatten the flange. Account is taken of the bending and twisting resistance of the flange itself, the restraint afforded by the pipe, and the fact that the bolt circle is displaced from the gasket circle. The analysis applies to flanges whose warping can be adequately described by considering it to vary as cos 2θ. Numerical examples are considered for several typical flanges.

46.1 Nomenclature

A, B	integration constants
C	centroid of flange cross section
E	Young's Modulus (lb/in^2)
F_B	bolt load (lb/in.)
F_G	gasket force (lb/in.)
F_P	pipe force (lb/in.)
G	shear modulus ($lb/in.^2$)
I_1, I_2	principal moments of inertia of flange cross section (in^4)
GJ	torsional stiffness
M_ξ, M_η, M_ζ	moments (lb/in)(Fig. 46.2)
$N_z, N_{z\theta}, N_\theta$	forces in pipe walls (lb/in)(Fig. 46.3)
R_B	radius of bolt circle (in.)
R_G	radius of gasket circle (in.)
R_T	radius at flexural center T (Fig. 46.1) (in.)
R	radius of mid-thickness of pipe (in.)
t	pipe wall thickness (in.)
T	flexural center of flange cross-section
w	warping displacement (in.)
z	axial coordinate along pipe (in.)
α	angular coordinate (Fig. 46.2)
β	parameter (Eq. 22)(1/in.)
γ	angle between ξ and 1 axes (Fig. 46.1)
$\gamma_{z\theta}$	shear strain in pipe wall
δ_r, δ_θ	radial and circumferential displacements (in.)
ξ, η, ζ	coordinates (Fig. 46.2)
ϵ_z	axial strain in pipe wall
θ	angular coordinate (Fig. 46.2)
ϕ	axial load function (lb/in.)
ν	Poisson's ratio, taken as 0.25.

46.2 Introduction

Many aspects of the rational design of flanged joints are considered in the ASME's Pressure Vessels and Piping Design Collected Papers 1927-1959. This work is all based on the assumption of circular symmetry. It provides formulas for stress and deformation for the many loading conditions where circular symmetry is present. Experience shows, however, that the contact surfaces of flanges may deviate from a plane either due to machining tolerances or due to distortions in service. Dudley (Ref. 1) considered the bolt loads necessary to overcome this warping and attain a flat contact surface on the assumption that the flange and pipe wall could be considered developed into a flat surface. Waters (Ref. 2) in discussing Dudley's paper, and Dudley in replying, indicated that when twisting due to three-dimensional loads is considered, the Dudley analysis somewhat overestimates the bolt stress required for flattening. This section takes better account of the three-dimensional nature of the problem and does, in fact, show substantially lower bolt stresses than would be predicted from Dudley's analysis. It does, however, make use of some substantial simplifying assumptions. They are: (1) that the flange is sturdy and does not change cross-sectional shape; and (2) that the resistance of the pipe to bending into an oval shape is all due to hoop bending.

The equations are based on elastic theory and do not consider possible yielding. It is assumed that the pipe length is long enough to prevent deformations at one flange from affecting the flange at the other end of the pipe. (The solution shows that a pipe more than several diameters long should achieve this.)

The analysis considers only the case where warping varies as cos 2θ whereas the actual warping would ordinarily have higher frequency components. The higher-frequency terms can be computed from Dudley's solution with good accuracy.

46.3 Strain Energy in Flange

Fig. 46.1 is a cross-sectional view of a typical flange and shell. The increment in forces acting on the flange and hub to counteract warping are the bolt force F_B, the gasket force F_G, and the force F_P between hub and pipe. All these forces are taken per circumferential inch. The forces are all considered to vary as cos 2θ circumferentially, giving

$$\begin{aligned} F_B &= F_{B\ Max} \cos 2\theta \\ F_G &= F_{G\ Max} \cos 2\theta \\ F_P &= F_{P\ Max} \cos 2\theta \end{aligned} \tag{1}$$

These forces cause the flange to twist about its axis, ζ in Fig. 46.2 and to bend out of its plane about the ξ axis and in its plane about the η axis.

Considering a cross-section at D, Fig. 46.2, and taking coordinate axes as shown, the increments in the moment about D due to a force F_B are:

$$\begin{aligned} dM_\xi &= -F_B R_B^2 \sin(\theta-\alpha)\,d\alpha \\ dM_\eta &= 0 \\ dM_\eta &= F_B R_B \left[R_T - R_L \cos(\theta - \alpha)\right] d\alpha \end{aligned} \tag{2}$$

Similar equations apply for F_G and F_D. We can show by integration and symmetry that

$$\begin{aligned} M_\xi &= (1/3\left[F_{B\ Max} R_B^2 - F_{G\ Max} R_G^2 - F_{P\ Max} R^2\right] \cos 2\alpha \\ M_\eta &= 0 \\ M_\zeta &= (1/6)\left[F_{B\ Max} R_B^2\left(\frac{4R_B - 3R_T}{R_B}\right)\right. \\ &\qquad \left. - F_{G\ Max} R_G^2\left(\frac{4R_G - R_T}{R_G}\right) - F_{P\ Max} R^2\left(\frac{4R - R_T}{R}\right)\right] \sin 2\alpha \end{aligned} \tag{3}$$

Since ξ and η are not the principal bending axes of the cross-section the moments must be resolved along these axes in determining deformations. The component M_η is of course zero. The component of M_ξ along principal axis 1, Fig. 46.1, is $M_\xi \cos\gamma$ while that along principal axis 2 is $M_\xi \sin\gamma$. The strain energy stored in the flange is

$$U = \int_0^{2\pi} \left[\frac{M_\xi^2}{2E}\left(\frac{\cos^2\gamma}{I_1} + \frac{\sin^2\gamma}{I_2}\right) + \frac{M_\zeta^2}{2GJ}\right] R_T\,d\alpha \tag{4}$$

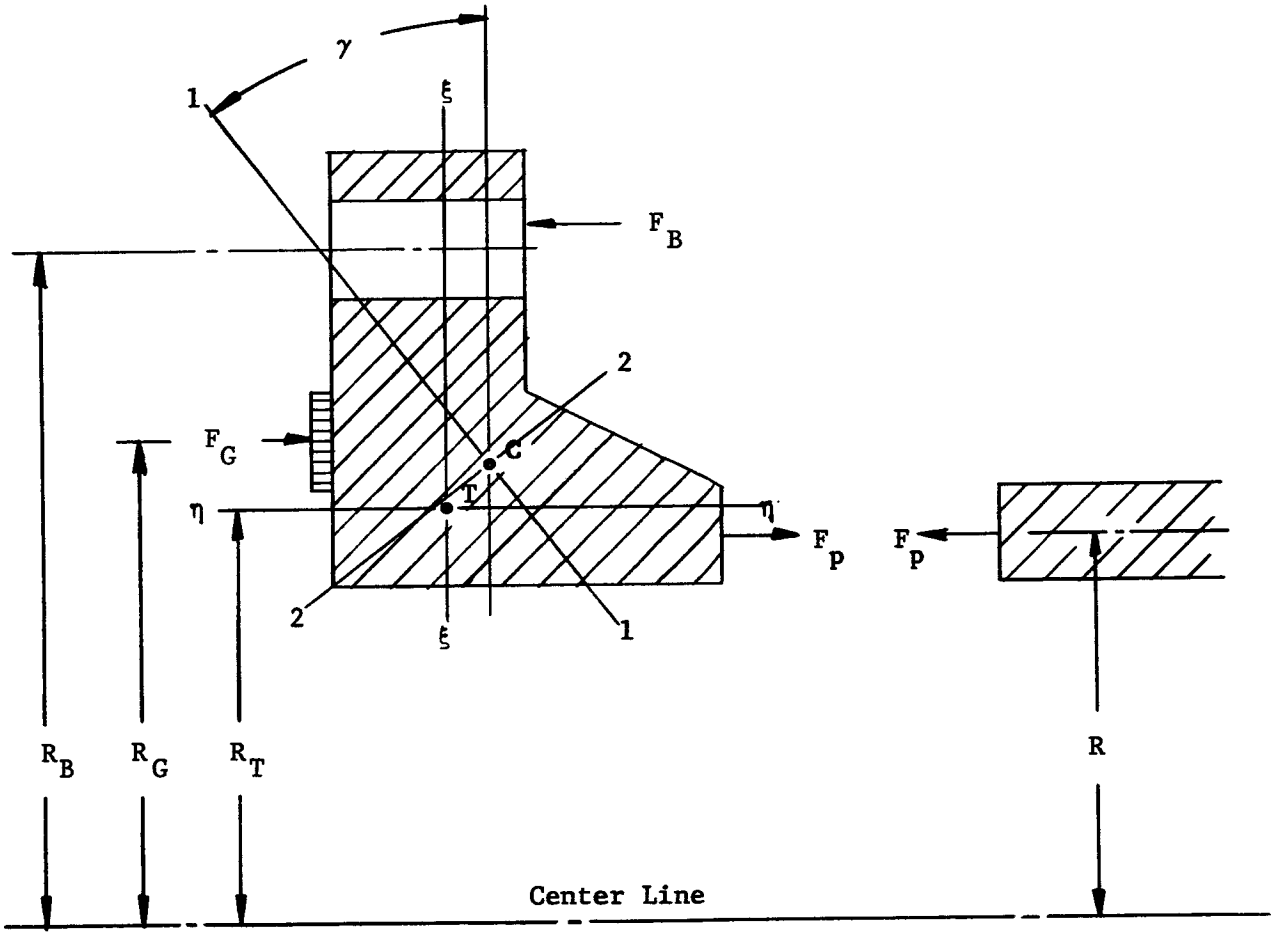

FIG. 46.1 Cross-section of typical flange showing forces

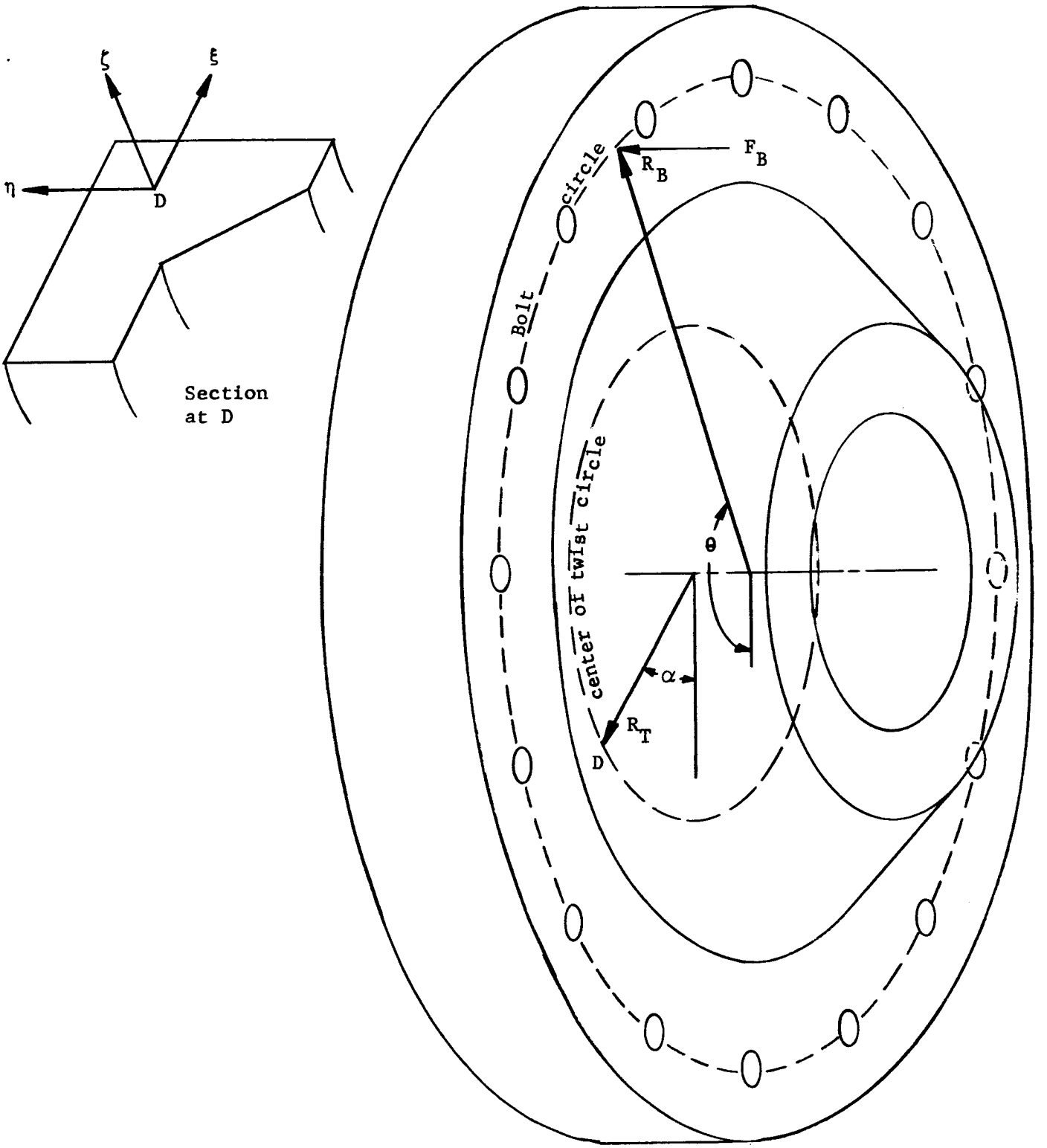

FIG. 46.2 Coordinates for flange bending and twisting

The first term is the contribution due to bending about the 1 axis, Fig. 46.1. The second term is that due to bending about the 2 axis. The third term is the energy stored due to twisting about point T, Fig. 46.1. Substituting (3) into (4), integrating, and taking the partial derivatives with respect to the generalized forces gives

$$w_{B\ Max} = \frac{\partial U}{\pi R_B \partial F_{B\ Max}} = \frac{R_T}{9E}\left(\frac{\cos^2\gamma}{I_1} + \frac{\sin^2\gamma}{I_2}\right)\left[F_{B\ Max} R_B^3 - F_{G\ Max} R_B R_G^2 - F_{P\ Max} R_B R^2\right]$$
$$+ \frac{R_T}{36GJ}\left[F_{B\ Max} R_B^3\left(\frac{4R_B - 3R_T}{R_B}\right)^2 - F_{G\ Max} R_B R_G^2\left(\frac{4R_B - 3R_T}{R_B}\right)\left(\frac{4R_G - 3R_T}{R_G}\right)\right.$$
$$\left. - F_{P\ Max} R_B R^2\left(\frac{4R_B - 3R_T}{R_B}\right)\left(\frac{4R - 3R_T}{R}\right)\right] \qquad (5a)$$

$$w_{G\ Max} = \frac{\partial U}{\pi R_G \partial F_{G\ Max}} = \frac{R_T}{9E}\left(\frac{\cos^2\gamma}{I_1} + \frac{\sin^2\gamma}{I_2}\right)\left[- F_{B\ Max} R_B^2 R_G + F_{G\ Max} R_G^3 + F_{P\ Max} R_G R^2\right]$$
$$+ \frac{R_T}{36GJ}\left[- F_{B\ Max} R_B^2 R_G\left(\frac{4R_B - 3R_T}{R_B}\right)\left(\frac{4R_G - 3R_T}{R_G}\right) + F_{G\ Max} R_G^3\left(\frac{4R_G - 3R_T}{R_G}\right)^2\right.$$
$$\left. + F_{P\ Max} R_G R^2\left(\frac{4R_G - 3R_T}{R_G}\right)\left(\frac{4R - 3R_T}{R}\right)\right] \qquad (5b)$$

$$w_{P\ Max} = \frac{\partial U}{\pi R \partial F_{P\ Max}} = \frac{R_T}{9E}\left(\frac{\cos^2\gamma}{I_1} + \frac{\sin^2\gamma}{I_2}\right)\left[- F_{B\ Mas} R_B^2 R + F_{G\ Max} R_G^2 R + F_{P\ Max} R^3\right]$$
$$+ \frac{R_T}{36GJ}\left[- F_{B\ Max} R_B^2 R\left(\frac{4R_B - 3R_T}{R_B}\right)\left(\frac{4R - 3R_T}{R}\right)\right.$$
$$\left. + F_{G\ Max} R_G^2 R\left(\frac{4R_G - 3R_T}{R_G}\right)\left(\frac{4R - 3R_T}{R}\right) + F_{P\ Max} R^3\left(\frac{4R - 3R_T}{R}\right)^2\right] \qquad (5c)$$

where

$$w_B = w_{B\ Max} \cos 2\theta$$
$$w_G = w_{G\ Max} \cos 2\theta$$
$$w_P = w_{P\ Max} \cos 2\theta \qquad (6)$$

The positive directions of the flange warping deflections is in the same sense as the corresponding forces in Fig. 46.1.

46.4 Stress and Deformation of Pipe

Fig. 46.3 is an element of the wall of the pipe. We take z as axial coordinate, positive away from the flange, θ as angular coordinate, and R as radius to mid-thickness of wall. N, with suitable subscript, denotes the load per unit length. Equilibrium in the z- and θ- directions gives,

$$\frac{\partial N_{z\theta}}{R\partial\theta} + \frac{\partial N_z}{\partial z} = 0 \tag{7a}$$

$$\frac{\partial N_\theta}{R\partial\theta} + \frac{\partial N_{z\theta}}{\partial z} = 0 \tag{7b}$$

At $z = 0$ we know from Eq. (1) that N_z, which equals F_p, varies as cos 2θ. We will see if all equations can be satisfied by taking

$$N_z = \emptyset(z) \cos 2\theta \tag{8}$$

where $\emptyset$ is a function of z only. Substituting Eq. (8) into Eq. (7a) and integrating, with the integration constant zero since there is no net torque on the pipe, gives

$$N_{z\theta} = \frac{-R}{2}\frac{d\emptyset}{dz} \sin 2\theta \tag{9}$$

Substituting Eq. (9) into Eq. (7b) and integrating with the integration constant zero, since internal pressure is considered separately,

$$N_\theta = -\frac{R^2}{4}\frac{d^2\emptyset}{dz^2} \cos 2\theta \tag{10}$$

We next consider an elemental ring from the pipe formed by cutting out a length Δz. This ring will have acting on it a differential shear

$$\Delta q = \frac{\partial N_{z\theta}}{\partial z}\Delta z = -\left[\frac{R}{2}\frac{d^2\emptyset}{dz^2} \sin 2\theta\right]\Delta z \tag{11}$$

The ring will distort to an elliptical shape as a result of this differential shear. The resulting displacements are

$$\delta_\theta = \delta_{\theta\ \mathrm{Max}} \sin 2\theta$$

$$\delta_r = -\delta_{\theta\ \mathrm{Max}} \cos 2\theta \tag{12}$$

The work done by the shear in distorting the ring is

$$\Delta W = \frac{1}{2}\int_0^{2\pi} \Delta q \delta_\theta R d\theta = -\frac{\pi R^2}{4}\left[\delta_{\theta\ \mathrm{Max}}\frac{d^2\emptyset}{dz^2}\right]\Delta z \tag{13}$$

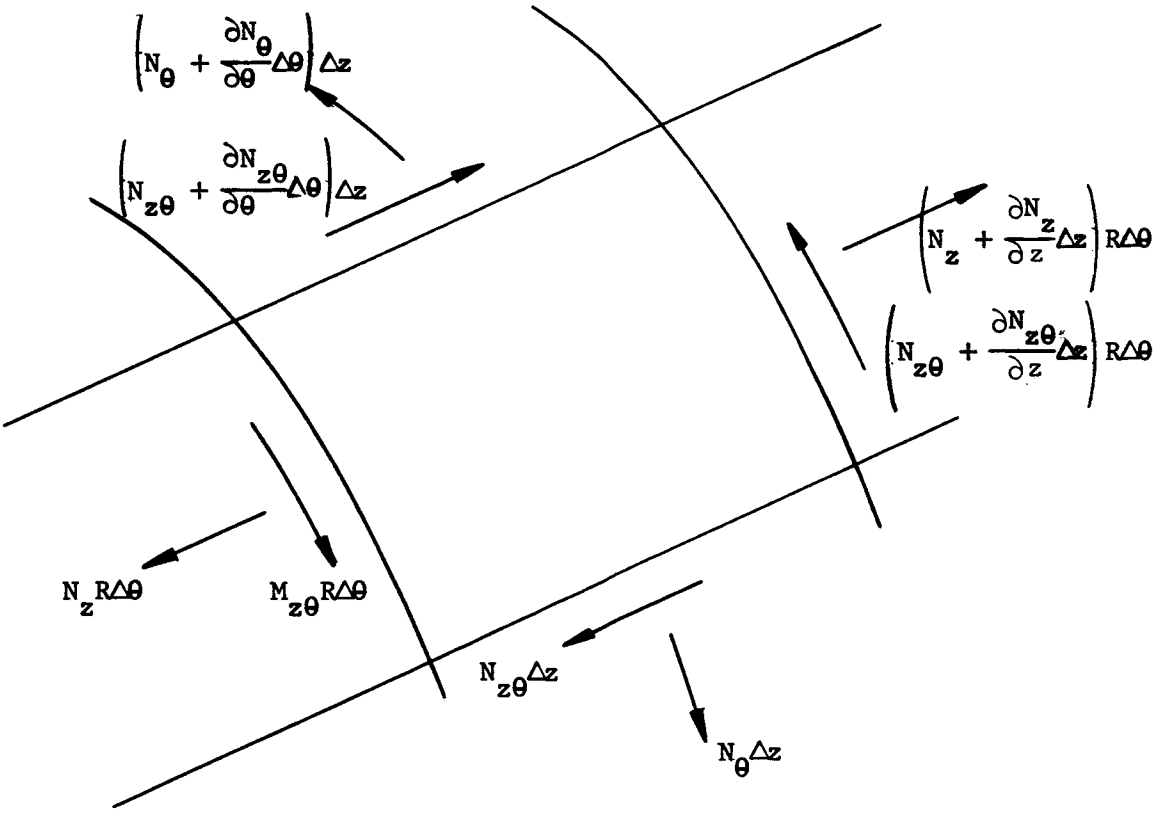

FIG. 46.3 Element of pipe wall showing membrane forces

This must equal the energy stored in hoop bending of the ring

$$\Delta W = \frac{1}{2}\int_0^{2\pi}\left[\frac{Et^3\Delta z}{12(1-\nu^2)}\right]\left(\frac{\partial^2\delta_r}{R^2\partial\theta^2}\right)Rd\theta = \frac{2\pi}{3R^3}\left(\frac{Et^3}{1-\nu^2}\right)\delta^2_{\theta\ Max}\,\Delta z \qquad (14)$$

(In obtaining Eq. 14 it has been assumed that the variation of δ_r axially is much more gradual than it is circumferentially so that the energy stored as a result of axial curvature and twisting of the pipe wall can be omitted.) Equating the values of ΔW in Eqs. (13) and (14) gives

$$\delta_{\theta\ Max} = -\frac{3R^5}{8}\left(\frac{1-\nu^2}{Et^3}\right)\frac{d^2\phi}{dz^2} \qquad (15)$$

The shear strain in the wall is given by

$$\frac{N_{z\theta}}{Gt} = \gamma_{z\theta} = \frac{\partial\delta_\theta}{\partial z} + \frac{\partial w}{R\partial\theta} \qquad (16)$$

where w is the out-of-plane distortion, Fig. 46.4.

Substituting from Eqs. (9), (12) and (15) into (16) and integrating gives

$$w = \left[\frac{R^2}{4Gt}\left(\frac{d\phi}{dz}\right) - \frac{3R^6}{16}\left(\frac{1-\nu^2}{Et^3}\right)\frac{d^3\phi}{dz^3}\right]\cos 2\theta \qquad (17)$$

where the integration constant, which corresponds to axial displacements of the entire cross-section, is omitted.

The axial strain is given by

$$\frac{N_z - \nu N_\theta}{Et} = \epsilon_z = \frac{\partial w}{\partial z} \qquad (18)$$

Substituting Eqs. (8), (10) and (17) into (18) and setting $\nu = 0.25$ gives,

$$\frac{R^6}{t^2}\frac{d^4\phi}{dz^4} - 3.20R^2\frac{d^2\phi}{dz^2} + 5.70\phi = 0 \qquad (19)$$

The corresponding auxiliary equation is

$$\frac{R^6m^4}{t^2} - 3.20\frac{t}{R}\left(\frac{R^3m^2}{t}\right) + 5.70 = 0 \qquad (20)$$

Solving, $m = \pm 1.265(t/R^2)\sqrt{1 \pm \sqrt{1-2.225R^2/t^2}}$

$$\simeq \pm 1.265(t/R^2)\sqrt[4]{-2.225R^2/t^2}$$

$$= (\pm 1 \pm \sqrt{-1})(1.091\sqrt{t/R^3}) \qquad (21)$$

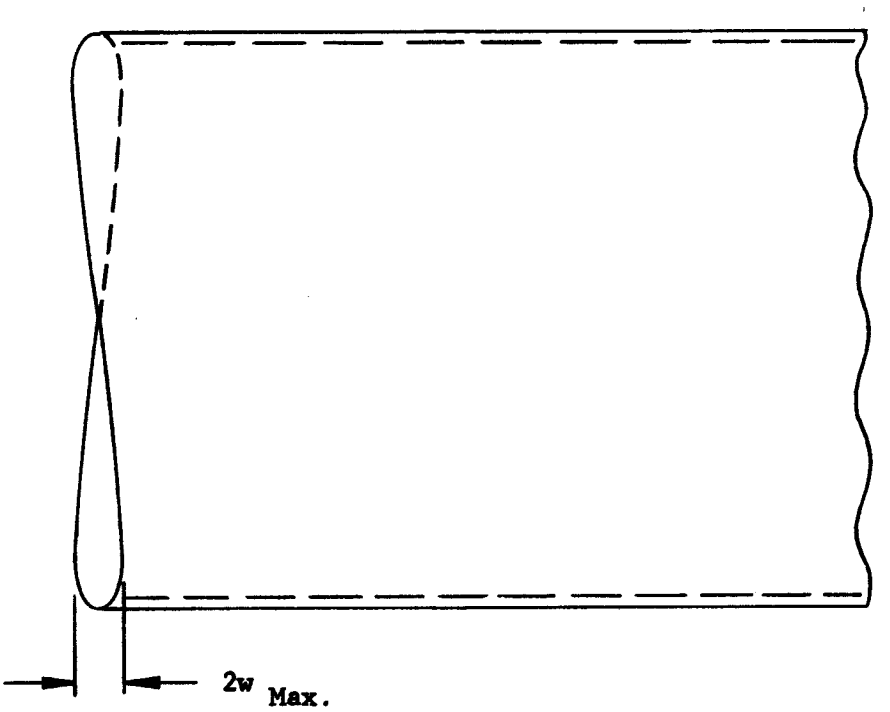

FIG. 46.4 Out-of-plane distortion

where the approximation is excellent for the usual case where R is much larger than t. If we require ϕ to remain finite for large values of z we need consider only the roots having a negative real part. The solution of Eq. (19) is therefore

$$\phi = e^{-\beta z} (A \cos \beta z + B \sin \beta z) \tag{22}$$

where $\beta = 1.091\sqrt{t/R^3}$

and A and B are arbitrary constants satisfying conditions at the flange.

Substituting Eq. (22) into Eq. (15) and the result into Eq. (12) gives

$$\delta_r(z=0) = -0.839\left(\frac{BR^2}{Et^2}\right) \cos 2\theta \tag{23}$$

It can be shown that the hoop bending stiffness of the flange is usually so much greater than that of the pipe that $\delta_r(z = 0)$ is very small and B is negligible compared with A. With this Eq. (22) becomes

$$\phi = Ae^{-\beta z} \cos \beta z \tag{24}$$

Substituting Eq. (24) into Eq. (17) with $\nu = 0.25$ gives

$$w_p = w(z = 0) = -0.681\frac{A}{E}\sqrt{\frac{R}{t}}(1+ 0.670\frac{R}{t}) \cos 2\theta \tag{25}$$

Substituting Eq. (24) into (8) gives

$$F_p = N_z(z = 0) = A \cos 2\theta \tag{26}$$

Since the displacement of the pipe and flange are the same at their junction and the forces are in equilibrium, Fig. 46.1, we see from Eqs. (1), (6), (25) and (26)

$$w_{P\ Max} = -.681\sqrt{R/t}\ (1 + 0.670R/t)F_{P\ Max}/E \tag{27}$$

46.5 Interaction of Pipe and Flange

A sufficient additional bolt force is applied to correct the initial warping deflection at the gasket. When this is done the flange will be flat at the gasket location and the gasket force will have no variable component,

$$F_G = 0 \tag{28}$$

The magnitude of the pipe force will be such that the deflections given by (5c) and (27) are equal. Equating these and using (28) gives

$$\frac{F_{P\ Max}}{F_{B\ Max}} = \frac{R_B^2\left[\frac{\cos^2\gamma}{I_1} + \frac{\sin^2\gamma}{I_2} + \frac{E}{4GJ}\left(\frac{4R_B - 3R_T}{R_B}\right)\left(\frac{4R - 3R_T}{R}\right)\right]}{\frac{6.12}{RR_T}\left(1 + 0.670\frac{R}{t}\right)\sqrt{\frac{R}{t}} + R^2\left(\frac{\cos^2\gamma}{I_1} + \frac{\sin^2\gamma}{I_2}\right) + \frac{E}{4GJ}(4R - 3R_T)^2} \tag{29}$$

Substituting Eq. (28) into (5b) gives the correction of warping displacement as a function of bolt force

$$\frac{w_{G\ Max}}{F_{B\ Max}} = -\frac{R_B^2 R_G R_T}{9E}\left[\frac{\cos^2\gamma}{I_1} + \frac{\sin^2\gamma}{I_2} + \frac{E}{4GJ}\left(\frac{4R_B - 3R_T}{R_B}\right)\left(\frac{4R_G - 3R_T}{R_G}\right)\right]$$
$$+ \frac{F_{P\ Max}}{F_{B\ Max}}\left(\frac{R^2 R_G R_T}{9E}\right)\left[\frac{\cos^2\gamma}{I_1} + \frac{\sin^2\gamma}{I_2} + \frac{E}{4GJ}\left(\frac{4R - 3R_T}{R}\right)\left(\frac{4R_G - 3R_T}{R_G}\right)\right] \tag{30}$$

For a given corrective warping displacement $w_{G\ Max}$, Eqs. (29) and (30) can be used to determine $F_{P\ Max}$ and $F_{B\ Max}$. Eqs. (3) then give the corresponding maximum bending and twisting moments in the flange.

46.6 Examples

The use of the equations will be clarified by several examples.

(a) A flange requires a warping displacement $w_{G\ Max} = -0.020$ in/2 = -0.010 in. to achieve flatness. Values of the dimensional constants for the flange and pipe are

$R_B = 21$ in. $\qquad R_T = 19.0$ in.

$R_G = 19.5$ in. $\qquad R = 17.84$ in.

$t = 1.00$ in. $\qquad E/G = 2.5$

$E = 30{,}000{,}000$ lb/in.^{2} $\qquad J = 88$ in.^{4}

$(\cos^2 \gamma/I_1 + \sin^2 \gamma/I_2) = 1/(52\ \text{in.}^4)$

Using Eq. (29)

$$(F_{P\ Max}/F_{B\ Max}) = 1.381$$

Using Eq. (30)

$$(w_{G\ Max}/F_{B\ Max}) = -2.3 \times 10^{-6}\ \text{in.}^2/\text{lb}$$

With the given value of $w_{G\ Max}$ and E

and $F_{B\ Max} = +4400$ lb/in

$F_{P\ Max} = +6000$ lb/in

This is about one-third the value given in Ref. 1 for a similar problem. In this example the pipe provides high restraint of the flange at the pipe-flange interface.

(b) Consider example (a) with R_G changed to 17.84 in. In that case $(F_{P\ Max}/F_{B\ Max}) = 1.381$, $(w_{G\ Max}/F_{B\ Max}) = -1.52 \times 10^{-6}\ \text{in}^2/\text{lb}$

$$F_{B\ Max} = 6600\ \text{lb/in, and } F_{P\ Max} = 9100\ \text{lb/in}$$

Thus moving the gasket location inwards increases the required bolt load.

(c) Consider example (a) with t changed to 0.5 in. In that case $(F_{P\ Max}/F_{B\ Max}) = 1.128$, $(w_{G\ Max}/F_{B\ Max}) = -5.26 \times 10^{-6}\ \text{in}^2/\text{lb}$

$$F_{B\ Max} = 1900\ \text{lb/in, and } F_{P\ Max} = 2100\ \text{lb/in}$$

The reduction in pipe wall thickness in this case gives a nearly proportionate reduction in bolt force.

46.7 Discussion

Equations have been derived from which the additional bolt force to correct warping at the gasket can be computed. Equations are also given for the increment in moment in the flanges. In an example, comparable to that given by Dudley, Ref. 1, the bolt loads were about one-third of those given by him. This reduction seems reasonable for the use of a three-dimensional rather than a two-dimensional model. Additional examples show that the necessary bolt load is least when the gasket is nearest the bolts. They also show, for the cases chosen, that reductions in the pipe wall thickness give almost proportionate reductions in the necessary bolt loads. The stresses obtained, though lower than those given by Dudley, are still so high that his comment, "any unequal warping of mating surfaces is evidently a serious problem," must be taken as a guide. Experimental confirmation of the equations is desirable because of the simplifying assumptions regarding cross-sectional distortion of the flange and bending energy in the pipe wall.

It will ordinarily not be necessary to get the gasket circle completely flat in order to achieve adequate sealing. The permissable initial warping will depend not only on the gasket requirements but also on the available additional load capacity of the bolts and flanges over that already imposed by the usual axisymmetric loading. Where the permissable variation in gasket force is significant Eqs. (28) and (30) can be appropriately modified with little difficulty.

46.8 References

1. W.M. Dudley, "Deflection of Heat Exchanger Flanged Joints as Affected by Barreling and Warping", Trans. A.S.M.E., Journal of Engineering for Industry, Vol. 83, Series B, No. 4, Nov. 1961, pp. 460-466.

2. E.O. Waters, Discussion of above paper, loc. cit.

138

47. EFFECT OF BENDING MOMENT AND MISALIGNMENT ON FLANGE CONNECTORS

by

B. T. Fang

47.0 Summary

Bending loads on the pipe and flange assembly will result in an uneven distribution of bolt loads and gasket compression. At the location where the gasket compression falls below the internal pressure, leakage is likely to occur.

If the flange surface is assumed to remain plane during bending, simple relations are obtained which relate the changes in the bolt load and gasket compression to the bending moment and the component stiffnesses. However, bending moment also changes the originally uniform flange "rolling moment" to a variable twisting moment and causes twist of the flanges. The determination of the twist of flanges is comparatively complex. The governing equations are given and a numerical example is computed. The result shows that the relief of gasket compression due to flange twist is more than that due to simple bending and should not be neglected. This does not seem to have attracted the attention of previous investigators. It is highly desirable that experimental work be undertaken to substantiate this finding.

When pipe misalignment exists, an uneven bolt load is needed to bring the flanges together and secure a uniform gasket compression. This is a consideration to be kept in mind when a torque wrench is used to tighten the bolts.

47.1 Effect of Bending Moment

It is well known that even a moderate bending moment influences the sealing ability of a flange connector considerably (Ref. 1). Essentially, the bending moment changes the distribution of gasket compression, relieving the compression at some places and increasing the compression at other places. Leaking passages are likely to form at those places where the gasket compression falls below the internal pressure.

The redistribution of the gasket compression and the bolt load can be found as follows:

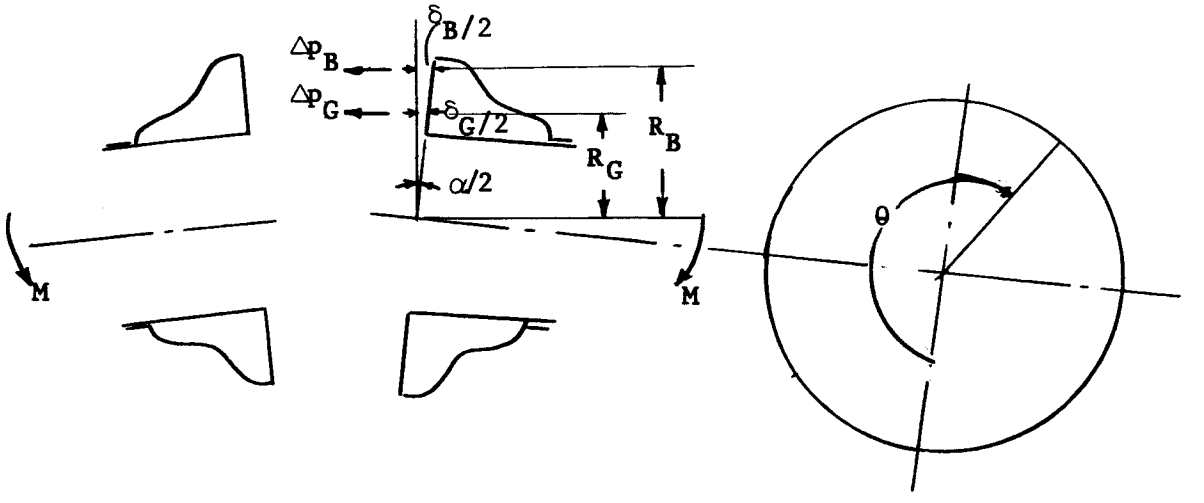

140

Prior to the application of the bending moment, the bolt load is P_B (lb/in) and the gasket compression P_G (lb/in). Ideally, these loads are uniform, and the two faces of the flanges are parallel. When a moment M is now applied, the two flanges will rotate with respect to each other. If the flange surfaces are assumed to remain plane, the elongation of the bolts and the gasket can be represented in the form

$$\delta_B = \delta_{B\ max} \cos \theta \tag{1a}$$

$$\delta_G = \delta_{G\ max} \cos \theta$$

$$= \frac{R_G}{R_B} \delta_{B\ max} \cos \theta \tag{1b}$$

The change in bolt loads Δp_B and gasket compression Δp_G are related to these elongations by the appropriate stress-strain laws. For the bolts, Hook's law holds and we have

$$\Delta p_B = \frac{E_B A_B}{(2\pi R_B)\ell_B} \delta_B \tag{2a}$$

$$= \Delta p_{B\ max} \cos \theta$$

where $$\Delta p_{B\ max} = \frac{E_B A_B}{(2\pi R_B)\ell_B} \delta_{B\ max} \tag{2b}$$

E_B = Young's modulus of bolt material

A_B = total bolt area

ℓ_B = length of bolt

Gaskets as a rule do not follow Hooke's law very closely. But if the stress-strain law for a gasket is known from experimental data, the change in gasket compression Δp_G can be expressed in terms of the gasket elongation δ_G. As a simple case, we will assume a gasket material which obeys Hooke's law. Then, similar to the above, the change in gasket compression can be written as

$$\Delta p_G = \Delta p_{G\ max} \cos \theta \tag{3a}$$

where $$\Delta p_{G\ max} = \frac{E_G A_G}{(2\pi R_G)\ell_G} \frac{R_G}{R_B} \delta_{B\ max} \tag{3b}$$

E_G = Young's modulus of gasket material

A_G = gasket area

ℓ_G = gasket thickness

From Eqs. (2a) and (3a) we obtain the following relation between the change in bolt load and gasket load

$$\Delta p_{G\ max}/\Delta p_{B\ max} = (E_G A_G/\ell_G)\Big/(E_B A_B/\ell_B) \tag{4}$$

Since the bending moment M on one section of the pipe is transmitted to the other section of the pipe through the bolts and the gasket, these changes in bolt load and gasket compression must have a resultant moment equal to M. Therefore,

$$\begin{aligned} M &= \int (\Delta p_B R_B d\theta) R_B \cos(\theta - \pi) + \int (\Delta p_G R_G d\theta) R_G \cos(\theta - \pi) \\ &= -\Delta p_{B\ max} R_B^2 \int \cos^2\theta d\theta - \Delta p_{G\ max} R_G^2 \int \cos^2\theta d\theta \\ &= -\pi \left[\Delta p_{B\ max} R_B^2 + \Delta p_{G\ max} R_G^2\right] \end{aligned} \tag{5}$$

We obtain from Eqs. (4) and (5),

$$\Delta p_{G\ max} = \frac{-M}{\pi R_G^2} \frac{1}{1 + \left(\frac{R_B}{R_G}\right)^2 \left(\frac{E_B A_B}{\ell_B}\right)\Big/\left(\frac{E_G A_G}{\ell_G}\right)} \tag{6}$$

Eq. (3a) now becomes

$$\Delta p_G = \left\{\frac{-M}{\pi R_G^2} \frac{1}{1 + \left(\frac{R_B}{R_G}\right)^2 \left(\frac{E_B A_B}{\ell_B}\right)\Big/\left(\frac{E_G A_G}{\ell_G}\right)}\right\} \cos\theta \tag{3c}$$

The change of gasket compressive stress is, therefore,

$$\Delta p_G \Big/ \text{width of gasket} \tag{7}$$

In arriving at Eq. (5) above, we have neglected the contribution to the bending moment due to the bending of individual bolts and the variation of gasket stress across its width. This approximation is justified as long as the diameter of the bolt circle is large compared to the bolt diameter

and the diameter of the gasket circle is large compared with the gasket width.

If in addition to the bolts and gasket, there is also a spacer in between the flanges, or the flanges themselves contact each other, Eq. (6) can be generalized as

$$\Delta p_{G\ max} = \frac{-M}{\pi R_G^2} \frac{1}{1 + (R_B/R_G)^2(K_B/K_G) + (R_S/R_G)^2(K_S/K_G) + \cdots} \tag{6a}$$

where $K_G = E_G A_G/\ell_G$, $K_B = E_B A_B/\ell_B$ and $K_S = E_S A_S/\ell_S$ are the stiffnesses of the gasket, the bolts and the spacer, and R_S is the spacer radius.

To obtain the change in bolt load, spacer load, etc., simply interchange the subscript G to B, to S etc. in Eq. (6a).

In the above we have assumed that the bending moment M on the flange is known. Eqs. (3c) and (7) then give us the change of gasket compression due to the moment. There are cases, however, where the pipe and flange together constitute a statically indeterminate system under the load. In that case, the moment on the flange will not be known until we know the bending rigidity of every component of the system. The bending rigidity of the pipe and the flange is given by the well-known expression

Bending rigidity = (Young's modulus)(area moment of inertia of the cross-section)

The bending rigidity of the components (bolts, gaskets, spacers, etc.) connecting the two flanges can be defined as

$$\text{Bending rigidity} = \frac{M}{\alpha/\ell_G} = \frac{M}{\delta_{G\ max}/R_G\ell_G}$$

$$= \frac{M}{2\pi\Delta p_G/K_G\ell_G}$$

$$= \frac{\ell_G}{2}\left[K_G R_G^2 + K_B R_B^2 + K_S R_S^2 + \cdots\right] \tag{8}$$

To illustrate our result, we consider the following flange connector:

(1) Gasket

Material = iron jacketed asbestos, $E_G = 4.8 \times 10^5$ psi

Thickness = $\frac{1}{8}$ in.

Width = $\frac{1}{2}$ in.

Mean radius = $R_G = 18\frac{3}{4}$"

Gasket area = $2\pi\ (18\frac{3}{4})(\frac{1}{2}) = 58.9$ in.^{2}

(2) Bolts

Diameter = $1\frac{3}{8}$ in.

Number = 24

Equivalent length = $\ell_B = 10$ in.

Young's modulus = $E_B = 30 \times 10^6$ psi

Radius of bolt circle = 21 in.

Total bolt area = $(24)(\frac{\pi}{4})(1\frac{3}{8})^2 = 35.6$ in.^{2}

For a bending moment of 10,000 in-lb., the maximum reduction in gasket compression is, from Eqs. (6) and (7)

$$\frac{\Delta p_{G\ max}}{\text{Width of gasket}} = \frac{10{,}000}{\pi(18.75)^2\left[1+\left(\frac{21}{21.75}\right)^2\left(\frac{30\times10^6\times35.6}{10}\right)\Big/\left(\frac{4.8\times10^5\times58.9}{\frac{1}{8}}\right)\right]}$$

$$= 546 \text{ psi}$$

If a softer gasket (600 psi series spiral-wound gasket) of Young's modulus 7.87×10^4 psi is used instead, the reduction in gasket compression will be 183 psi. The rigidity of the bolts and gasket in resisting the bending of the pipe and flange is, from Eq. (8)

$$\frac{1/8}{2}\left[(21)^2\left(\frac{30\times10^6\times35.6}{10}\right) + (18.75)^2\left(\frac{4.8\times10^5\times58.9}{1/8}\right)\right]$$

$$= 7.95 \times 10^9 \text{ lb-in}^2/\text{rad}.$$

If the softer gasket is used, the bending ridigity will be 3.76×10^9 lb-in^2/rad. Suppose these flanges connect cast iron pipes of 17-1/2 in. inside radius and 1/2 in. thickness, the bending rigidity of the pipe section is

$$EI = 14 \times 10^6 \times \frac{\pi}{4} \left[(18)^4 - (17.5)^4 \right]$$
$$= 1.25 \times 10^{11} \text{ lb-in}^2/\text{rad.}$$

which is much greater than the corresponding rigidity of the bolts and gasket in resisting bending.

145

47.2 Effect of Pipe Misalignment

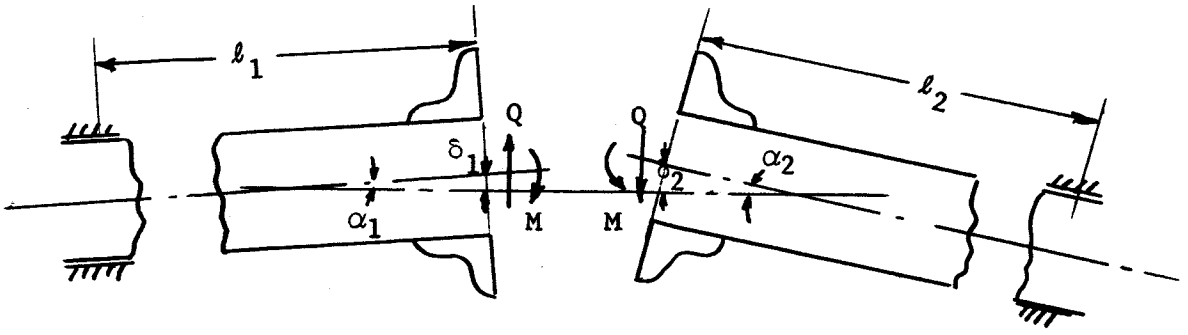

The above figure shows that the two sections of a pipe are misaligned. In order to bring the flanges of the two sections together and secure a uniform gasket compression, bending moments and shear forces are required. These forces and moments are applied through tightening of bolts and appear as uneven bolt tension and cross shearing of bolts. The magnitude of the moment and the shear force is to be determined from the condition that for uniform gasket compression, the axes of the opposing flanges should be collinear.

We shall assume that the pipe is "clamped" at its points of support. Due to the moment M and shear Q, the rotation and deflections at the flange ends are (Ref. 2)

$$\theta_1 = \frac{M\ell_1}{EI} - \frac{Q\ell_1^2}{2EI} \quad \text{clockwise} \tag{9}$$

$$y_1 = \frac{M\ell_1^2}{2EI} - \frac{Q\ell_1^3}{3EI} \quad \text{downward} \tag{10}$$

for the left-hand section, and

$$\theta_2 = \frac{M\ell_2}{EI} + \frac{Q\ell_2^2}{2EI} \quad \text{counterclockwise} \tag{11}$$

$$y_2 = \frac{M\ell_2^2}{2EI} + \frac{Q\ell_2^3}{3EI} \quad \text{downward} \tag{12}$$

for the right-hand section. The requirement that the axes of the flanges are collinear is

$$\alpha_1 - \theta_1 = -(\alpha_2 - \theta_2) \tag{13}$$

$$\delta_1 - y_1 = \delta_2 - y_2 \tag{14}$$

From these equations we obtain

$$M = \frac{EI\left[4(\alpha_1+\alpha_2)(\ell_1^2-\ell_1\ell_2+\ell_2^2)-6(\delta_1-\delta_2)(\ell_1-\ell_2)\right]}{(\ell_1+\ell_2)^3} \tag{15}$$

$$Q = \frac{EI\left[6(\alpha_1+\alpha_2)(\ell_1-\ell_2)-(\alpha_1-\alpha_2)\right]}{(\ell_1+\ell_2)^3} \tag{16}$$

Notice that in arriving at our result, we have:

(1) Neglected the contribution of the bending rigidity of the flange.

(2) Idealized the support of the pipeline by the "clamped" condition.

The bending rigidity of the flange is not important as long as the length of the pipe is much greater than the length of the flange. The support of the pipeline, however, may be more like "continuous beam on many supports" than "clamped." The present result can be easily generalized to account for these effects.

From the point of view of leakage prevention, we desire a uniform gasket compression and arrive at the conclusion that uneven bolt loads are required whenever there is any misalignment in the pipeline. This is a consideration to be kept in mind when the flange connector is assembled using torque wrenches. From the point of view of not overstressing the bolts, however, the bolt loads should be uniform. A compromise will sometimes have to be made. Eqs. (15) and (16) serve as the basis for establishing the tolerance of pipe misalignment.

Numerical Example:

Consider the following two sections of a pipeline

Length = $\ell_1 = \ell_2 = 10$ ft.

Young's modulus = 30×16^6 psi

Moment of inertia of cross section = 127 $in.^4$
(corresponding to a 10 in. diameter, 1/4 in. thickness pipe)

Initial misalignment = $\alpha_1 = 0.01$ radian

$\alpha_2 = 0.02$ radian

$\delta_1 = 1.0$ in.

$\delta_2 = 1.5$ in.

From Eq. (15) we have

$$M = \frac{4(0.03)(10\times12)^2 \times 30\times10^6\times127}{(20\times12)^3}$$

$$= 3970 \text{ in-lb}$$

$$Q = \frac{30\times10^6\times127(+0.5)}{(20\times12)^3}$$

$$= 138 \text{ lb.}$$

148

47.3 Twisting of Flanges

In the preceding sections we assumed that the flange surface remains plane during bending. It was shown that the bending moment relieves the bolt and gasket load at some places while increasing the bolt and gasket load at other places. The result is that the originally uniform flange "rolling moment" becomes non-uniform, or the flange is now subjected to a twisting moment variable along the flange circumference. To determine the twist of the flange we proceed as follows. We formulate the equations relating the changes in bolt and gasket load to the angle of twist of the flange; the equations governing the bending of the adjoining pipes; the equations relating the load on the flange and its angle of twist. By matching these equations together we can determine the twist of the flange and the stresses in the components.

47.3.1 Equations Relating the Changes in Bolt and Gasket Stresses to the Angle of Twist and Bending Moment

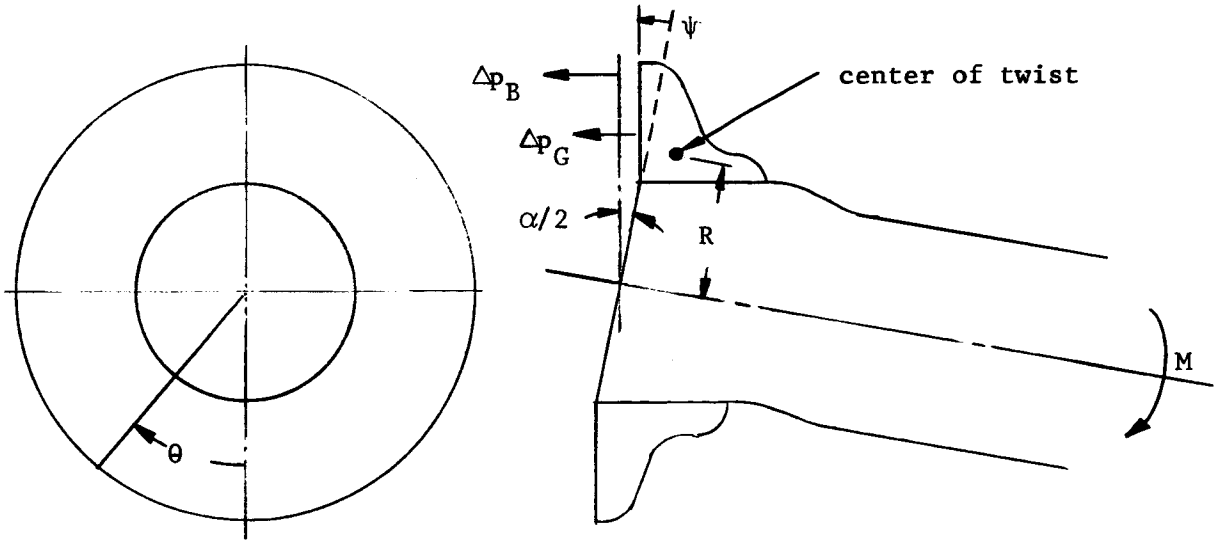

Let the relative rotation of the flange surfaces be α and the twist of the flange cross-section be $\psi = \psi_{max} \cos \theta$.

The extension of the bolts is

$$\delta_B = \left[- \alpha R_B + 2\psi_{max} (R_B - R) \right] \cos \theta = \delta_{B\,max} \cos \theta \qquad (17)$$

The extension of the gasket is

$$\delta_G = \left[- \alpha R_G + 2\psi_{max} (R_G - R) \right] \cos \theta = \delta_{G\,max} \cos \theta \qquad (18)$$

We can eliminate α from the equations and obtain

$$2\psi_{max}\left[R(1 - R_B/R_G)\right] = -\delta_{B\ max} + \left(R_B/R_G\right)\delta_{G\ max} \tag{19}$$

or, in terms of the changes in bolt and gasket load

$$2\psi_{max}\left[R(1 - R_B/R_G)\right] = -\Delta p_{B\ max}\left(\frac{2\pi R_B}{K_B}\right) + \Delta p_{G\ max}\left(R_B/R_G\right)\left(\frac{2\pi R_G}{K_G}\right) \tag{20}$$

From Eqs. (5) and (20) we obtain the changes in bolt and gasket load in terms of the bending moment M and the angle of twist ψ_{max} as follows

$$\Delta p_{G\ max} = \frac{K_G}{\pi\left(K_B R_B^2 + K_G R_G^2\right)}\left[\psi_{max}\ K_B R R_B(1 - R_B/R_G) - M\right] \tag{21}$$

$$\Delta p_{B\ max} = \frac{K_B}{\pi\left(K_B R_B^2 + K_G P_G^2\right)}\left[\psi_{max}\ K_G R R_G\left(1 - R_G/R_B\right) - M\right] \tag{22}$$

47.3.2 Adjoining Pipes Analyzed as Cylindrical Shells

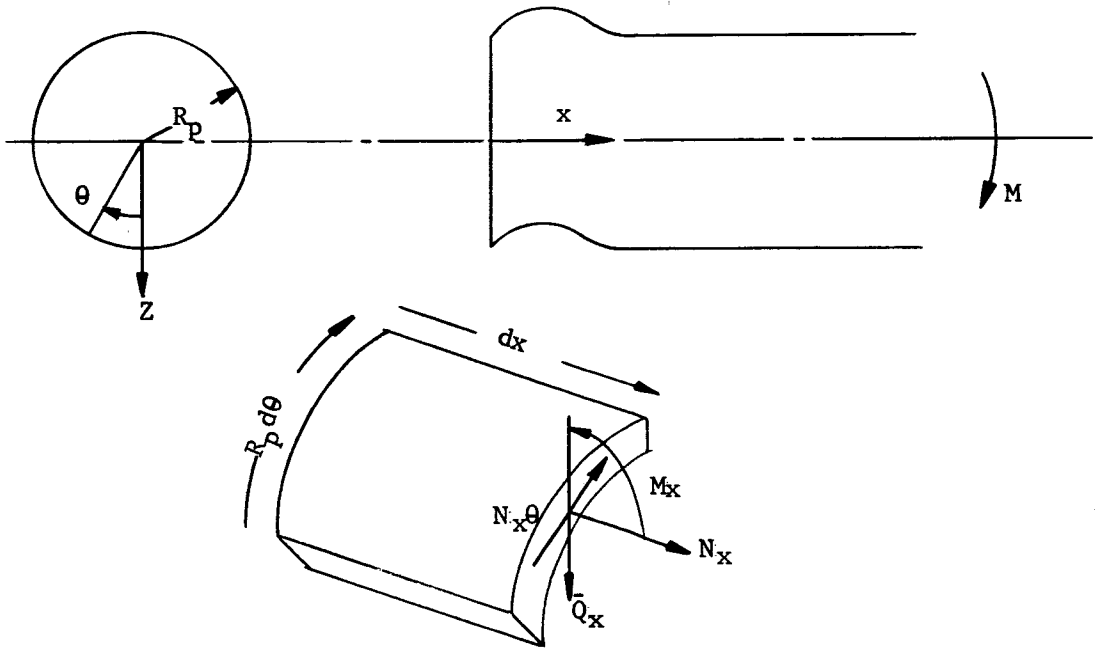

At a large distance from the flange, a membrane state of stress

$$N_x = - (M/\pi R_p^2) \cos \theta \tag{23}$$

exists in the pipe. In the vicinity of the flange, in addition to the above state of stress, a self-equilibrating bending state of stress exists. A complete solution is given in Ref. 3 as

$$w = \left[e^{-\alpha x}(H_1 \cos \beta x + H_2 \sin \beta x) + M (x^2/R_p^2)/2\pi RhE + H_5(x/R_p) - H_1 \right] \cos \theta \tag{24}$$

$$u = \left[e^{-\alpha x}(H_5 \cos \beta x + H_6 \sin \beta x) - M(x/R_p)/\pi RhE - H_5 \right] \cos \theta \tag{25}$$

$$v = \left[e^{-\alpha x}(H_7 \cos \beta x + H_8 \sin \beta x) - M(x^2/R_p^2 - 2\nu)/2\pi RhE - H_5(x/R_p) + H_1 \right] \sin \theta \tag{26}$$

where u, v, w = displacement components in x, θ, z directions

E = Young's modulus

ν = Poisson's ratio

h = wall thickness of pipe

$$\alpha = \frac{1}{R_p}\left[1 - \frac{\nu}{2} + \frac{R_p}{h}\sqrt{3(1 - \nu^2)}\right]^{1/2}$$

$$\beta = \frac{1}{R_p}\left[\frac{\nu}{2} - 1 + \frac{R_p}{h}\sqrt{3(1 - \nu^2)}\right]^{1/2}$$

$$H_5 = L_1H_1 + L_2H_2$$

$$H_6 = -L_2H_1 + L_1H_2$$

$$H_7 = L_3H_1 + L_4H_2$$

$$H_8 = -L_4H_1 + L_3H_2$$

$$L_i = K_i/K_5 \qquad (i = 1,2,3,4)$$

$$K_1 = R_p\alpha\left[-(1 + \nu^2) + 2\nu R_p^2\beta^2\right]$$

$$K_2 = -R_p\beta\left[-(1 + \nu^2) - 2\nu R_p^2\alpha^2\right]$$

$$K_3 = 1 - 2\nu + \nu^2$$

$$K_4 = 2(2 + \nu) R_p^2\alpha\beta$$

$$K_5 = 12(1 - \nu^2)(R_p/h)^2$$

It is obvious that the exponentially decaying terms represents the self-equilibrating bending solution while other terms represent the membrane solution. From these equations we obtain, at the flange end of the pipe,

$$\text{circumferential strain } \epsilon_\theta = \left(\frac{\cos\theta}{R_p}\right)\left[\frac{\nu M}{\pi R_p h E} + H_1(1 + L_3) + L_4 H_2\right] \tag{27}$$

$$\text{slope } \frac{\partial w}{\partial x} = (H_2\beta - H_1\alpha)\cos\theta \tag{28}$$

Stress resultants

$$M_x = \frac{Eh^3}{12(1-\nu^2)}\cos\theta\left\{H_1\left[\alpha^2 - \beta^2 - \nu(1+L_3)/R_p^2 + (L_1\alpha + L_2\beta)/R_p\right] - H_2\left[2\alpha\beta + \frac{\nu L_4}{R_p^2} + (L_1\beta - L_2\alpha)/R_p\right]\right\} \tag{29}$$

$$N_x = \frac{Eh}{1-\nu^2}\cos\theta\left\{H_1\left[\nu(1 + L_3)/R_p - (L_1\alpha + L_2\beta)\right] + H_2\left[L_1\beta - L_2\alpha + \nu L_4/R_p\right]\right\} - M\cos\theta/\pi R_p^2 \tag{30}$$

$$N_{x\theta} = \frac{Eh}{2(1+\nu)}\sin\theta\left\{H_1\left[-\frac{L_1}{R_p} - \beta L_4 - \alpha L_3\right] + H_2\left[-\frac{L_2}{R_p} + \beta L_3 - \alpha L_4\right]\right\} \tag{31}$$

$$\bar{Q}_x = \frac{Eh^3}{12(1-\nu^2)}\cos\theta\left\{H_1\left[-\alpha(\alpha^2 - 3\beta^2) + \frac{(2-\nu)\alpha}{R_p^2} + (3-\nu)(\alpha L_3 + \beta L_4)/3R_p^2 - \frac{1}{R_p}\left((\alpha^2 - \beta^2)L_1 + 2\alpha\beta L_2\right) - \frac{(1-\nu)L_1}{2R_p^3}\right] + H_2\left[\beta(3\alpha^2 - \beta^2) - \frac{(2-\nu)\beta}{R_p^2} - (3-\nu)(-\alpha L_4 + \beta L_3)/2R_p^2 - \left((\alpha^2 - \beta^2)L_2 - 2\alpha\beta L_1\right)/R_p - \frac{(1-\nu)L_2}{2R_p^3}\right]\right\} \tag{32}$$

Since the bending solution is self-equilibrating we should have

$$M_{x\ max} = R_p(N_{x\ max} + M/\pi R_p^2) \tag{33}$$

and

$$N_{x\theta\ max} = -\bar{Q}_{x\ max} \tag{34}$$

These relations are convenient since it often happens that some of these expressions are much easier to compute numerically than the others.

47.3.3 Equations Relating the Loads on the Flange and Its Angle of Twist

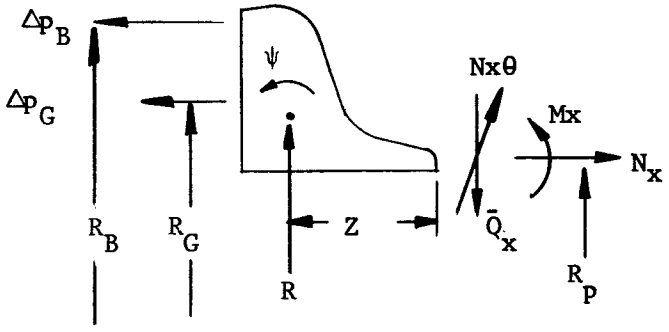

Assuming that the cross-section of the flange remains rigid we may resolve these forces and moments into a force in the axial direction and passing through the center of twist,

$$q = (\Delta p_B R_B + \Delta p_G R_G - N_x R_p)/R = q_{max} \cos\theta \tag{35}$$

a twisting moment

$$T = \Big[\Delta p_B R_B(R_B - R) + \Delta p_G R_G(R_G - R) + N_x R_p(R - R_p) + M_x R_p - \bar{Q}_x R_p Z\Big]/R = T_{max} \cos\theta \tag{36}$$

and a bending moment

$$M = -N_{x\theta} Z R_p/R = M_{max} \sin\theta \tag{37}$$

The following figure shows a differential element of the flange and forces acting on it

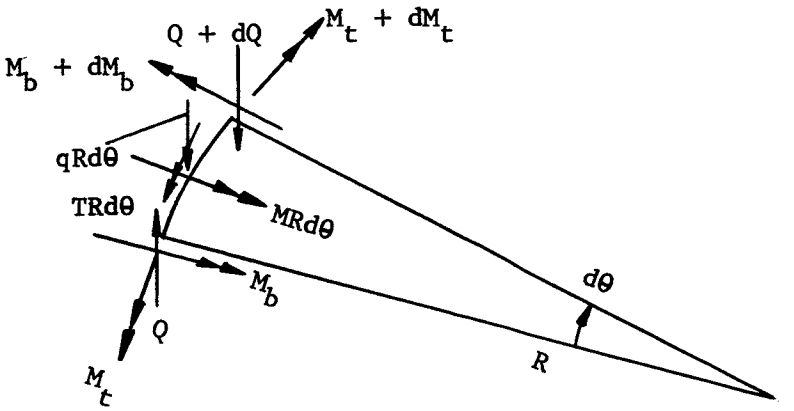

There exist the following equilibrium equations

$$qRd\theta + dQ = 0, \quad \text{or } \frac{dQ}{d\theta} = -qR \tag{38}$$

$$TRd\theta - dM_t - M_b d\theta = 0, \text{ or } \frac{dM_t}{d\theta} = TR - M_b \tag{39}$$

$$dM_b - MRd\theta - M_t d\theta + QRd\theta = 0, \text{ or } \frac{dM_b}{d\theta} = M_R + M_t - QR \tag{40}$$

They admit the following solutions

$$\text{shear, } Q = -q_{max} R \cos\theta$$
$$\text{Bending moment, } M_b = 0$$
$$\text{Twisting moment, } M_t = T_{max} R \sin\theta$$

The angle of twist is given by

$$d\psi = M_t Rd\theta/GJ, \quad \text{or} \quad \psi = -T_{max} R^2 \cos\theta/GJ \tag{41}$$

where GJ is the torsional rigidity of the flange.

47.3.4 Compatibility of Deformation at Junction of Flange and Pipe

The deformation of the flange and pipe as given in Section 47.3.2 and 47.3.3 should be compatible at their junction. Equality of rotation gives us

$$H_2\beta - H_1\alpha = \psi_{max} \tag{42}$$

The circumferential strain should also be equal. Since twist does not introduce circumferential strain and the flange cross-section is large compared with pipe cross-section, we can take the circumferential strain in the flange as zero approximately. Therefore Eq.(27) becomes

$$\nu M/\pi R_p hE + H_1(1 + L_3) + L_4 H_2 = 0 \qquad (43)$$

Eqs. (42), (43) and (36) are three equations for the three unknowns H_1, H_2 and ψ_{max}. When the geometric and material properties of the fluid connector are known these equations can be solved to give the twist of the flange and the stresses in the components.

47.3.5 A Numerical Example

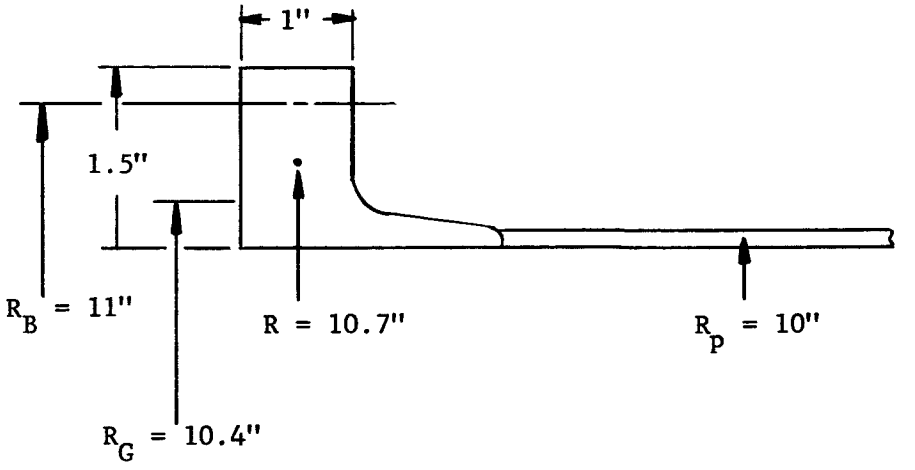

The flange and pipe are made of aluminum alloy with

$$E = 10 \times 10^6 \text{ psi}$$
$$\nu = 0.33$$
$$GJ = (0.141)(1.5)(1)^3(4 \times 10^6) = 8.47 \times 10^5 \text{ lb-in}^2$$

The gasket used is iron-jacketed asbestos gasket with

$$E_G = 5 \times 10^5 \text{ psi}$$
$$A_G = 2\pi(10.4)(1/4) = 16.3 \text{ sq. in.}$$
$$\ell_G = 1/8 \text{ in.}$$
$$K_G = \frac{E_G A_G}{\ell_G} = 6.52 \times 10^7 \text{ lb/in.}$$

Forty 7/16" alloy steel bolts are used

$$E_B = 30 \times 10^6 \text{ psi}$$
$$A_B = (40)(0.106) = 4.24 \text{ sq. in.}$$
$$\ell_B = 2\text{-}3/8 \text{ in.}$$
$$K_B = 5.33 \times 10^7 \text{ lb/in.}$$

The connector is subjected to a bending moment of

$$M = 400{,}000 \text{ in-lb.}$$

We can calculate from Eqs. (21) and (22) that

$$\Delta p_{G\ max} = \frac{6.52 \times 10^7}{\pi\left[5.33 \times 10^7 (11)^2 + 6.52 \times 10^7 (10.4)^2\right]} \left[\psi_{max}\ (5.33 \times 10^7)(10.7)(11)(1-11/10.4) - (400{,}000)\right]$$

$$= -5.56 \times 10^5 \psi_{max} - 615 \qquad (44)$$

$$\Delta p_{B\ max} = 4.98 \times 10^5\ \psi_{max} - 503$$

Since the hub is rather thin, it is more convenient to treat it as part of the pipe rather than part of the flange. The hub and pipe is then taken as having an average thickness of 0.2 in. The numerical values of the parameters appearing in the shell equations are obtained as

$$\alpha = 0.91 \qquad \alpha^2 - \beta^2 = 0.0167$$

$$\beta = 0.90$$

$$L_1 = 0.0178 \qquad L_3 = 1.68 \times 10^{-5}$$

$$L_2 = 0.0187 \qquad L_4 = 0.0143$$

Eqs. (29), (31), (33) and (34) then give us

$$M_{x\ max} = 125H_1 - 12300H_2$$

$$N_{x\ max} = 12.5H_1 - 1230H_2 - M/\pi R_p^2$$

$$\bar{Q}_{x\ max} = 11000H_1 + 11200H_2 \qquad (45)$$

A relation between H_1 and H_2 can be obtained from Eq. (43) as

$$H_1 = -0.0143H_2 - 0.0021 \qquad (46)$$

Substituting these equations in Eq. (36) we obtain

$$(4.98 \times 10^5 \psi_{max} - 503)(11)(11 - 10.7) + (-5.56 \times 10^5 \psi_{max} - 615) \times (10.4)(10.4 - 10.7) + \left(-1230\ H_2 - 400{,}000/\pi(10^2)\right)(10)(10.7 - 10)$$

$$+ (-12300\ H_2 - 0.262)(10) - (11100\ H_2 - 23.1)(10)(0.5)$$

$$= (10.7)\left(-8.47 \times 10^5/(10.7)^2\right)\psi_{max}$$

Or, after simplification,

$$3.46 \times 10^6 \psi_{max} - 1.87 \times 10^5 H_2 - 8550 = 0 \qquad (47)$$

Another equation relating ψ_{max} and H_2 is Eq. (42) which becomes

$$0.89 H_2 + 0.0019 = \psi_{max}$$

From these two equations we obtain

$$\psi_{max} = 2.51 \times 10^{-3} \text{ rad.}$$
$$H_2 = 6.85 \times 10^{-4} \qquad (48)$$

and from Eq. (44)

$$\Delta P_{G\ max} = -5.56 \times 10^5\ \psi_{max} - 615$$
$$= -\ 1400 \text{ lb/in.} \qquad (49)$$

as compared with -615 lb/in when twisting of the flange is not considered.

This example shows that the twist of the flange associated with the external bending moment may adversely affect the gasket compression and should not be neglected.

157

47.4 References

1. A.R.C. Markl, Discussion of "Gaskets and Bolted Joints," J. of Applied Mechanics, Vol. 17, 1950, pp. 454-455.

2. R. J. Roark, Formulas for Stress and Strain, Third Ed., McGraw-Hill, 1954.

3. P. P. Bijlarrd, "Stresses in a Spherical Vessel from External Moments Acting on a Pipe", Welding Research Council Bulletin No. 49, April, 1959.

4. E. O. Waters, D. B. Wesstrom, D. B. Rossheim, and F. S. G. Williams, "Formulas for Stresses in Bolted Flanged Connections", Trans. ASME, Vol. 59, 1937, pp. 161-169.

5. D. B. Wesstrom and S. E. Bergh, "Effect of Internal Pressure on Stresses and Strains in Bolted-Flanged Connections," Trans. ASME, Vol. 73, 1951, pp. 553-568.

158

48. THERMAL DISTORTION OF FLANGES

by

S. Levy

48.0 Summary

This section considers the stresses and growth in radius and thickness of a flange having a radial variation of temperature. A plane stress analysis is presented for the case of a temperature rise given by the function $Ar^n + B$, where A, B, and n are constants and r is the radius. The flange material is considered to be homogeneous with a constant coefficient of expansion. Numerical examples are presented. These indicate that for given temperatures at the inner and outer surface of the flange, the stresses at these surfaces and the radial grouth are relatively insensitive to the actual values of A, B and n. It appears therefore that moderate variations in the shape of the temperature distribution curve, between the values at the inner and outer surfaces, have little effect on stress or radial growth. Formulas are also given for the growth in flange thickness. These are of interest in determining the change in bolt load accompanying the temperature rise.

48.1 Introduction

Heating causes thermal expansion of materials. Since pipes may carry fluids which are initially at different temperatures than the pipe wall, the pipe connectors will be subjected to a change in temperature. In the case of LOX, for example, there would be a sudden cooling. When the thermal constants of the two flanges of the connector are not the same, their change in radial dimensions might be expected to differ. This condition would be particularly marked where one flange is stainless steel and the other is aluminum. Such scrubbing may cause gasket leakage. Due to the much greater time lag in change of temperature of the bolts, relative expansion may cause a tightening or loosening of the bolts. This would also have a marked effect on sealing action. In the case of tightening it could cause yielding with subsequent leaking when equilibrium is achieved. In the case of loosening the gasket pressure would be released with resulting immediate leakage.

For moderate temperature ranges in the usual flange materials, the coefficient of expansion can be considered constant and independent of direction. For longer rises, however, it is necessary to consider the coefficient of expansion as a function of temperature. In this section the coefficient is considered constant.

When the temperature rise varies radially, unequal expansion takes place. This gives rise to thermal stresses. The change in flange dimensions is then the sum of that due to expansion and that due to thermal stress. The modulus of elasticity and Poissons ratio are involved in determining the change in dimensions with stress.

The elastic modulus can be considered to be constant over moderate temperature ranges but is a function of temperature for wider ranges of temperature. In this section the modulus is considered constant.

The importance of thermal stresses in Diesel and turbine engines as well as elsewhere has resulted in a substantial body of literature on this subject. Timoshenko, (Ref. 1), gives basic equations as well as some results for particular cases. Additional treatment of the subject by Manson is given in Ref. 2. A relatively simple solution results if the temperature rise can be approximated by the function $Ar^n + B$. This form of solution is used in this section with results given not only for stresses but also for the growth in radius and flange thickness.

48.2 Nomenclature

T = temperature rise

A, B, n constants in $T = Ar^n + B$

r = radius

t = flange thickness

a = inner radius

b = outer radius

α = coefficient of expansion

E = Young's modulus

ν = Poisson's ratio

σ_r = radial stress

σ_c = circumferential stress

δ_r = radial growth

δ_t = thickness growth

ϵ = unit change in length due to temperature expansion and stress combined

z = coordinate in thickness direction

48.3 Results

It is shown in the Appendix that for a temperature rise distribution given by

$$T = Ar^n + B, \tag{1}$$

the radial stress in the flange is given by

$$\sigma_r = \left(\frac{A\alpha E}{n+2}\right)\left[-r^n - \left(\frac{a^2b^2}{r^2}\right)\left(\frac{b^n-a^n}{b^2-a^2}\right) - \left(\frac{a^2}{b^2-a^2}\right)a^n + \left(\frac{b^2}{b^2-a^2}\right)b^n\right] \tag{2}$$

The circumferential stress is given by

$$\sigma_c = \left(\frac{A\alpha E}{n+2}\right)\left[-(n+1)\,r^n + \left(\frac{a^2b^2}{r^2}\right)\left(\frac{b^n-a^n}{b^2-a^2}\right) - \left(\frac{a^2}{b^2-a^2}\right)a^n + \left(\frac{b^2}{b^2-a^2}\right)b^n\right] \tag{3}$$

The radial growth at the inner and outer surfaces is given by

$$\sigma_{r,\ \text{inner}} = a\left\{\alpha B + \left(\frac{2\alpha A}{n+2}\right)\left[\frac{b^{(n+2)} - a^{(n+2)}}{b^2 - a^2}\right]\right\} \tag{4}$$

and,

$$\delta_{r,\ \text{outer}} = b\left\{\alpha B + \left(\frac{2\alpha A}{n+2}\right)\left[\frac{b^{(n+2)} - a^{(n+2)}}{b^2 - a^2}\right]\right\} \tag{5}$$

The growth in thickness at the inner and outer surfaces is given by

$$\delta_{t,\ \text{inner}} = \alpha Bt + \alpha At\, a^n + \left(\frac{\nu\alpha At}{n+2}\right)\left[na^n - 2b^2\left(\frac{b^n - a^n}{b^2 - a^2}\right)\right] \tag{6}$$

and,

$$\delta_{t,\ \text{outer}} = \alpha Bt + \alpha At\, b^n + \left(\frac{\nu\alpha At}{n+2}\right)\left[nb^n - 2a^2\left(\frac{b^n - a^n}{b^2 - a^2}\right)\right] \tag{7}$$

The circumferential stress at the inner and outer surfaces is given by

$$\sigma_{c,\ \text{inner}} = \left(\frac{A\alpha E}{n+2}\right)\left[-na^n + 2b^2\left(\frac{b^n - a^n}{b^2 - a^2}\right)\right] \tag{8}$$

and

$$\sigma_{c,\ \text{outer}} = \left(\frac{A\alpha E}{n+2}\right)\left[-nb^n + 2a^2\left(\frac{b^n - a^n}{b^2 - a^2}\right)\right] \tag{9}$$

48.4 Examples

Example (1): Consider a flange for which the inner radius is 1 inch and the outer radius 2 inches. Let the thickness t=0.5 inch. Let $T=500^{o}F$ at r=1 and $T=100^{o}F$ at r=2. Let $\nu=0.3$, E=10,000,000 psi, and $\alpha=10^{-5}/^{o}F$. Assume the temperature distribution is adequately given by $T=500/r^{2.32}$. What are the stresses and deformations?

$$a = 1,\ b = 2,\ t = 0.5,\ A = 500,\ B = 0,\ n = -2.32$$

Using equations (8) and (9)

$$\sigma_{e,\ inner} = \left(\frac{500 \times 10^{-5} \times 10^{7}}{2-2.32}\right)\left[2.32 + 8\left(\frac{2^{-2.32}-1}{4-1}\right)\right]$$

$$= -156{,}200\left[2.32 + 8\left(\frac{-1+0.2}{3}\right)\right] = -29{,}100 \text{ psi}$$

$$\sigma_{c,\ outer} = -156{,}200\left[2.32 \times 0.2 + 2\left(\frac{-.8}{3}\right)\right] = 10{,}800 \text{ psi}$$

Using Eqs (4) and (5)

$$\delta_{r,\ inner} = 1\left\{0 + \left(\frac{2\times500\times10^{-5}}{2-2.32}\right)\left[\frac{2^{-.32}-1}{4-1}\right]\right\}$$

$$= -.03125\left(\frac{-1+.801}{3}\right) = .00207 \text{ in}$$

$$\delta_{t,\ outer} = 2\ (.00207) = .00414 \text{ in}$$

Using Eqs. (6) and (7)

$$\delta_{t,\ inner} = 0.5\left\{500 \times 10^{-5} + \left(\frac{0.3\times500\times10^{-5}}{2-2.32}\right)\left[-2.32-8\left(\frac{-.8}{3}\right)\right]\right\}$$

$$= 0.5 \times 10^{-5}\left\{500 + 85.7\right\} = .00292 \text{ in}$$

$$\delta_{t,\ outer} = 0.5\ (500)10^{-5}\left\{2^{-2.32} + \left(\frac{.3}{2-2.32}\right)\left[-2.32 \times 2^{-2.32} - 2\left(\frac{-.8}{3}\right)\right]\right\}$$

$$= .0025\left\{0.2 + \frac{0.3}{-0.32}\left(-.4640 + .5333\right)\right\} = .00034 \text{ in}$$

It is of interest to note that the thickness increase is about eight times as much at the inner surface as at the outer although the temperature rise is only five times as great. The excess results from the thermal compressive stress at the inner surface.

Example (2): Suppose we repeat example (1) with the same temperature at inner and outer walls but assuming the temperature distribution to be adequately given by $T= 1000/r^{0.737}-500$.

Now A=1000, B= -500, n= -0.737 and a, b, t are unchanged
Substituting values in Eqs. (4) to (9) gives

$\sigma_{t,\ inner} = -26{,}100$ psi ; $\sigma_{t,\ outer} = 13{,}800$ psi.

$\delta_{r,\ inner} = 0.00238$ in $\delta_{r,\ outer} = 0.00476$ in

$\delta_{t,\ inner} = .00289$ in $\delta_{t,\ outer} = 0.00034$ in

The change in temperature distribution from Exam. 1 has not markedly affected the stress or deformation.

Example (3): Same as Exam. (1) and (2) except T= 800/r -300

Now A= 800, B= -300, n=-1

Eqs. (4) to (9) give,

$\sigma_{t,\ inner} = -26{,}700$ psi $\sigma_{t,\ outer} = 13{,}300$ psi

$\delta_{r,\ inner} = 0.00233$ in $\delta_{r,\ outer} = 0.00466$ in

$\delta_{t,\ inner} = 0.00290$ in $\delta_{t,\ outer} = 0.00030$ in

Example (4): Same as Exam. (1) to (3) except $T= 400.5/r^{10} + 99.5$

Now A= 400.5, B= 100, n= -10

Eqs. (4) to (9) give,

$\sigma_{c,\ inner} = -36{,}700$ psi $\sigma_{c,\ outer} = 3{,}300$ psi

$\delta_{r,\ inner} = 0.00133$ in $\delta_{r,\ outer} = 0.00266$ in

$\delta_{t,\ inner} = 0.00305$ in $\delta_{t,\ outer} = 0.00045$ in

It is noted that changing n to -10 in this example has resulted in some modification of the resulting stresses and displacements. Even in this case comparison with Exam.(1) shows that the results are within 26% for the largest stress, 56% for the largest radial displacement, and 5% for the largest thickness change.

The results of the examples are plotted in Figs. 48.1 and 48.2 as a function of the shape factor n. In Fig. 48.3 the corresponding temperature distributions are shown. It is apparent from Fig. 48.3 that a considerable range of temperature distributions has been considered.

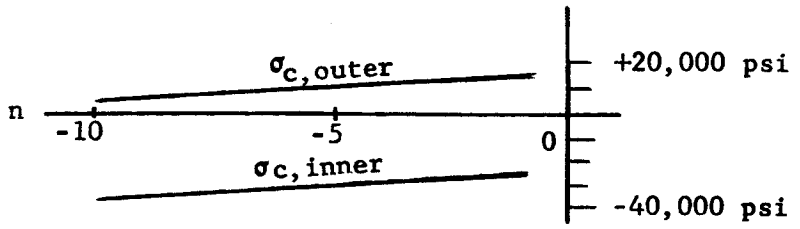

Fig. 48.1 - Stresses in Flange as a Function of Shape Factor n.

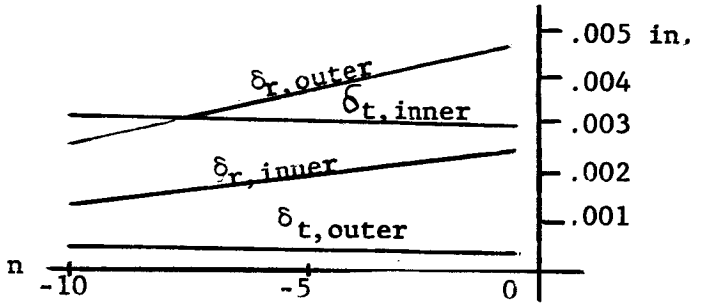

Fig. 48.2 - Radial Deflections and Thickness Changes as a Function of Shape Factor n.

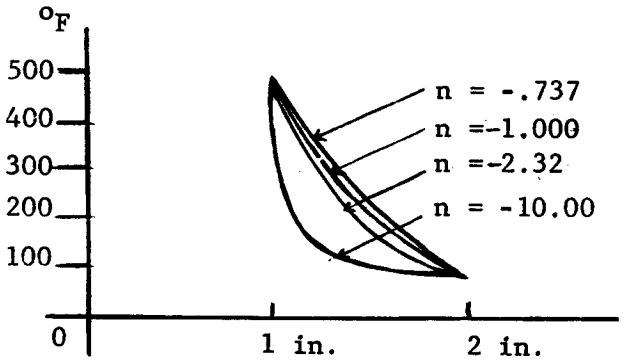

Fig. 48.3 - Temperature Distribution as a Function of Radius for Various Shape Factors n.

48.5 Discussion:

Formulas have been presented for stresses and deformations in flanges due to temperature effects. The numerical examples presented indicate a marked insensitivity to the actual temperature distribution so long as inner and outer surface temperatures are unchanged. This is of special importance because of the difficulty of obtaining exact solutions of the transient heat flow in such a flange.

The solution is based on constant material properties. If the need arises, it appears possible to include temperature-dependent properties where the temperature dependence fits the polynomial nature of the solution.

48.6 Appendix

48.6.1 Derivation of Thermal Stress Equations

The solution of the thermal stress problem presented earlier in this section is based on satisfying the conditions of equilibrium and compatibility.

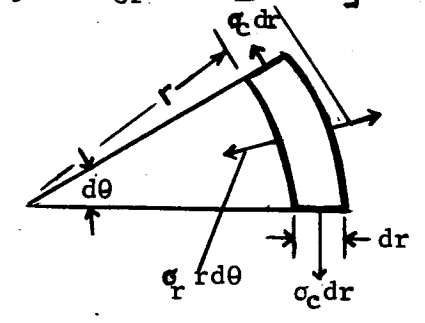

Equilibrium requires that

$$\sigma_c = \sigma_r + r \frac{\partial \sigma_r}{\partial r} \tag{1A}$$

The unit change in length is given by,

$$\epsilon_r = \alpha T + \frac{\sigma_r}{E} - \nu \frac{\sigma_c}{E} \tag{2A}$$

$$\epsilon_c = \alpha T + \frac{\sigma_c}{E} - \nu \frac{\sigma_r}{E} \tag{3A}$$

$$\epsilon_z = \alpha T - \nu \frac{\sigma_c}{E} - \nu \frac{\sigma_r}{E} \tag{4A}$$

Compatibility requires that

$$\epsilon = \frac{\partial}{\partial r}\left(r \epsilon_c\right) = r \frac{\partial \epsilon_c}{\partial r} + \epsilon_c \tag{5A}$$

Using Eqs. (2A) and (3A) in (5A) gives

$$\left(\frac{1+\nu}{E}\right)\left(\sigma_r - \sigma_c\right) = r \alpha \frac{\partial T}{\partial r} + \frac{r}{E}\left(\frac{\partial \sigma_c}{\partial r} - \nu \frac{\partial \sigma_r}{\partial r}\right) \tag{6A}$$

Substituting for σ_c from (1A) gives after re-arranging terms and using differentials because circular symmetry removes θ as an argument,

$$r^2 \frac{d^2 \sigma_r}{dr^2} + 3 r \frac{d\sigma_r}{dr} = - \alpha E r \frac{dT}{dr} \tag{7A}$$

If we consider the temperature distribution as being describable by the function

$$T = A r^n + B \tag{8A}$$

we find the solution of (7A) is

$$\sigma_r = - A\left(\frac{\alpha E}{n+2}\right) r^n + C_1 E / r^2 + C_2 E \tag{9A}$$

where C_1 and C_2 are constants of integration. Setting $\sigma_r = 0$ at the inner and outer radius r = a and r = b gives

$$0 = -A\left(\frac{\alpha}{n+2}\right) a^n + C_1/a^2 + C_2 \tag{10A}$$

$$0 = -A\left(\frac{\alpha}{n+2}\right) b^n + C_1/b^2 + C_2 \tag{11A}$$

Solving (10A) and (10B) for C_1 and C_2,

$$C_1 = A\left(\frac{\alpha}{n+2}\right)\left(b^n - a^n\right)\frac{a^2b^2}{a^2-b^2} \tag{12A}$$

$$C_2 = A\left(\frac{\alpha}{n+2}\right)\left[b^n\left(\frac{b^2}{b^2-a^2}\right) - a^n\left(\frac{a^2}{b^2-a^2}\right)\right] \tag{13A}$$

Substituting Eqs. (12A) and (13A) into (9A) gives Eq.(2) in the earlier part of this section. Substituting Eq. (2) into Eq.(1A) gives Eq.(3).

The radial growth is

$$\delta_r = r\,\epsilon_c = r\left(\alpha T + \sigma_c/E - \nu\,\sigma_r/E\right) \tag{14A}$$

Substituting Eqs.(2) and (3) in this and evaluating for r= a and r= b gives Eqs.(4) and (5).

The thickness growth is

$$\delta_t = t\,\epsilon_z = t\left(\alpha T - \nu\frac{\sigma_c}{E} - \nu\frac{\sigma_r}{E}\right) \tag{15A}$$

Substituting Eqs. (2) and (3) in this and evaluating for r= a and r= b gives Eqs. (6) and (7). Evaluating Eq. (3) for r= a and r= b gives Eqs. (8) and (9).

48.7 References

1. S. Timoshenko, Theory of Elasticity, McGraw-Hill Book Co., 1934, pp. 366-376.

2. S.S. Manson, "Thermal Stresses in Design: Elastic Stress Analysis," Machine Design, Vol. 31, Jan. 22, 1959, pp. 126-131.

49. ANALYSIS OF FLARE-TYPE DEMOUNTABLE TUBING CONNECTORS

by

S. Levy

49.0 Summary

In this section the sealing pressure in flare-type demountable tubing connectors is considered. Equations are given for the elastic and plastic behavior of variable thickness tubes. From these it is shown that both the fitting and tube yield in hoop stress in the area where sealing occurs. An equation is given for determining the sealing pressure in terms of the geometry of the connector and the material properties. In an example, for a stainless steel tube of 0.385" I.D. and 37° flare angle, it is shown that the maximum sealing pressure is about 50,000 psi and occurs about 0.1 inch from the tip. Tightening the nut on such a fitting is shown to increase the sealing pressure and move the maximum sealing pressure point farther from the tip.

49.1 Introduction

It is common experience that flare-type demountable tubing connectors appear to be permanently deformed in the seal region after tightening. Some investigators feel that in addition yielding occurs at the threads and that the nut tends to expand.

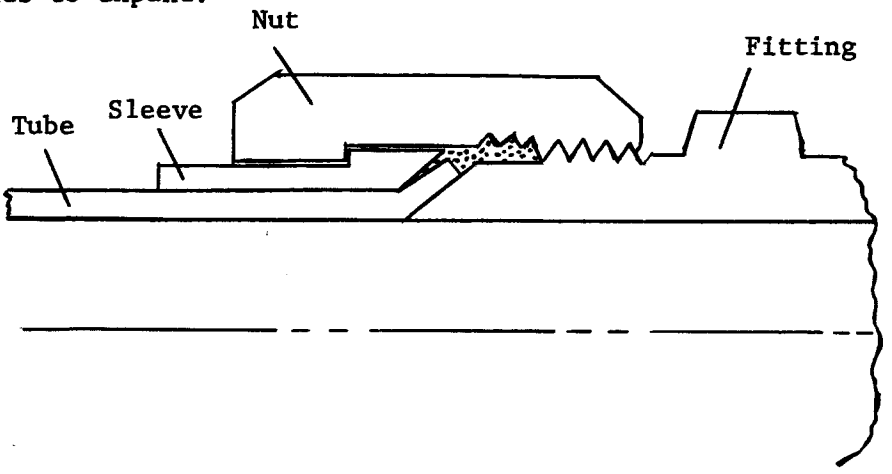

In studies of leaky connectors (Ref. 1), it has been found that contributing factors to leakage include:

1. Ovality in excess of 0.0005 inches.
2. Step changes in surface "out-of-round" in excess of 0.0001 inch in 60^{o} of arc.
3. Scratches, tool marks, chatter, and waviness which can breech the closure path.
4. Step changes in tube wall thickness.
5. Overstressing fitting sleeve with creep effects resulting in delayed leakage.

It has been found that polished fittings (RMS8) against precision flares can tolerate ovality of up to 0.0005 inches. MoS_2 has been found to be an excellent pore filler and lubricant. Copper "crush washers" have been found to improve sealing ability. These washers may by up to 0.005-inch thick for tubes up to 3/8-inch size and up to 0.010-inch thick for tubes up to 2-inch size. The use of a double angle on the sleeve tends to be beneficial.

A review of these experience factors for this type of connector suggests that even with tightness causing yielding in some places, the "sealing pressure" is on the low side for the mechanical properties of the materials used.

The relation between "sealing" pressure, σ_s, at the tube-fitting interface and axial stress, σ_a, in the fitting is illustrated in

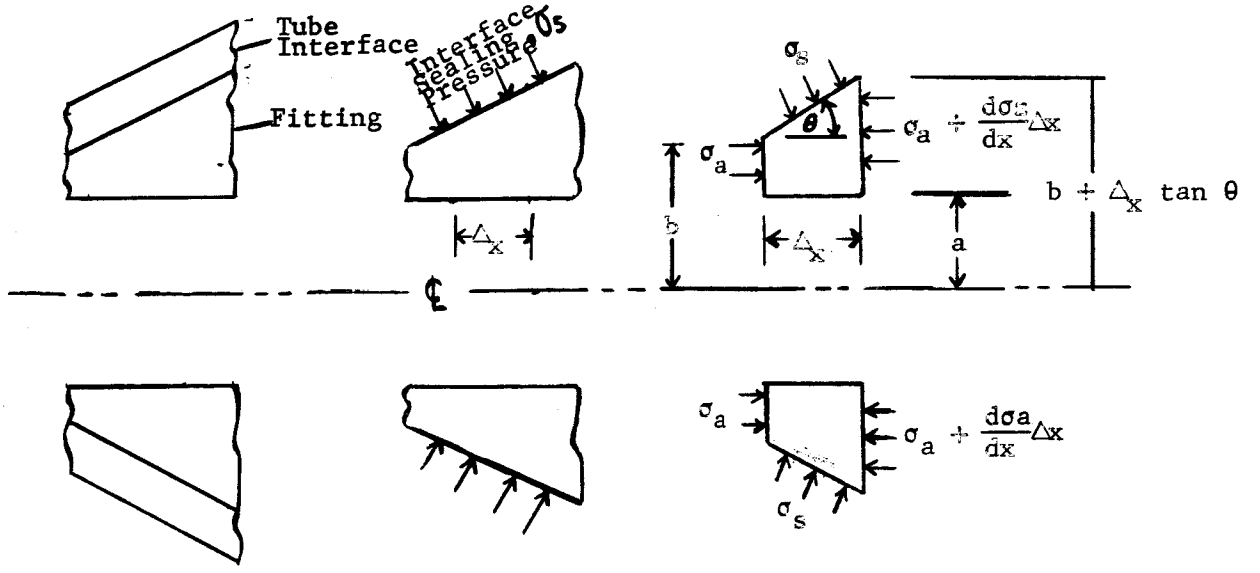

the sketch. Equilibrium of horizontal forces gives

$$\sigma_s\left(\frac{\Delta x}{\cos\theta}\right)\sin\theta\left[2\pi\left(b+\frac{\Delta x}{2}\tan\theta\right)\right]+\sigma_a\pi(b^2-a^2)=\left(\sigma_a+\frac{d\sigma_a}{dx}\Delta x\right)\left[\pi(b+\Delta x\tan\theta)^2-\pi a^2\right]$$

Neglecting Δx^2 this equation reduces to

$$2\pi b\,\Delta x\tan\theta\sigma_s=2\pi b(\Delta x)\tan\theta\sigma_a+\pi(b^2-a^2)(\Delta x)\frac{d\sigma_a}{dx}$$

which in turn reduces to

$$\sigma_s=\sigma_a+\left(\frac{b^2-a^2}{2\tan\theta}\right)\frac{d\sigma_a}{dx}$$

A solution of this equation for constant σ_s is $\sigma_s=\sigma_a$.

For radial equilibrium, the radial force component of the "sealing" pressure on the disk of axial length Δx is

$$\sigma_s\left(\frac{\Delta x}{\cos\theta}\right)\cos\theta=\sigma_s\Delta x$$

A disk of thickness Δx subjected to an external radial force can resist this force in either of two ways. First, by transferring the load to neighboring disks through the action of shear forces τ. In the elastic range this transfer requires an axial distance of about the square root of the thickness times the radius or $\sqrt{(a + b)(b - a)/2}$ (Ref. 2, p. 397). This is so short a distance that each disk supports its own external radial force by hoop action. In the plastic range shear transfer drops to zero so that the same conclusion applies.

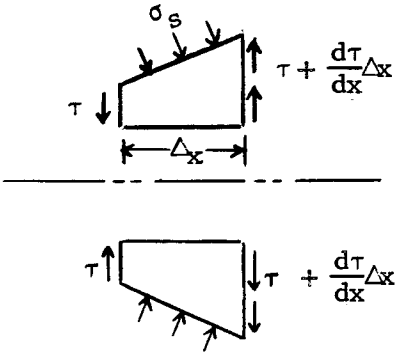

The second way of resisting is by hoop compression which we will now discuss.

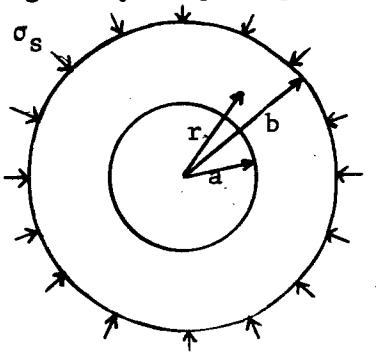

In the elastic range the stresses in a disk of thickness Δx subjected to an external radial force $\sigma_s \Delta x$ is given by Lame's theory as

$$\sigma_{hoop} = -\left(\frac{b^2}{b^2 - a^2}\right)\left(\frac{a^2 + r^2}{r^2}\right)\sigma_s$$

It is evident from this equation that

$$\sigma_{hoop} = -2\sigma_s/(1 - a^2/b^2) \text{ when } r = a$$

$$\sigma_{hoop} = -\sigma_s(1 + a^2/b^2)/(1 - a^2/b^2) \text{ when } r = b$$

These equations show that the hoop stress at r = a is many times the "sealing" pressure σ_s near the tip of the fitting where a is nearly equal to b. Even far from the tip where b = 1.5a, the hoop stress is 3.6 times the "sealing" pressure σ_s.

If the hoop stress is computed on the basis of full plasticity hoopwise, the hoop stress is everywhere σ_{yp}, the yield stress in compression. Equilibrium of forces in a vertical direction in the sketch gives

$$2\sigma_{yp}(b-a)\Delta x = \int_0^{\pi} \sigma_s \Delta x b d\theta \sin\theta$$

giving, $\sigma_s = \sigma_{yp}(1 - a/b)$

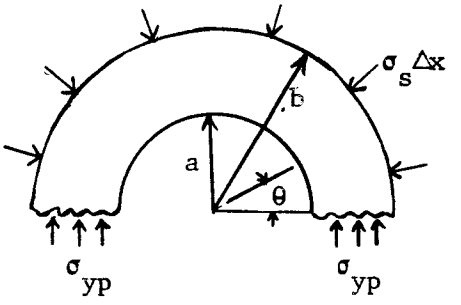

This equation shows that in the yield range, as in the elastic range, the hoop stress, σ_{yp} in this case, is many times the "sealing" pressure near the tip of the fitting where a is nearly equal to b. Even far from the tip where b = 1.5a, the hoop stress is 3.0 times the "sealing" pressure σ_s.

The low ratio of "sealing" pressure to hoop stress for this connector is probably the reason why a good seal is achieved only when it is very smoothly fitted or when a soft washer material is used.

In this section we will develop methods for predicting the "sealing pressure," taking into account the effects of hoop yielding, as well as the interaction between fitting and tube.

49.2 Elastic-Plastic Analysis

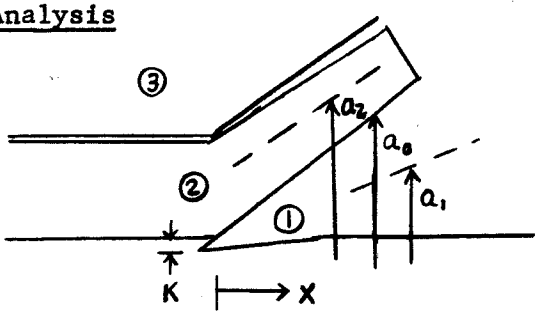

A sketch of the geometrical relationship between the fitting (1), the tube (2) and the sleeve (3) is shown. In a possible configuration, the angle between the axis and the interface between pieces (1) and (2) is 37°. Due to loss of thickness of the tube while expanding, the outer wall of (2) is at an angle of about 33.5°. The inner side of (3) is taken at an angle of 37° in this example. It should be noted, however, that a more realistic value of the angle at the inner side of (3) is 28° (Ref. 1, Fig. 1). As an example, the value chosen is considered adequate. Tightening of the nut will force (1) into (2) such that a radial interference K develops at x = 0.

The difference in angle between the inner and outer walls of the tube is inherent in the manufacturing process. The remaining angles are, however, subject to the designer's decision. In some configurations the angle on the inner face of (3) can be less than that on the outer face of (2). There are configurations in which a double angle is used for the inner face of (3).

Considering the stresses in part (1), it is seen that a hoop compression is developed near the tip in proportion to the radially inward deflection K. This compression reacts on part (2) so that part (2) is deflected outward. At a small value of x part (2) will "bottom" on (3). At a somewhat larger value of x, the stresses are such that (2) becomes free of (3). The point of maximum pressure between parts (1) and (2) will occur in the region where (2) is "bottomed" on (3). As an example, we will now consider these stresses for the case sketched.

For purposes of understanding, we postulate a pressure between parts (2) and (3) such that (1), (2), and (3) are all in intimate contact. This results in radial deflections of pieces (1) and (2), positive inward, given by:

$$w_1 = K - x\,(\tan 37^{\circ} - \tan 33.5^{\circ}) = K - .092x \qquad (1)$$

$$w_2 = -.092x$$

In addition, we denote

h_1 = radial thickness of (1) = $x \tan 37^{\circ} = 0.754x$

h_2 = radial thickness of (2) = $0.064 - (\tan 37^{\circ} - \tan 33.5^{\circ})x$

$= 0.064 - 0.092x$

(the initial tube wall thickness has been taken as 0.064)

$D_1 = Eh_1^3/12(1 - \nu^2) = 0.038Ex^3$

(Poisson's ratio ν has been taken as 0.25)

$D_2 = 0.000,0691E\ (0.696 - x)^3$

a_1 = radius of mid-thickness of (1) = 0.190 + 0.335x

(the initial tube radius has been taken as 0.190)

$a_2 = 0.222 + \tan 35^\circ x = 0.222 + 0.700x$

a_{12} = radius of (1) - (2) interface = 0.190 + 0.754x

a_{23} = radius of (2) - (3) interface = 0.254 + 0.754x

Z_{12} = pressure at (1) - (2) interface

Z_{23} = pressure at (2) - (3) interface

Timoshenko (Ref. 2, pages 413 to 422) considers the case of a cylinder with non-uniform wall thickness and gives as the governing equation

$$\frac{d^2}{dx^2}\left(D\frac{d^2w}{dx^2}\right) + \left(\frac{Eh}{a^2}\right)w = Z$$

where w is the radial deflection, positive inward
Z is the external pressure, positive inward
D is the flexural rigidity, variable
h is the thickness, variable

In this equation, the first term on the left-hand side corresponds to the lateral load resisted by wall flexure. The wall, in flexing, carries load much as does a tapered beam. The second term on the left-hand side corresponds to the lateral load resisted by hoop compression of the cylinder. The wall carries hoop compression much as a ring does.

In deriving this equation, Timoshenko tacitly assumes that the wall thickness varies slowly and that the inner and outer radii are nearly equal. We will now examine how this equation should be modified to apply to the fitting, for example, for which the taper is large and for which the inner and outer radii may be substantially different.

First, we consider the right-hand side of the equation. In the case where the pressure is applied externally, we must take the effective value of Z as being larger in proportion to the ratio of the outer radius to the mid-thickness radius. In the case where the pressure is applied internally, we must take the effective value of Z as being smaller in proportion to the ratio of inner radius to mid-thickness radius.

Second, we consider the second term on the left-hand side of the equation. Since w/a represents the average hoop strain, the value of

'a' referred to is the mid-thickness value.. The remaining 'a' factor is also the mid-thickness value, since it converts the average hoop load Ehw/a into an equivalent pressure at the mid-thickness radius.

Finally, we consider the first term in Timoshenko's equation. The degree of error in this term due to taper is difficult to judge. As the best available approximation we will keep this term in the same form as Timoshenko gives it.

In the elastic range then, Timoshenko's equation for pieces (1) and (2) becomes:

$$\frac{d^2}{dx^2}\left(D_1\frac{d^2w_1}{dx^2}\right) + \frac{Eh_1w_1}{a_1^2} = Z_{12}\frac{a_{12}}{a_1}$$

$$\frac{d^2}{dx^2}\left(D_2\frac{d^2w_2}{dx^2}\right) + \frac{Eh_2w_2}{a_2^2} = Z_{23}\frac{a_{23}}{a_2} - Z_{12}\frac{a_{12}}{a_2} \qquad (2)$$

In the plastic region for hoop stress, the first term in Eqs. (2) drops to zero, and we replace Ew/a by σ_{yp} in the first of Eqs. (2) and by $-\sigma_{yp}$ in the second. Doing this gives

$$h_1\sigma_{yp} = Z_{12}a_{12}$$

$$h_2\sigma_{yp} = -Z_{23}a_{23}+Z_{12}a_{12} \qquad (3)$$

Consider first part (1) with K large enough to cause yielding. As a reasonable approximation we take $\sigma_{yp} = 0.006E$. Then from the first of Eqs. (3) for $w_1/a_1 > 0.006$ (yielding in compression)

$$0.754x(.006E) = Z_{12}(0.190 + 0.754x) \qquad (4)$$

$$\left(w_1/a_1 > .006 \text{ gives } \frac{K-.092x}{.190+.335x} > 0.006\right)$$

From the first of Eqs. (2) for $w_1/a_1 < 0.006$

$$E(0.754x)(K-.092x) = Z_{12}(0.190+0.754x)(0.190+0.335x) \qquad (5)$$

$$\left(\text{for } \frac{K-.092x}{.190+.335x} < 0.006\right)$$

From the second of Eqs. (2) for $-w_2/a_2 < 0.006$ (yielding in tension)

$$E(0.064-0.092x)(-.092x) = Z_{23}(0.254+.754x)(0.222+0.700x) - Z_{12}(0.190+.754x)(0.222+0.700x) \qquad (6)$$

$$\left(-w_2/a_2 < 0.006 \text{ gives } \frac{+0.092x}{0.222+0.700x} < 0.006, \text{ that is, } x < .0153\right)$$

From the second of Eqs. (3) for $-w_2/a_2 > 0.006$

$$(0.064-0.092x)(.006E) = -Z_{23}(.254+.754x)+Z_{12}(0.190+.754x) \qquad (7)$$

$$\left(\text{for } \frac{.092x}{0.222+0.700x} > 0.006\right)$$

Setting $Z_{23} = 0$ in Eq. (7) and substituting for Z_{12} the value given in Eq. (4) shows that reversal in the sign of Z_{23} occurs at $x = 0.0757$ so long as $K > 0.00825$. One can expect part (2) to first contact the sleeve then at $x = 0.0757$ for interferences $K > 0.00825$.

Setting $Z_{23} = 0$ in Eq. (7) and substituting for Z_{12} the value given in Eq. (5) shows that the next reversal in the sign of Z_{23} occurs at $x = 0.10$ for $K = 0.01017$ and at $x = 0.20$ for $K = 0.01887$. One can expect, therefore, that when $K = 0.01017$, part (2) will bear on part (3) from $x = .0757$ to $x = 0.1000$. Similarly, when $K = .01887$, part (2) will bear on part (3) from $x = .0757$ to $x = 0.2000$.

The highest value of sealing pressure, Z_{12}, occurs at the value of x where part (1) makes a transition from the plastic solution, Eq. (4) to the elastic solution, Eq. (5). This transition occurs when $x = x_m$ where $(K-.092x_m)/(.190+.335x_m) = 0.006$. Substituting this value of x_m into Eq. (4) gives

$$(\text{Sealing Pressure})_{max} = Z_{12} = (.006E)\left(\frac{K-.00114}{K+.0226}\right) \qquad (8)$$

Thus, when $K = .01017$, $Z_{12}/E = .00165$, at $x_m = .096$
and when $K = .0189$, $Z_{12}/E = .00257$, at $x_m = .189$

Since these sealing pressures are roughly a third of the yield pressure, it is apparent that a good seal will only be attained where the surfaces are very smooth and match in contour.

177

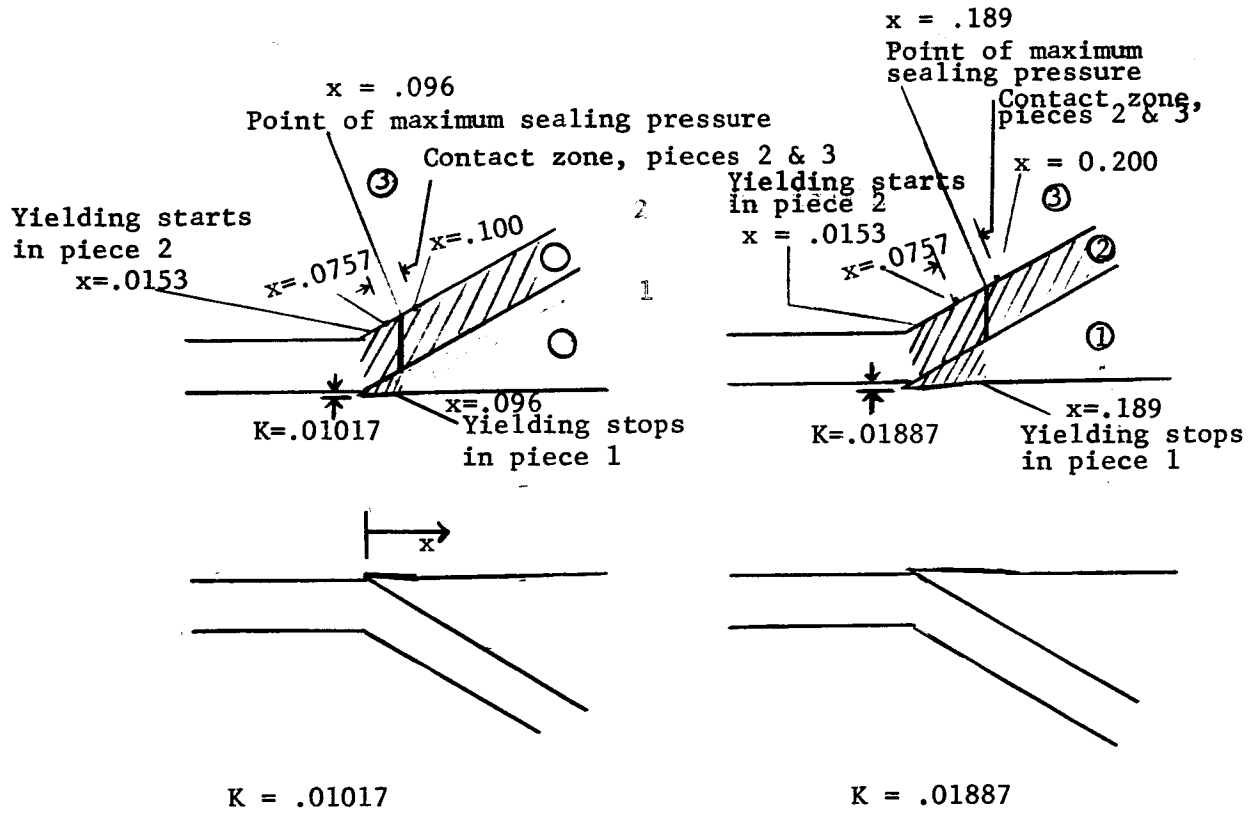

The sketches give a description of the contact regions and areas of plastic hoop stress. Cross-hatching is used to indicate plastic hoop stress. For the interference K = .01017, it is seen that contact between pieces (2) and (3) occurs between x = .0757 and x = .100. The maximum contact pressure between pieces (1) and (2) occurs at x = .096 which is also the point where piece (1) has a transition from plastic to elastic behavior. With an interference K = .01887 the zone of contact between (2) and (3) is broadened and extends from x = .0757 to x = .200. The maximum contact pressure between pieces (1) and (2) now occurs farther from the tip at x = .189. As before, yielding stops in piece (1) at the point where maximum contact pressure occurs between pieces (1) and (2).

In the particular example treated here we have seen that both tube and fitting have both elastic and plastic zones. The contact zone between pieces (2) and (3) is seen to have broadened as the interference K has increased. With other geometries for the sleeve (3) it is evident that the "contact zone" between the tube (2) and the sleeve (3) can be established at other values of x. For example, if the sleeve has the double-angle shown in the sketch, the "contact zone" will tend to center in the region A of first contact of pieces (2) and (3). Similarly, if the angle on (3) is lower than the angle on (2) (as is frequently the case), the "contact zone" will tend to center in the region B where x is large. In this regard, however, it should be noted that piece (3) can be expected to deform so that

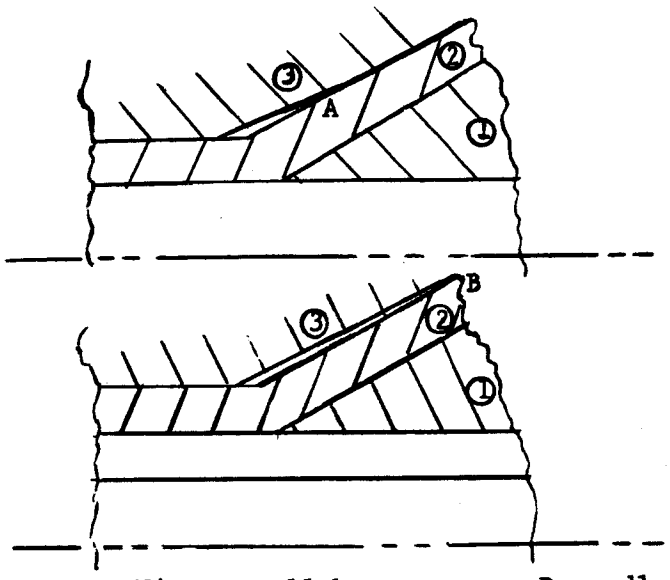

the final angle on piece (3) may well be greater. Regardless of the specific contouring of (3), it is apparent that a "contact zone" between (2) and (3) will develop. In the neighborhood of this "contact zone" the deformations and stresses will be similar to those in the example. The tube (2) may or may not be yielded in the "contact zone" depending on the backing provided by (3). Piece (1), however, will always be yielded in the contact zone, and the maximum "sealing pressure" will occur where piece (1) has a transition from plastic to elastic hoop action. The "sealing pressure" increases with increasing x in the plastic zone, since the thickness increases while the hoop stress is constant at the yield stress; in the elastic region beyond, although the thickness continues to increase, the hoop stress now decreases more rapidly.

49.3 Other Considerations

The interference between parts (1) and (2) is achieved by the pressure of nut (4) in pushing sleeve (3) against tube (2) which in turn bears on

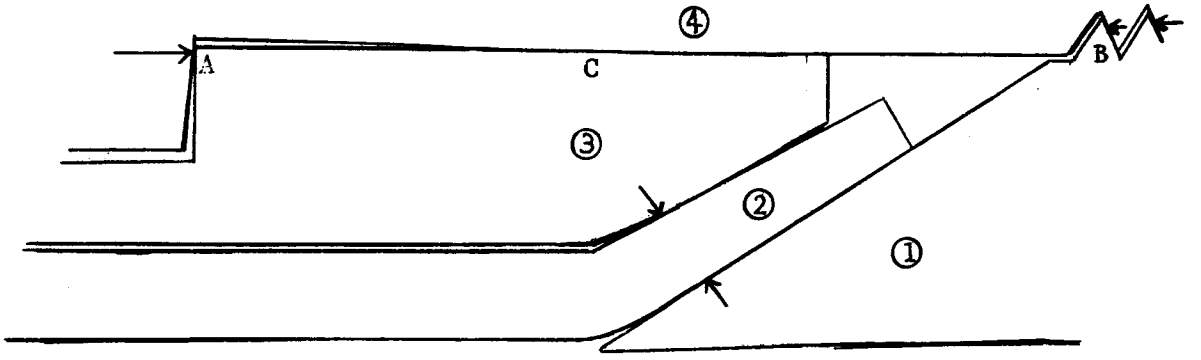

fitting (1). It is evident that at point A there is a need for close tolerances to prevent variations in contact pressure circumferentially. Similarly, at point B there is such a need. The sleeve will ordinarily be too light to back-up the tube by itself. It will bear in turn on the nut at C. Deviations from concentricity between sleeve, nut, and tube, as well as ovality, can cause substantial circumferential variations in sealing pressure. No detailed analysis of these effects will be given here.

In the preceding section we have assumed that the force between mating parts can be described as a normal pressure. In actuality, frictional forces will also be present, particularly in the absence of lubricants. The frictional force will diminish the ratio of "sealing pressure" to axial stress in proportion to $1/(1 + \nu \cot \beta)$ where ν is the coefficient of friction and β is the angle between the (1) - (2) interface and the fitting axis. As a result, friction tends to decrease the "sealing pressure" for a given nut tightness. On the other hand, friction increases the ratio of "sealing pressure" to hoop stress in proportion to $1/(1 - \nu \tan \beta)$.

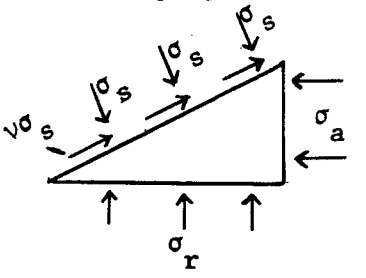

$$\sigma_r = \sigma_s(1-\nu \tan \beta)$$
$$\sigma_a = \sigma_s(1+\sigma \cot \beta)$$

As a result, it appears that friction can be favorable where hoop stress is a limiting factor and unfavorable where axial stress is limiting. In addition, of course, galling and similar related phenomena are more likely where friction is large.

In addition, friction at A and B in the preceding sketch will increase the torque required to attain a given normal force between nut and sleeve.

Temperature will tend to affect part (1) much earlier in time than it affects part (4). In addition, the presence of several interfaces, i.e., (1)-(2), (2)-(3), and (3)-(4) makes it likely that a steady-state temperature difference between (1) and (4) will develop whenever the fluid is either much hotter or much colder than the external environment. Since yielding is present from the beginning, it is likely that many temperature effects will result in additional yielding with a corresponding reduction in tightness after equilibrium is reached.

Internal pressure will have some tendency to increase seal tightness by relieving compressive hoop stress in part (1) and causing some additional yielding in hoop tension in part (2) and additional loading of the "back-up" structure, part (3). In view of the additional yielding in part (2), it seems likely that the sealing effectiveness at lower pressures will have been reduced by a previously higher internal pressure.

The use of a soft washer between parts (1) and (2) can be expected to substantially improve the leak effectiveness because the "sealing pressure" will be relatively unaffected, while the surface "softness" will be much improved.

Another means of improving the sealing effectiveness may involve the use of an elevated contact surface at A on piece (1) to localize the sealing area. In so doing, it should be possible to increase the ratio of "sealing pressure" to hoop stress, particularly where the "contact length" can be made substantially smaller than the thickness of (1) in the vicinity of A. Such a change in shape of (1) may adversely affect flow, cleanliness, strength, or other factors and requires thorough investigation. It should be noted that localizing the contact zone between (2) and (3), as by a double-angle sleeve, is not nearly so effective, since the localization will spread out in going through (2) to the (1)-(2) seal interface.

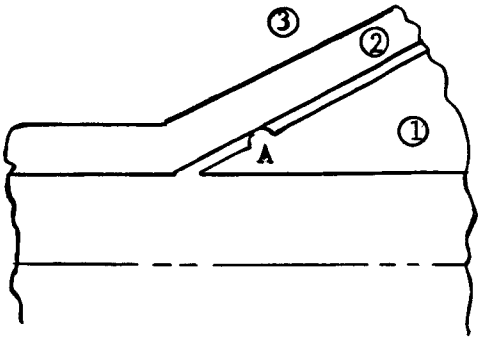

It would appear that increasing the fitting angles would also be beneficial. With larger angles, the presence of some friction prevents hoop stress from being limiting and makes the "sealing pressure" approach the axial stress in magnitude.

49.4 Conclusions

The elastic-plastic behavior of flare-type demountable tubing connectors shows that hoop yielding in the "seal" area is probably always present. The "sealing" radial pressure is, however, only 1/4 to 1/2 the yield stress, depending on geometry and degree of tightening. As a result, this form of connector benefits little from surface yielding in getting a better "fit" between the sealing surfaces. Such a connector, therefore, requires excellent surfaces if a tight seal is to be achieved. The presence of unusual pressure or temperature conditions will cause a worsening of the leakage characteristics in most cases. Greatest improvement in the performance of these connectors can be expected from:

(1) The use of "crush" washers or soft gaskets.

Some benefit can also be obtained from:

(2) The use of "double-angle" sleeves.

49.5 References

1. W. G. Groth, "Flare Type Demountable Stainless Steel Tubing Connections for Space Vehicle Service," Report No. M-F&AE-MTP-61-25, NASA, Marshall Space Flight Center, March 22, 1961.

2. S. Timoshenko, Theory of Plates and Shells, McGraw-Hill Book Co., 1940.

3. S. Timoshenko, Theory of Elasticity, McGraw-Hill Co., 1934.